NASA-CR-202394

FINAL REPORT: MS Thesis

NASA GRANT NUMBER NCC 2-743
Cal Poly Project 5318

Development of a Computer Program for Analyzing Preliminary Aircraft Configurations in Relationship to Emerging Agility Metrics

Brent Bauer
Graduate Student

PI: Doral Sandlin

OCT 1 5 1996

December 1993

Development of a Computer Program for Analyzing Preliminary
Aircraft Configurations in Relationship to Emerging Agility Metrics

A Thesis

Presented to

the Faculty of the Aeronautical Engineering Department

California Polytechnic State University, San Luis Obispo

In Partial Fulfillment

of the Requirements for the Degree

Master of Science

by

Brent Alan Bauer

December 1993

AUTHORIZATION FOR REPRODUCTION OF MASTER'S THESIS

I grant permission for the reproduction of this thesis in its entirety or any of its parts, without further authorization from me.

_____

Signature

_____

Date

APPROVAL PAGE

TITLE: Development of a Computer Program for Analyzing
          Preliminary Aircraft Configurations in Relationship to
          Emerging Agility Metrics

AUTHOR: Brent Alan Bauer

DATE SUBMITTED: December 1993

Dr. Ruben Rojas-Oviedo   _____
Advisor   Signature

Dr. Russell Cummings   _____
Committee Member   Signature

Dr. Daniel Biezad   _____
Committee Member   Signature

ABSTRACT

This paper discusses the development of a FORTRAN computer code to perform agility analysis on aircraft configurations. This code is to be part of the NASA-Ames ACSYNT (AirCraft SYNThesis) design code. This paper begins with a discussion of contemporary agility research in the aircraft industry and a survey of a few agility metrics. The methodology, techniques and models developed for the code are then presented. Finally, example trade studies using the agility module along with ACSYNT are illustrated. These trade studies were conducted using a Northrop F-20 Tigershark aircraft model. The studies show that the agility module is effective in alalyzing the influence of common parameters such as thrust-to-weight ratio and wing loading on agility criteria. The module can compare the agility potential between different configurations. In addition one study illustrates the module's ability to optimize a configuration's agility performance.

TABLE OF CONTENTS

TABLES

FIGURES

SYMBOLS

a_F	Acceleration normal to flight path due to aerodynamic and thrust forces
a_{cent}	Centripetal acceleration (reaction)
a_x	Acceleration along flight path direction
C_L	Aircraft lift coefficient
C_D	Aircraft drag coefficient
$C_{L\alpha}$	Aircraft lift slope $\left(\dfrac{\partial C_L}{\partial \alpha}\right)$
$C_{L\alpha_c}$	Canard lift slope
$C_{L\alpha_h}$	Horizontal tail lift slope
$C_{M\alpha}$	Aircraft pitching moment coefficient due to angle of attack $\left(\dfrac{\partial C_M}{\partial \alpha}\right)$
$C_{M_{\dot\alpha}}$	Aircraft pitching moment coefficient due to angle of attack rate $\left(\dfrac{\partial C_M}{\partial \dot\alpha}\right)$
C_{Mq}	Aircraft pitching moment coefficient due to pitch rate $\left(\dfrac{\partial C_M}{\partial q}\right)$
D_{aero}	Parasite plus induced drag force $\left(D_{aero} = qSC_D\right)$
D_{ram}	Ram drag force $\left(T_g - T_n\right)$
$\left(\dfrac{\partial \varepsilon}{\partial \alpha}\right)_c$	Upwash gradient at canard
$\left(\dfrac{\partial \varepsilon}{\partial \alpha}\right)_h$	Downwash gradient at horizontal tail

g gravitational acceleration

L Aircraft lift force $(L = qSC_L)$, or aircraft rolling moment

L_p Roll damping derivative $\left(\dfrac{\partial L}{\partial p}\right)$

L_{δ_A} Aileron effectiveness derivative $\left(\dfrac{\partial L}{\partial \delta_A}\right)$

M Mach number

M_α Aircraft pitching moment derivative due to angle of attack $\left(\dfrac{\partial M}{\partial \alpha}\right)$

$M_{\dot\alpha}$ Aircraft pitching moment derivative due to angle of attack rate $\left(\dfrac{\partial M}{\partial \dot\alpha}\right)$

M_q Aircraft pitching moment derivative due to pitch rate $\left(\dfrac{\partial M}{\partial q}\right)$

M_δ Aircraft pitching moment derivative due to control surface deflection- elevator/canardvator $\left(\dfrac{\partial M}{\partial \delta}\right)$

n Load factor

n_{dyn} Transient load factor term due to pitch rate

p Roll rate

Ps Specific excess power

p_{ss} Steady state roll rate

R Turn radius

t	Time
T_g	Gross thrust
T_n	Net thrust
U_1	Steady state forward airspeed
V	Instantaneous forward airspeed
V_c	Canard volume coefficient or aircraft corner speed
V_h	Horizontal tail volume coefficient
$\dot{V}$	Acceleration along flight path, equivalent to a_x
W	Aircraft weight
X	Downrange distance, used to track movement of aircraft
X_{ac_c}	Longitudinal location of canard aerodynamic center on aircraft
X_{ac_h}	Longitudinal location of horizontal tail aerodynamic center on aircraft
X_{cg}	Longitudinal location of center of gravity on aircraft
Y	Crossrange distance, used to track movement of aircraft
Z_α	Normal force derivative due to angle of attack $\left(\dfrac{\partial Z}{\partial \alpha}\right)$
Z_δ	Normal force derivative due to control surface deflection-elevator/canardvator $\left(\dfrac{\partial Z}{\partial \delta}\right)$
α	Angle of attack
δ	Pitch control surface deflection

δ_A	Aileron deflection	
Δ	Incremental difference	
η_c	Dynamic pressure ratio at canard location	
η_h	Dynamic pressure ratio at horizontal tail location	
Θ	Aircraft pitch angle	
λ	Thrust vector angle	
Φ	Bank angle	
Ψ	Heading angle	
$\dot{\Psi}$	Turn Rate	

CHAPTER 1

INTRODUCTION

Much of present fighter performance research centers on agility. Projects such as NASA's High Angle of Attack Research Vehicle (HARV)[1] and Rockwell/MBB's X-31 agility research platform[2,3] represent the flight test efforts at agility research. In addition, in the past five to ten years, increased interest from industry and NASA have created a host of analysis methods and agility philosophies.[4,5,6,7] Several companies have developed their own measures of merit, or metrics, that they believe best measure an aircraft's agility. However, the industry as a whole has not yet adopted a solid definition of agility nor accepted any of the analysis methods or metrics as superior.

Some of the agility definitions used by industry are:

> The ability to change aircraft attitude and
> flight path with quickness and precision
>   Air Force Flight Center[8]

> Agility is directly proportional to the inverse
> of the time to transition from one maneuver
> to another
>   Pierre Sprey[7]

> Agility is the ability to rapidly change both
> the magnitude and direction of the aircraft
> velocity vector
>   Northrop[7]

> Agility is an attribute of a fighter aircraft
> that measures the ability of the entire
> weapon system to minimize the time delays
> between target acquisition and target
> destruction
> Eidetics[7]

While all of these definitions appeal to the intuitive sense of what agility should address, they each place emphasis on different facets of the concept of agility. These different approaches have thus provided different tools and parameters to analyze the agility potential of an aircraft configuration. It is these various facets and their respective tools and parameters that have produced the myriad of agility metrics. Chapter Two discusses in detail some of these metrics.

The importance of agility is to provide a combat advantage over other aircraft. Combat advantage can be provided by superior training, better weapons, as well as many other sources. However, improvement in an airframe's performance has always been a key element in providing combat advantage. Historically, this has been created through improvements in energy maneuverability; the ability to generate high turn rates and high speeds and accelerations. The energy maneuverability envelope has been continuously expanded from the days of World War I until today. However, the last generation of fighters reached an envelope boundary. This boundary is the physiological limit of the pilot. Contemporary aircraft have surpassed the g tolerance of humans and this has placed a limit on combat advantage through improving energy maneuverability.

Given the physiological barrier, the industry began to look not at expanding the energy maneuverability envelope but at how quickly an aircraft could transition from one point in the envelope to another. This school of thought guides today's agility research and is seen as the main source of airframe related combat advantage for at least the next generation of combat aircraft.

Improvement in aircraft agility places certain requirements and constraints on an aircraft configuration. Proper trade studies need to be performed at the preliminary design stage in order to create a balanced airframe. The purpose of this project is to include agility analysis into the ACSYNT (AirCraft SYNThesis) design code developed at the NASA Ames Research Center. To illustrate how agility analysis can be incorporated into the ACSYNT code a description of how it operates must first be covered.

ACSYNT is a FORTRAN program developed as a tool to be used in the preliminary design of aircraft. It is composed of modules that each perform a different analysis function or analyze a separate discipline relevant to aircraft design.

The primary modules in ACSYNT are geometry, trajectory (mission profile), aerodynamics, propulsions, and weights. These modules and others such as takeoff/landing and economics are each called separately. When a module is called it then performs its analysis and applies its constraints to the aircraft configuration. The modules are each called repeatedly until they converge on the solution of an aircraft configuration that can perform the specified mission.

The real power of ACSYNT is achieved when it is linked to another NASA code called COPES. This code is a generic optimization code. When ACSYNT and COPES are coupled, multivariable optimizations can be performed. A large array of variables from all modules are available to be constrained or optimized. Typically the gross takeoff weight is optimized for the least value. This procedure provides the lightest preliminary configuration that satisfies mission requirements.

The main use of the ACSYNT-COPES package is to perform trade studies of configurations and to evaluate the impact of technologies on configurations. The improvements in materials, propulsions and other technologies can be incorporated and their effect on aircraft configurations can be readily determined. In this way the feasibility and penalty of technology can be assessed.

The objective of the agility module in ACSYNT is to provide analysis of agility metrics and, when developed, agility criteria. Implementation of technologies to improve aircraft agility could be analyzed and optimized in ACSYNT and their penalty and impact on other design constraints determined. This analysis will provide some insight into the utility of agility technologies and the combat effectiveness of an aircraft configuration.

The objective of this study is to develop the framework for the agility module. The basic code architecture is to be designed with emphasis on adaptability so that many different agility metrics can be analyzed. In addition, the code should be able to apply various constraints for use in optimization.

CHAPTER 2

DISCUSSION ON AGILITY METRICS

The discussion on agility metrics begins with a description of a general maneuverability diagram- the doghouse plot- and the definition of corner speed. Their significance to agility analysis is discussed.

The second section of this chapter is a survey of several agility metrics developed and used by industry. Finally, the relation between these metrics and the project scope and code architecture is discussed. The ultimate goal of ACSYNT's agility module is to be able to both analyze existing metrics and be adaptable enough to analyze metrics yet to be created.

The Doghouse Plot and Definition of Corner Speed

The general character of the agility module is to operate on the upper boundary of what is frequently referred to as the doghouse plot. This is a graph of turn rate versus speed or Mach number. Figure 2.1 illustrates a typical doghouse plot. The upper boundary of this graph indicates the maximum turn rate for a given Mach number.

As shown in Figure 2.1, there is a peak in the upper boundary. This peak represents the highest turn rate for any Mach number. The Mach number corresponding to the peak is usually called corner speed.

The aircraft's turn rate is limited by different constraints depending on which side of corner speed it is flying. Above corner

speed, the aircraft can aerodynamically generate a higher load factor than the aircraft's structure can withstand. The aircraft is said to be "load limited" with the maximum turn rate determined by the maximum designed load factor. Below corner speed, the aircraft is operating at its maximum lift coefficient and cannot aerodynamically generate the design load factor. In this region the aircraft is said to be "lift limited".

From the above discussion, the definition of corner speed can be inferred: the Mach number that produces the maximum design load factor at maximum lift coefficient is the corner speed.
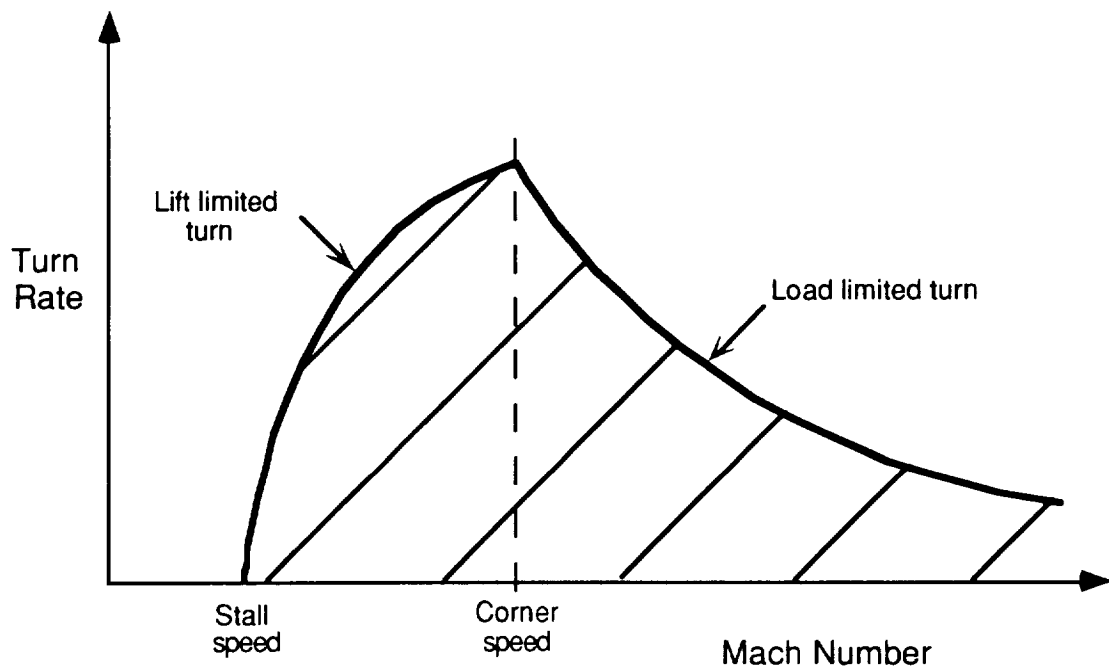
Figure 2.1

Illustration of the Doghouse Plot

Survey of Agility Metrics

This section describes several of the many agility metrics introduced by industry. It also provides a good sample of the spectrum of agility metrics. The uniqueness of each metric illustrates how the different concepts of agility have produced differing opinions on which parameters are important.

Combat Cycle Time[6]

The combat cycle time metric measures the time it takes to turn through a specified heading change and then accelerate to regain the energy lost during the turn. The objective is to complete this maneuver in the least amount of time. In this maneuver the aircraft operates along the upper boundary of the doghouse plot discussed earlier in the chapter. Figure 2.2 illustrates the path the aircraft follows on this plot over the course of the maneuver.

Figure 2.2

Combat Cycle Time Maneuver Circuit
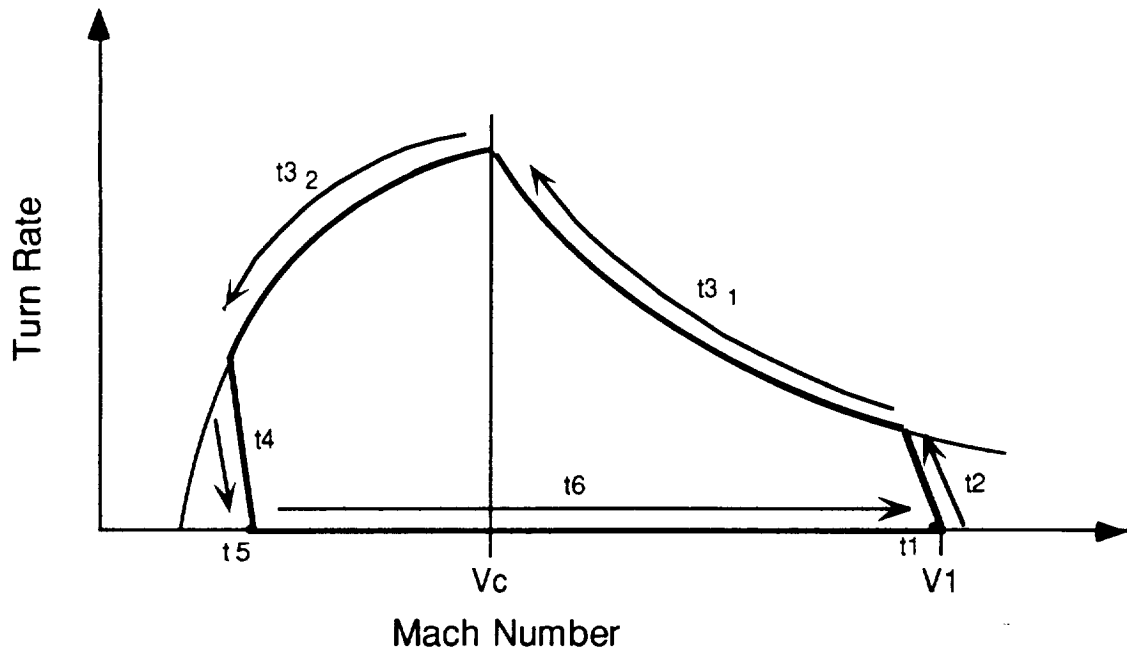
Legend:

V1-starting and ending speed

t1-time to bank into turn

t2-pitch up to load factor

t3₁-time spent in load limited turn

t32- time spent in lift limited turn

Vc-corner speed

t4-pitch down to unity load factor

t5-roll to wings level

t6-time to accelerate back to V1

Pointing Margin

The pointing margin metric measures how fast an aircraft can point his nose at an adversary aircraft. The two aircraft begin at nearly the same location in space but pointed in opposite directions (see Figure 2.3). The aircraft also begin at the same Mach number.

At the start of the metric both aircraft begin a maximum acceleration turn toward one another. The aircraft that first brings his line of sight upon the opposing aircraft's position is considered the most agile. The measure of merit is the pointing margin or the angle between the two aircrafts' lines of sight just as the inferior aircraft is captured. The greater this angle the longer it takes the losing aircraft to acquire the winning aircraft's position. This provides the winning aircraft a longer missile flight time and a better chance of a kill.
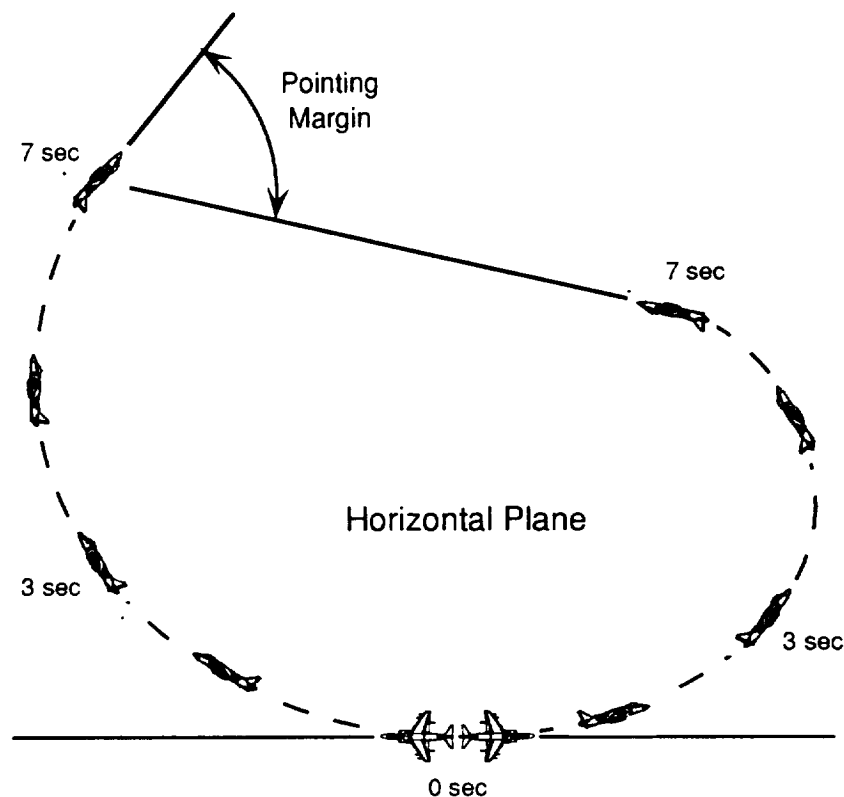
Figure 2.3
Pointing Margin Agility Metric

Torsional agility[7]

Torsional agility measures an aircraft's ability to quickly rotate the acceleration vector about the aircraft's longitudinal axis. Its definition is simple and straightforward. For a given altitude and Mach number, torsional agility is the maximum possible turn rate divided by the time to perform a 90 degree roll maneuver.

Axial agility[9]

Axial agility measures the influence of the propulsion system on the aircraft's ability to quickly gain or lose energy. For a given altitude and Mach number, axial agility measures the difference between maximum and minimum specific excess power divided by the time for the aircraft to transition between these two power levels, ie.

$$\frac{Ps_{max} - Ps_{min}}{\Delta t}$$

For this metric not only is the transient time important but the range of excess power levels is also important. Thus the maximum and mimimum values of available power (engine) and required power (airframe drag) are important as well as the ability to quickly transition between these maximums and minimums.

Dynamic Speed Turn[5]

The dynamic speed turn metric does not track one specific measurable quantity. Instead, it consists of a pair of graphs that

relate two parameters over an entire flight envelope. The plots are maximum turn rate versus bleed rate and the maximum straight and level acceleration versus Mach number. These plots correspond to a given altitude. Two example dynamic speed turn plots are illustrated in Figure 2.4.

The bleed rate graph plots the maximum turn rate for all possible Mach numbers versus the corresponding axial acceleration (bleed rate). This acceleration is calculated at full thrust. The bleed rate and the maximum level acceleration curves illustrate how an aircraft loses energy during maneuvering and how fast it can gain energy after maneuvering.
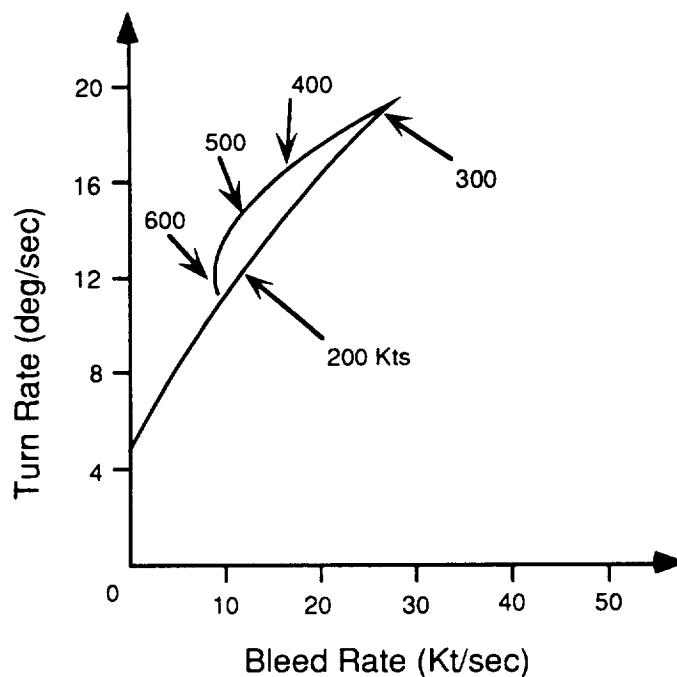
Figure 2.4a

Plot of Turn Rate Versus Bleed Rate
for the Dynamic Speed Turn Metric
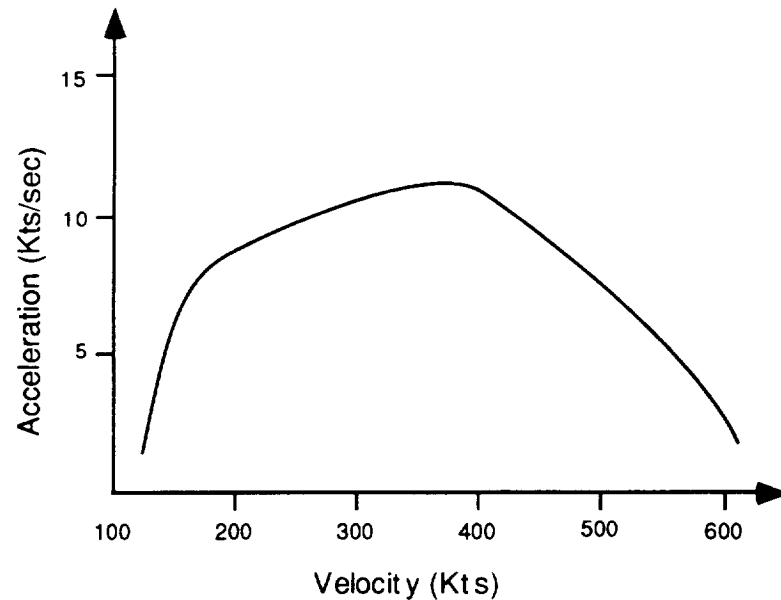
Figure 2.4b

Plot of Level Acceleration Versus Velocity
for the Dynamic Speed Turn Metric

Agility Metrics in Relation to Project Scope and Code Architecture

The metrics previously discussed illustrate the differences of opinion on what agility is. Some metrics analyze how efficiently aircraft use energy to achieve an objective and also how quickly they can regain lost energy. Other metrics analyze the quick-action nose pointing capability of a configuration. For this project it was decided not to select just one of these philosophies for the agility module but to make the module adaptable enough to accomodate several of the philosophies and their respective metrics.

To limit the project scope, the development of the overall architecture was considered the most important task and the primary responsibility of this project. One metric, combat cycle time, was used as an archetype for the development of the architecture. This metric was selected because it contained almost every element of the agility philosophy spectrum. While combat cycle time's main focus is on the gain and loss of energy, it also contains quick-action maneuvers (roll and pitch) within it. It was therefore considered the best metric for use as an archetype for the code architecture. Because of this selection, the complete development of the combat cycle time metric as a separate subroutine is included in the project scope.

The methodology used to develop the agility module architecture is the subject of the next chapter.

CHAPTER 3

GENERAL METHODOLOGY

The overall structure of the code is a time-stepping routine that tracks pertinent parameters over the course of the agility maneuver. This method is basically a simulation technique. Although many metrics, such as Lateral Agility, involve parameters that can be solved for directly, others, such as combat cycle time and pointing margin, require parameters that are tracked throughout the maneuver's time interval. It is these latter type of metrics that require the simulation methodology.

Since combat cycle time was selected as an archetype for the simulation package there exists a separate subroutine dedicated to analyzing this metric. To evaluate other agility metrics, one of two options may be used. First, the main input file allows the user to directly call the simulation package and construct the desired metric maneuver. The second option is to create a dedicated subroutine similar to the one for combat cycle time to conduct the metric maneuver.

The time stepping routine tracks important parameters such as Mach number, turn rate, and horizontal position. The time histories of these parameters forms the bulk of the data used in metric analysis. The final section of this chapter describes the list of tracked variables but first some other basic characteristics of the simulation package will be discussed.

Constant Altitude

Most of the agility metrics discussed previously involve maneuvers that occur at constant altitude. Therefore a constant altitude assumption was made throughout the development of the flight mechanics. This assumption greatly simplified the resulting equations. However, this is not to say the aircraft was constrained to fly level. Instead, the vertical excursions were ignored. For example, imagine an aircraft flying straight and level at constant airspeed. If the aircraft is suddenly banked, without altering the angle of attack, the unity load factor vector no longer counters gravity as is shown in Figure 3.1. This results in a downward acceleration. In the agility module, the downward acceleration was ignored and the vertical displacement was not tabulated. However, during the short time of a roll, this displacement was considered negligible.

If the purpose of the roll was to enter a level turn, the roll segment would be followed by a pitch segment. The purpose of pitching the aircraft would be to raise the load factor to that required for a level turn at the given bank angle. Again, the vertical excursion was considered negligible. This technique requires some orchestration of the maneuver segment sequence and thus it is somewhat the user's responsibility to ensure maneuvers are level.
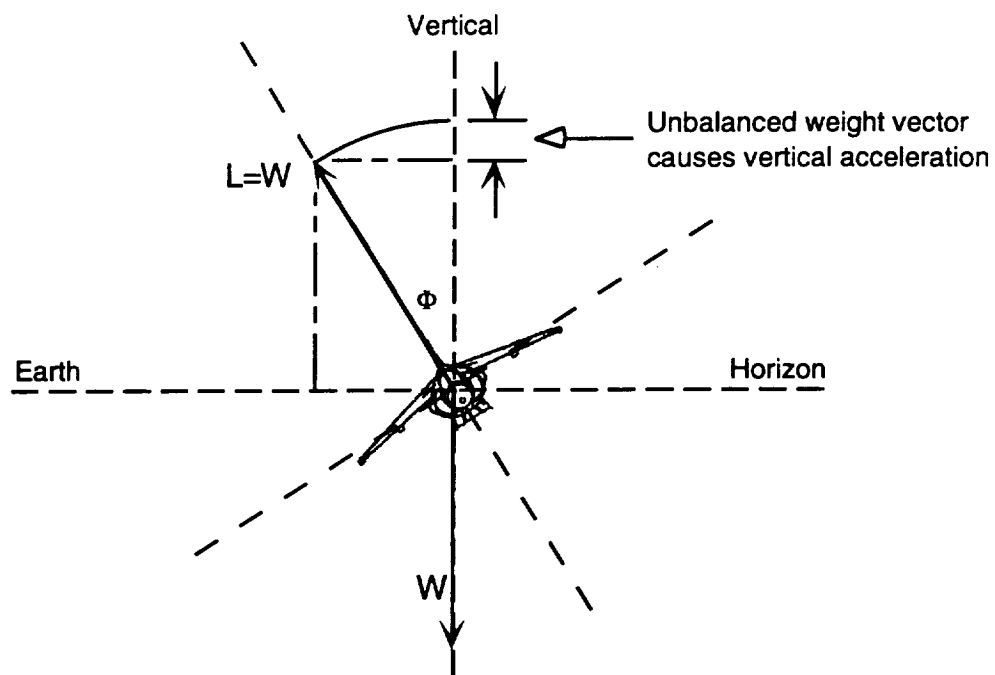
Figure 3.1

Downward Vertical Acceleration Due to
Unbalanced Weight Vector at a Bank Angle

Breakup of Maneuvers Into Segments

The metric maneuvers were divided into separate maneuver segments to simplify analysis. Each of the agility metrics discussed previously consisted of at least one maneuver segment. Most metrics are a combination of several segments of different types. Figures 3.2 and 3.3 illustrate the four types of maneuver segments; rolls, pitches, turns, and accelerations. Figure 3.3 also shows the segments divided into two categories; functional and transient. This classification, which is similar to the agility metric

classification system in reference 9, is used to separate the flight mechanics development in Chapter 4.

Functional maneuver segments deal with long-term changes in aircraft energy state, position and attitude. Equations of motion for the functional segments were steady-state equations for turns and rectilinear flight.

Transient maneuver segments deal with short-term changes in aircraft accelerations, positions and orientation. Equations of motion for the transient segments were standard longitudinal and lateral-directional perturbation equations.

The functional segments, turns and accelerations, actually represent quasi-steady turns and straight line accelerations. The term "quasi-steady turn" refers to a steady, level turn maneuver where the velocity may be changing. If a turn cannot be sustained the aircraft loses airspeed. In order to maintain the load factor, the angle of attack needs to gradually increase. Or, if the aircraft is lift-limited and cannot sustain the load factor, the bank angle will gradually have to decrease to maintain the level turn. These changes in angle of attack and bank angle are gradual enough that the steady turn equations of motion can be used and the perturbation equations need not be employed. It is this type of turning maneuver that is termed quasi-steady.
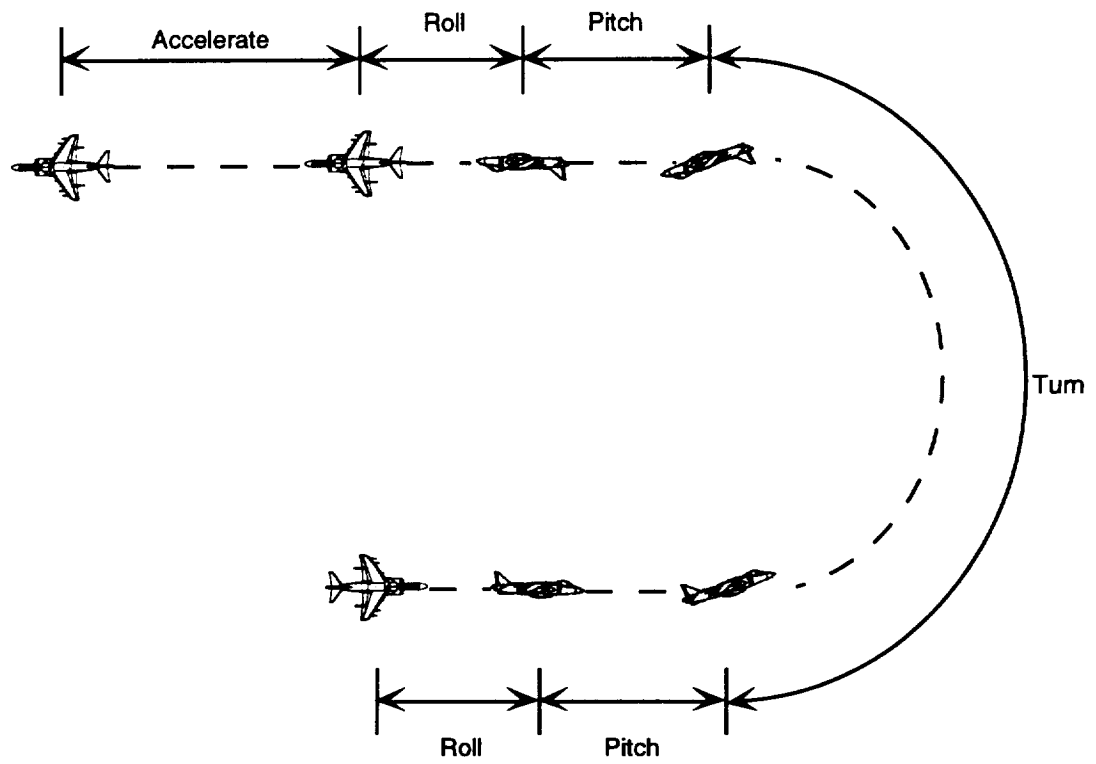
Figure 3.2
Breakup of Metric Maneuvers Into Maneuver Segments

```
┌─────────────────────────────────────────────────────────┐
│                                                          │
│              Maneuver Segment Categories                 │
│                                                          │
└─────────────────────────────────────────────────────────┘
        │                                    │
   ┌────────────────────┐         ┌────────────────────┐
   │                    │         │                    │
   │ Functional Segments│         │ Transient Segments │
   │                    │         │                    │
   └────────────────────┘         └────────────────────┘
      │           │                  │            │
  ┌───────┐  ┌────────────┐     ┌────────┐   ┌────────┐
  │ Turn  │  │Acceleration│     │ Pitch  │   │  Roll  │
  └───────┘  └────────────┘     └────────┘   └────────┘
```
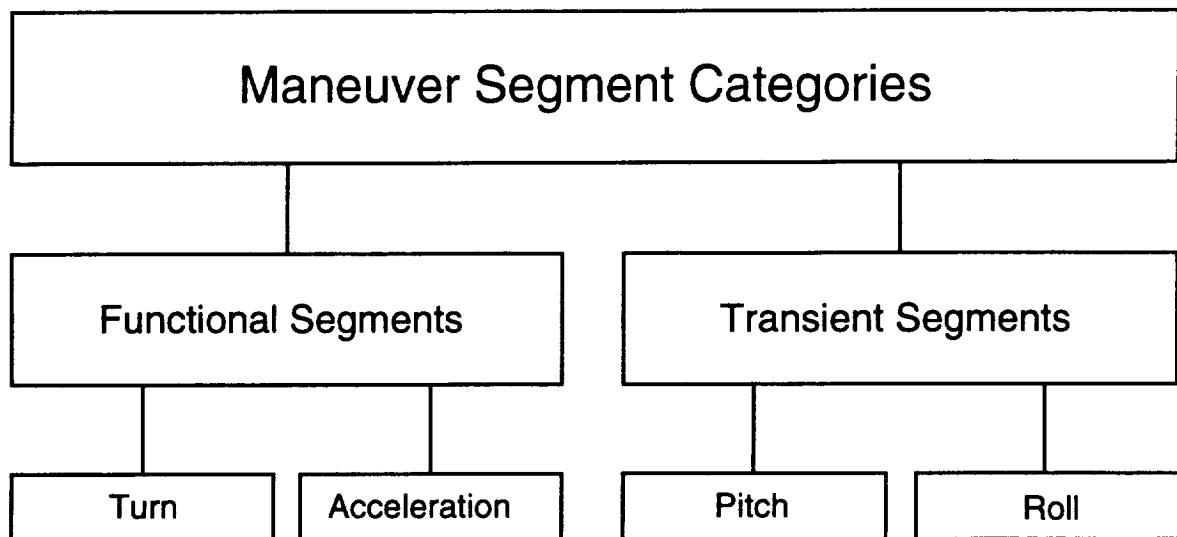
Figure 3.3

Illustration of the Agility
Maneuver Segment Categories

Tracked Variables

In order to evaluate agility metrics, nineteen parameters needed to be tracked. For each time step these parameters were calculated and stored. The primary output of the agility module is a time-stepped array of these parameters. The nineteen tracked variables are listed in Table 3.1.

Not all of the parameters in Table 3.1 are intuitive and therefore need explanation. Axial acceleration is the acceleration along the velocity vector and contributes solely to velocity changes. The throttle command is a variable whose value determines the pilot commanded thrust level; full afterburner, full dry, flight idle, etc.

The thrust vector angle parameter, which is also pilot commanded, does not represent pitch control thrust-vectoring but instead, thrust vector rotation about the aircraft center of gravity as in powered-lift aircraft such as the McDonnell Douglas AV-8B.

The second row in Table 3.1 involves the engine parameters. Gross thrust represents the total installed thrust force developed by the engine. Net thrust is gross thrust minus the momentum flux at the inlet (ram drag). At zero airspeed gross and net thrust are identical. As airspeed increases ram drag increases and the net thrust developed by the engine decreases. These two parameters are important during thrust-vectoring maneuvers. It is the gross thrust that is vectored normal to the flightpath. The ram drag (Tg-Tn) however, remains in the airflow (axial) direction.

The engine core percent and afterburner percent represent the core thrust over full dry thrust and the afterburner thrust over full afterburner thrust respectively. These parameters are not necessarily important for flight mechanics but are important for the throttle transient algorithm and will be discussed later.

The third row of Table 3.1 contains well known parameters. The fourth and fifth row contain lateral-directional motion variables and aircraft position variables, all of which will be defined in the next chapter.

Table 3.1

Variables Tracked Over Time by the Agility Module

M mach number	$\dot{V}$ axial acceleration (g's)	Throttle command logic (numeric)	λ thrust vector angle (degrees)
Tg gross thrust (pounds)	Tn net thrust (pounds)	Engine core thrust (% thrust)	Afterburner thrust (% thrust)
α angle of attack (degrees)	n normal accel. 'load factor' (g's)	C_L lift coefficient	C_D drag coefficient
Ψ heading angle (degrees)	$\dot{\Psi}$ turn rate (deg/sec)	Φ bank angle (degrees)	P roll rate (deg/sec)
X downrange distance (feet)	Y crossrange distance (feet)	R turn radius (feet)	

CHAPTER 4

FLIGHT DYNAMICS

In order to evaluate the tracked variables a flight dynamics strategy needed to be developed. First, the flight dynamics were divided into two categories, one for the functional maneuver segments (quasi-steady turns and straight line accelerations) and one for the transient segments (rolls and pitches). The functional maneuver strategy used steady state maneuver equations to develop equations of motion. The transient maneuver strategy used lateral and longitudinal perturbation equations of motion as developed in reference 10 for the roll and pitch segments. These two strategies are discussed in the last two sections of this chapter. First, however, appropriate coordinate systems are developed and some relevant tracked variables are defined.

Coordinate Systems

Tracking of parameters necessary to evaluate agility metrics required three coordinate systems. The first system was an inertial, Earth-fixed system designated (X1, Y1, Z1). The X1-Y1 plane lies in the horizontal with the Z1 axis pointing down toward the center of the Earth as shown in Figure 4.1. The downrange and crossrange parameters (X,Y) referenced in the previous chapter and listed in Table 3.1 correspond to the X1 and Y1 translations respectively.

22

The second coordinate system was designated (X2, Y2, Z2) and is also shown in Figure 4.1. This system translates with the aircraft but does not rotate with it. As the aircraft moves the X2 axis remains parallel with the X1 axis, Y2 remains parallel with Y1, and Z2 parallel with Z1.

The third coordinate system was designated (X3, Y3, Z3). This system and the second system (X2, Y2, Z2) are illustrated in Figure 4.2. This third system translates with the aircraft but also rotates laterally with it. The X3 axis remains pointed in the direction of the aircraft velocity vector but the Y3 axis remains pointed toward the aircraft's starboard wingtip. Since the aircraft is constrained in altitude the velocity vector (and hence X3) must always lie in the X1-Y1 plane.

The heading angle parameter (Ψ) described in the previous chapter is defined as the angle between the X2 axis and the X3 axis. The bank angle parameter (Φ) is defined as the vertically projected angle between the X2-Y2 plane and the Y3 axis. Both the heading angle and the bank angle are shown in Figure 4.2.

At the start of a metric (t=0), all three coordinate systems coincide with their origins at the aircraft center of gravity. All three X axes point along the aircraft's velocity vector, all Y axes point toward the starboard wingtip, and all Z axes point toward the center of the Earth.

Along with each of the three coordinate axes there corresponds a set of velocity components u,v,w and accelerations $\dot{u}, \dot{v}, \dot{w}$. However, not all of these parameters are of interest in metric

analysis. Instead of a complete set of coordinate transformation matrices, each parameter was calculated independently. This resulted in reduced computer time.
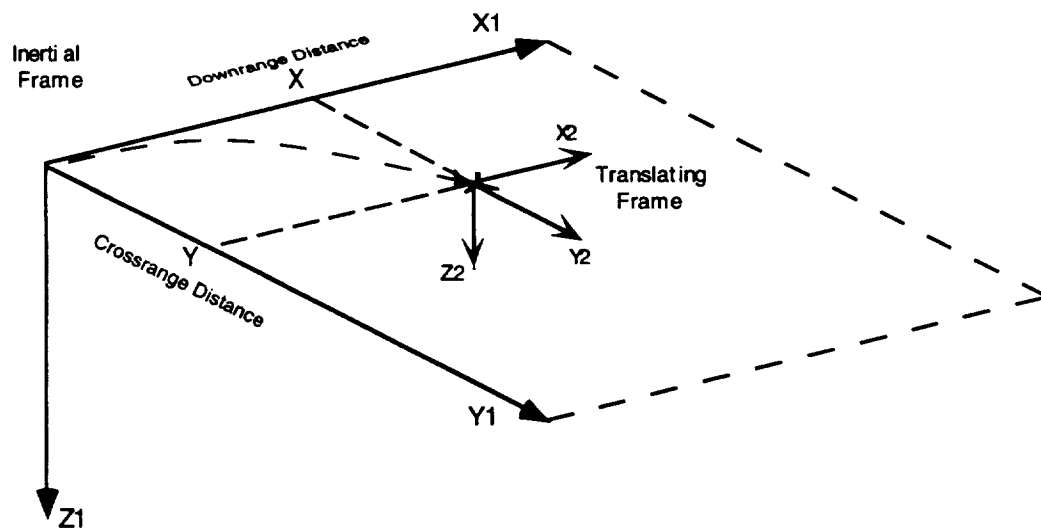
Figure 4.1

Orientation of the Inertial Coordinate Frame
and the Translating Coordinate Frame
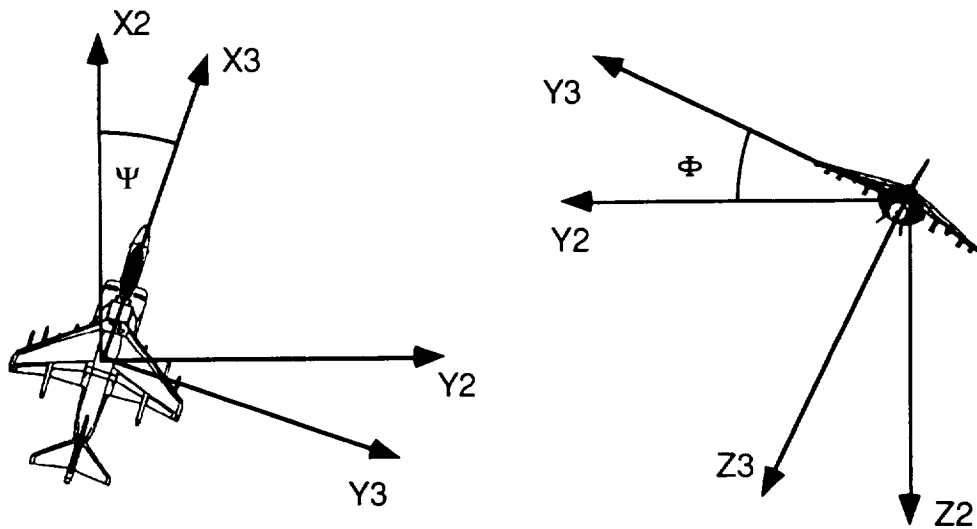
Figure 4.2

Orientation of the Rotating Coordinate Frame
With Respect to the Translating Coordinate Frame

Development of Free-Body Diagrams and Equations of Motion for Functional Maneuver Segments

To develop equations of motion for the functional maneuver segments, free-body diagrams were first created. From these diagrams the acceleration components normal and parallel to the flight path (X3 axis) could be determined. Figure 4.3 illustrates the free-body diagram used to determine the parallel (axial) acceleration component. From this diagram the force summation results in:

$$\Sigma F_x = ma_x \qquad\qquad (4.1)$$

Expanding into separate forces yields:

$$T_g \cos(\alpha + \lambda) - D_{aero} - D_{ram} = \left(\frac{W}{g}\right) a_x \qquad (4.2)$$

Substituting in identities for D_{aero} and D_{ram} and solving for a_x:

$$a_x = \left(\frac{g}{W}\right)\left[T_g \cos(\alpha + \lambda) - qSC_D - \left(T_g - T_n\right)\right] \qquad (4.3)$$

Rearranging results in the final expression for the axial acceleration:

$$a_x = g\left[\left(\frac{T_g}{W}\right)\cos(\alpha + \lambda) - \frac{qC_D}{\frac{W}{S}} - \frac{T_g - T_n}{W}\right] \qquad (4.4)$$

The free body diagram in Figure 4.4 illustrates the forces that generate the normal acceleration component. This component consists of three separate elements: acceleration due to aerodynamic and thrust forces, gravitational acceleration, and the reactive centripetal acceleration. The objective is to develop equations for the turn rate and turn radius through the centripetal acceleration element. The centripetal element is in turn developed from the other two acceleration elements.

For equilibrium in a steady level turn the aerodynamic and thrust acceleration element (a_F) must be balanced by the

gravitational (g) and the centripetal (a_{cent}) elements. The balance constraint gives:

$$a_F^2 = a_{cent}^2 + g^2 \qquad (4.5)$$

Solving for a_{cent}:

$$a_{cent} = \left(a_F^2 - g^2\right)^{\frac{1}{2}} \qquad (4.6)$$

The a_F element is represented by:

$$\Sigma F_F = ma_F \qquad (4.7)$$

$$-T_g \sin(\alpha + \lambda) - L = \left(\frac{W}{g}\right)a_F \qquad (4.8)$$

Substituting in the identity of L and solving for the component a_F:

$$a_F = \left(\frac{g}{W}\right)\left[-T_g \sin(\alpha + \lambda) - qSC_L\right] \qquad (4.9)$$

Rearranging results in:

$$a_F = g\left[\frac{-T_g}{W}\sin(\alpha + \lambda) - \frac{qC_L}{\frac{W}{S}}\right] \qquad (4.10)$$

Substituting in the a_F relationship into equation 4.6 produces the final identity for the centripetal acceleration:

$$a_{cent} = g\left\{ \left[\frac{T_g}{W}\sin(\alpha + \lambda) + \frac{qC_L}{\frac{W}{S}} \right]^2 - 1 \right\}^{\frac{1}{2}}$$

(4.11)

Equations for the turn radius and turn rate can be determined from basic rotational kinematics. The relationship between turn radius, velocity and centripetal acceleration is:

$$a_{cent} = \frac{V^2}{R}$$

(4.12)

Rearranging gives:

$$R = \frac{V^2}{a_{cent}}$$

(4.13)

Substitution of the a_{cent} identity of equation 4.11 results in:

$$R = \frac{V^2}{g\left\{ \left[\frac{T_g}{W}\sin(\alpha + \lambda) + \frac{qC_L}{\frac{W}{S}} \right]^2 - 1 \right\}^{\frac{1}{2}}}$$

(4.14)

The arc length (s) of a curved flight path is defined by:

$$s = R\Psi$$

(4.15)

The derivative with respect to time gives:

$$V = R\dot{\Psi}$$

(4.16)

Substitution of the R relationship of equation 4.14 results in the turn rate equation:

$$\dot{\Psi} = \frac{g\left\{\left[\dfrac{T_g}{W}\sin(\alpha + \lambda) + \dfrac{qC_L}{\dfrac{W}{S}}\right]^2 - 1\right\}^{\frac{1}{2}}}{V}$$ (4.17)

L

Tgross

λ

Dram   Daero   α

V   X3

WcosΦ

Z3
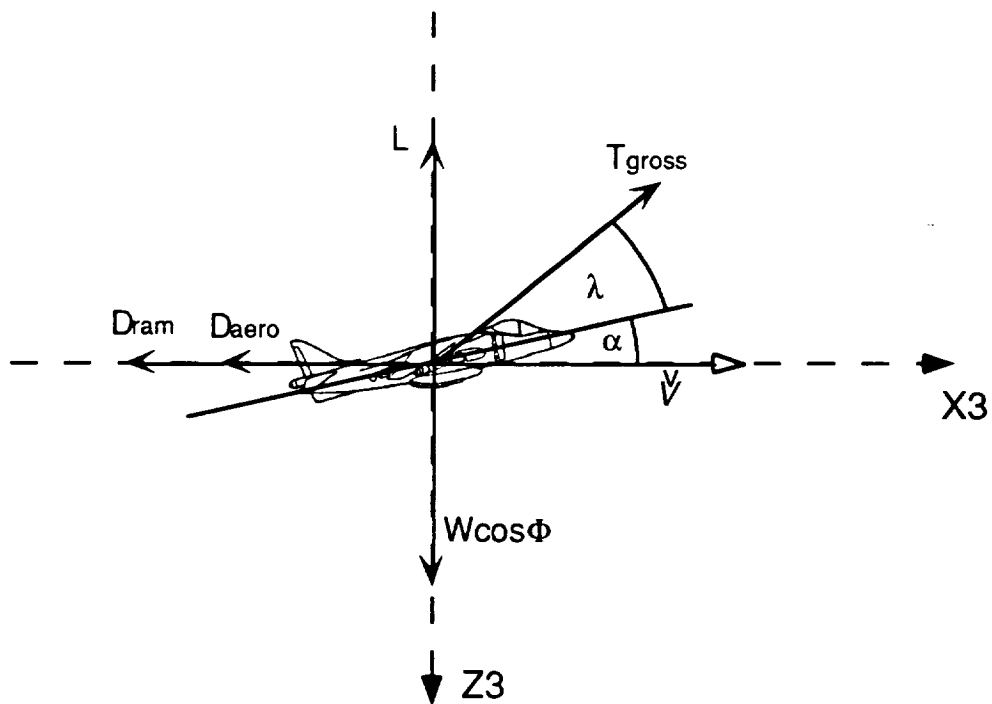
Figure 4.3

Free Body Diagram for the
Axial Acceleration Component
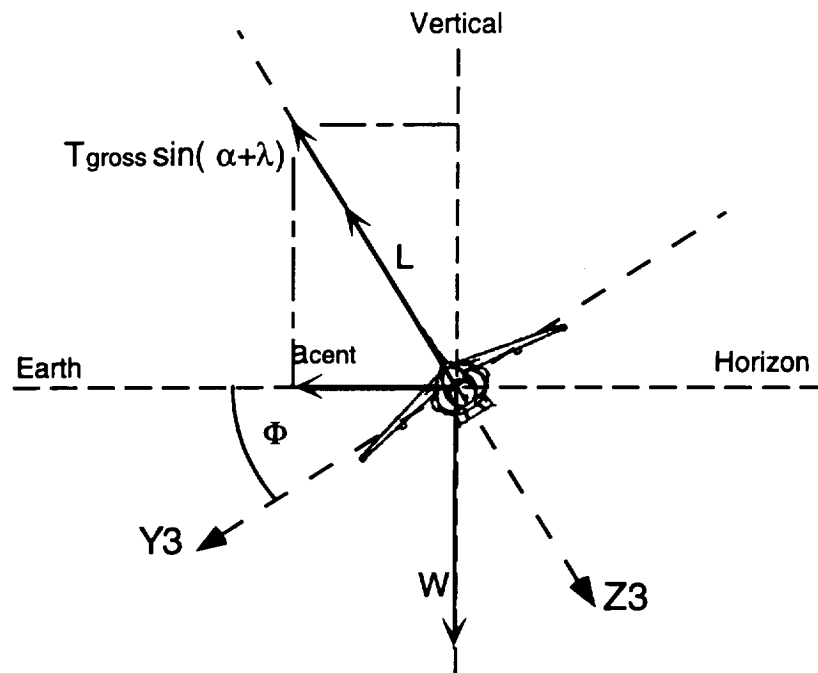
Figure 4.4

Free Body Diagram for the
Normal Acceleration Component

Equations of Motion for Transient Maneuver Segments

Equations of motion for the transient segments were standard lateral-directional and longitudinal perturbation equations. From these equations standard approximations were made to achieve simplified modal response models. The next two sections deal with the development of roll and pitch response modeling.

Roll Segments

The roll segments were modeled with a single degree of freedom, lateral equation of motion found in reference 10. This equation models roll response given: the roll damping derivative (L_p), aileron effectiveness derivative ($L_{\delta a}$), an aileron deflection (δa), and initial conditions. The basic equation is:

$$\dot{p} = L_p p + L_{\delta_a} \delta_a \qquad (4.18)$$

Construction of the dimensional derivatives in the above equation required stability derivatives that were difficult to obtain. No direct method was found to extract these derivatives from ACSYNT. Therefore, the dimensional derivatives L_p and $L_{\delta a}$ are input directly by the user.

Figure 4.5 illustrates a typical roll maneuver as conducted by the code. The control input strategy involved first deflecting the ailerons to the user specified angle causing a roll acceleration. As the roll progresses, and the bank angle approaches the target bank angle, the control input is reversed. This creates a strong roll deceleration. If this control reversal is timed properly, the roll rate drops to zero just as the target bank angle is acquired. This control strategy provides the quickest roll maneuver possible for a given aileron deflection. For simplicity, step control inputs were assumed.

The timing of the control input reversal required an iterative technique. Once the reversal time was determined the roll rate and

bank angle schedules were calculated by integration of the roll equation with the proper initial conditions. These equations were:

For roll rate during initial control input:

$$p(t) = p_{ss}\left(1 - e^{L_p t}\right)$$
(4.19)

where the steady state roll rate (p_{ss}) is:

$$p_{ss} = \frac{-L_{\delta a}\delta a}{L_p}$$
(4.20)

The bank angle during initial control input is:

$$\Phi(t) = \Phi_0 + p_{ss}\left(t + \frac{1}{L_p}\left(1 - e^{L_p t}\right)\right)$$
(4.21)

The roll rate after the control reversal is defined by:

$$p(t) = p_{ss}\left(2e^{L_p\left(t-t^*\right)} - e^{L_p t} - 1\right)$$
(4.22)

The bank angle after the control reversal is:

$$\Phi(t) = \Phi_0 + \frac{p_{ss}}{L_p}\left(2e^{L_p\left(t-t^*\right)} - e^{L_p t} - 1\right) - p_{ss}\left(t - 2t^*\right)$$
(4.23)

where t* is the time of the control input reversal
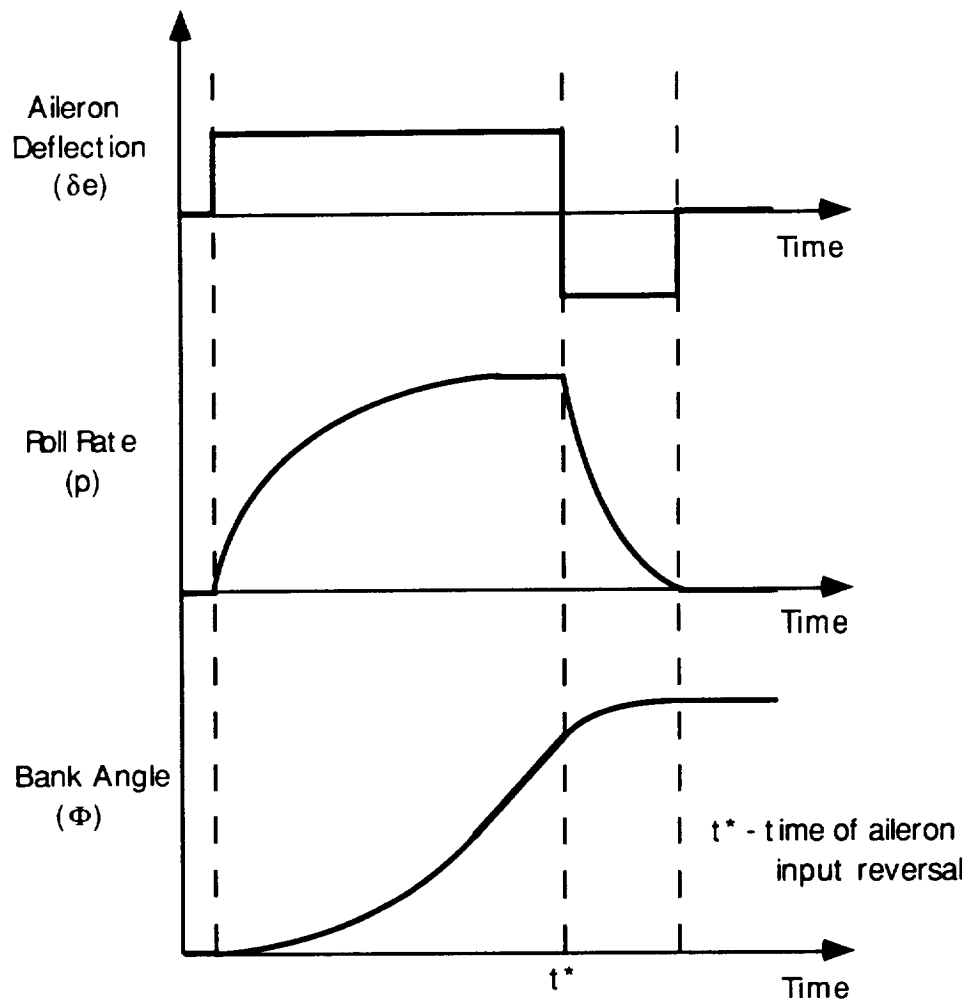
Figure 4.5

Illustration of a Typical Roll Maneuver

Pitch Segments

The pitch equations of motion were standard two degree of freedom short-period approximation equations as developed in reference 10. The s-domain matrix for these two equations is:

$$\begin{bmatrix} sU_1 - Z_\alpha & -U_1 s \\ -\{M_{\dot{\alpha}}s + M_\alpha\} & s^2 - M_q s \end{bmatrix} \begin{Bmatrix} \dfrac{\alpha(s)}{\delta(s)} \\ \dfrac{\Theta(s)}{\delta(s)} \end{Bmatrix} = \begin{Bmatrix} Z_\delta \\ M_\delta \end{Bmatrix}$$

(4.24)

The dimensional derivatives for the above matrix were constructed from the standard stability derivatives. The stability derivatives were in turn calculated from parameters found in ACSYNT's existing code. Some of the parameters were obtained directly from ACSYNT while others were constructed through equations found in reference 11. These stability derivatives are:

$C_{L\alpha} \sim$ obtained directly from ACSYNT

$C_{M\alpha} \sim$ obtained directly from ACSYNT

$$C_{M\dot{\alpha}} = -2 \left[C_{L\alpha_h} \eta_h V_h \left(X_{ac_h} - X_{cg}\right)\left(\frac{d\varepsilon}{d\alpha}\right)_h + C_{L\alpha_c} \eta_c V_c\left(X_{ac_c} + X_{cg}\right)\left(\frac{d\varepsilon}{d\alpha}\right)_c \right] \quad (4.25)$$

$$C_{Mq} = -2\left[C_{L\alpha_h} \eta_h V_h\left(X_{ac_h} - X_{cg}\right) + C_{L\alpha_c} \eta_c V_c\left(X_{ac_c} + X_{cg}\right) \right] \quad (4.26)$$

In the last two equations, only effects from the horizontal tail (subscript h) and the canard (subscript c) are included.

Reference 10 resolves the short-period matrix into time responses for both angle of attack (α) and pitch angle (Θ). A typical pitch time response is shown in Figure 4.6 These time responses are for a step control deflection. The angle of attack starts at zero and

ends at the steady state angle of attack corresponding to the new control deflection. If the $\alpha(t)$ equation is considered as $\Delta\alpha(t)$, it can be used for starting angles of attack other than zero.

The single-step input control strategy is not, however, typically the way pilots perform pitch maneuvers. To improve the model the $\alpha(t)$ response equation was modified to include initial conditions for α and Θ. With these initial conditions included, the response to multi-step control deflections could be constructed. A multi-step input schedule would better model a pilot's variable control input.

The desired pitch control input is that which provides the quickest rotation from the starting load factor to the desired load factor. When both the single-step and multi-step control strategies were tested with this goal in mind, little difference in pitch response was noticed. Figure 4.7 illustrates the close resemblance of the pitch responses for both control strategies. Since the multi-step control strategy increased the code complexity without providing a significant improvement in the response model, this strategy was rejected.

The load factor during a pitch maneuver consists of two elements: steady state and dynamic. At any given point in time, the present angle of attack produces a lift force and thus a load factor. This represents the steady state element. There is, however, a dynamic load factor element due to the pitch rate. This element was found from reference 12. This text defines the dynamic load factor as:

$$n_{dyn}(t) = V_\infty\left(\dot{\alpha} - \dot{\Theta}\right) \qquad (4.27)$$

When a comparison was made between load factor histories with and without the dynamic element little difference was found. A sample load factor response with and without the dynamic element is illustrated in Figure 4.8. Since the dynamic load factor element complicated the pitch coding and provided little benefit, it was discarded from the pitch model.

The final form of the pitch model will now be restated. The pitch model consists of a transient angle of attack time response due to a step control input. The load factor resulting from this control input consists of only the steady state load factor due to the instantaneous angle of attack. This strategy provided a satisfactory pitch transient with the least complicated and fastest computer code.

Aircraft configurations were constrained to a pitch damping ratio of at least 0.7. If the configuration did not have this level of damping the derivatives Cm_q and $Cm_{\dot{\alpha}}$ were artificially increased to provide sufficient damping. This constraint was employed to approximate the effects of a flight control system that limits pitch overshoot.

Unstable configurations were also artificially constrained. To prevent the pitch equations from blowing up, the pitching moment slope $Cm\alpha$ was forced to be -0.1 or less. Again, this constraint was employed to approximate the effects of a flight control system. It was recognized that this method was very rudimentary. However, it

was decided to use this technique in conjunction with a warning flag in the output file as apposed to no pitch analysis for unstable aircraft at all.

This procedure was considered feasible for two reasons. First, the objective of the pitch maneuver is to move from one load factor to another and to generate a representative angle of attack response. Whether the angle of attack response is generated by a simple constraint as above, or by a dedicated flight control system design is immaterial from a preliminary design point of view. The end result would not differ significantly.

The second reason the pitch constraints were considered feasible is that in functional agility metrics, transient segments like pitch contribute little to the overall maneuver performance.

Nevertheless, metric analysis where pitch response is significant is not recommended for negatively stable configurations. Adequate analysis for these types of maneuvers will be possible when ACSYNT's planned Flight Dynamics Module is introduced.
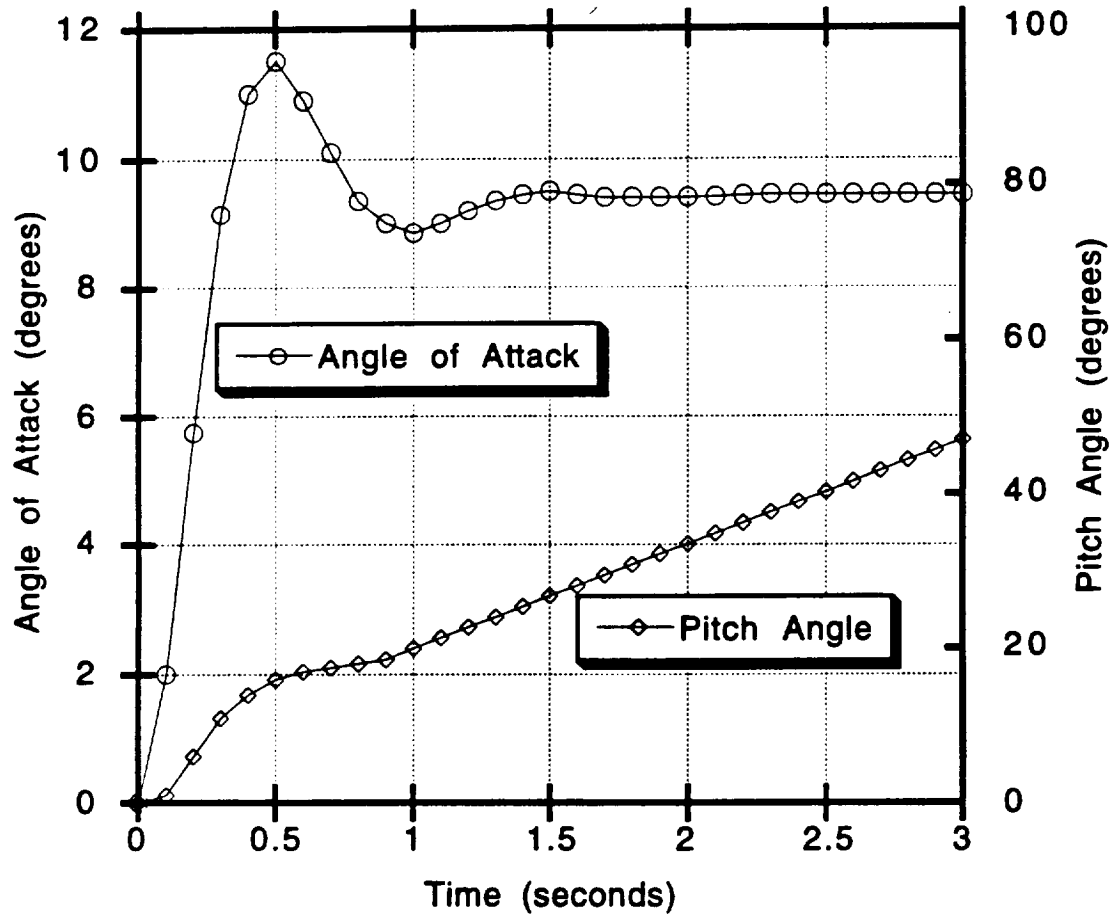
Figure 4.6

Typical Pitch Response to a
Step Elevator Deflection
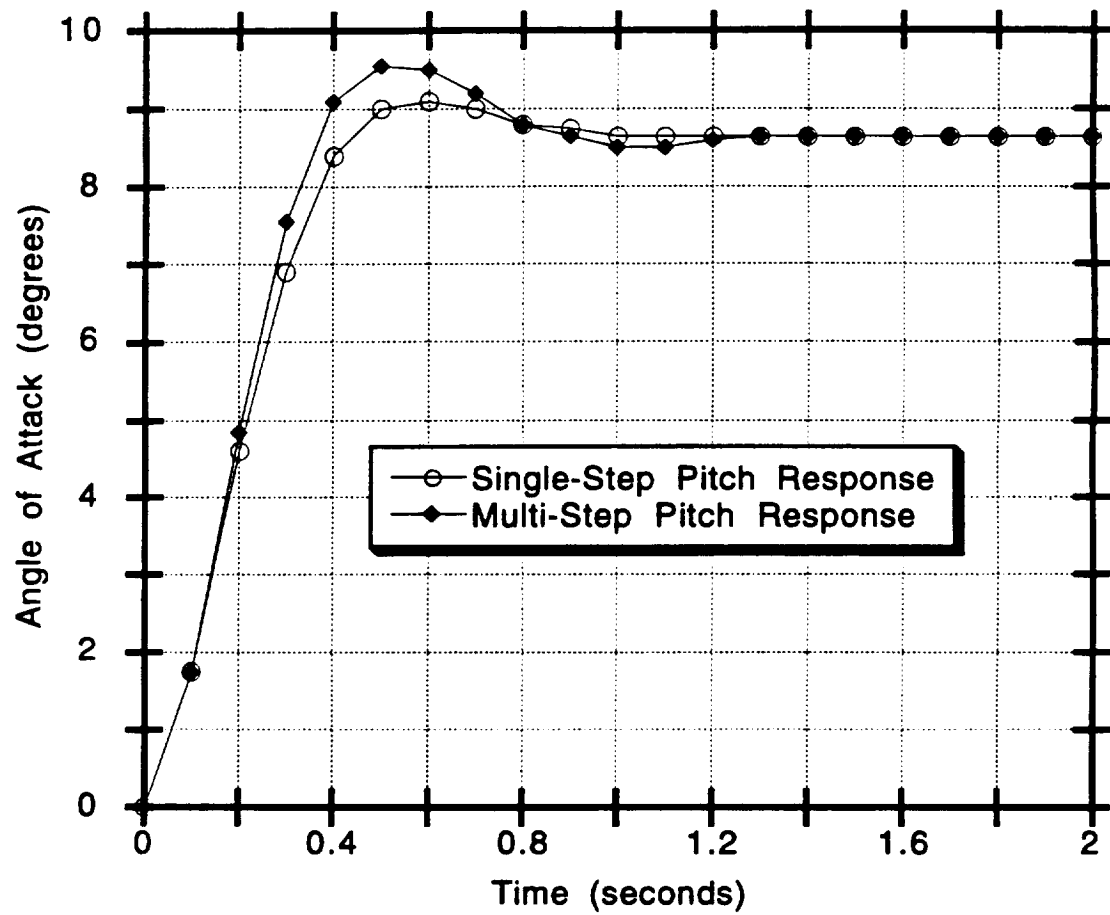
Figure 4.7

Comparison of Pitch Response Due to
Single and Multiple Elevator Deflections
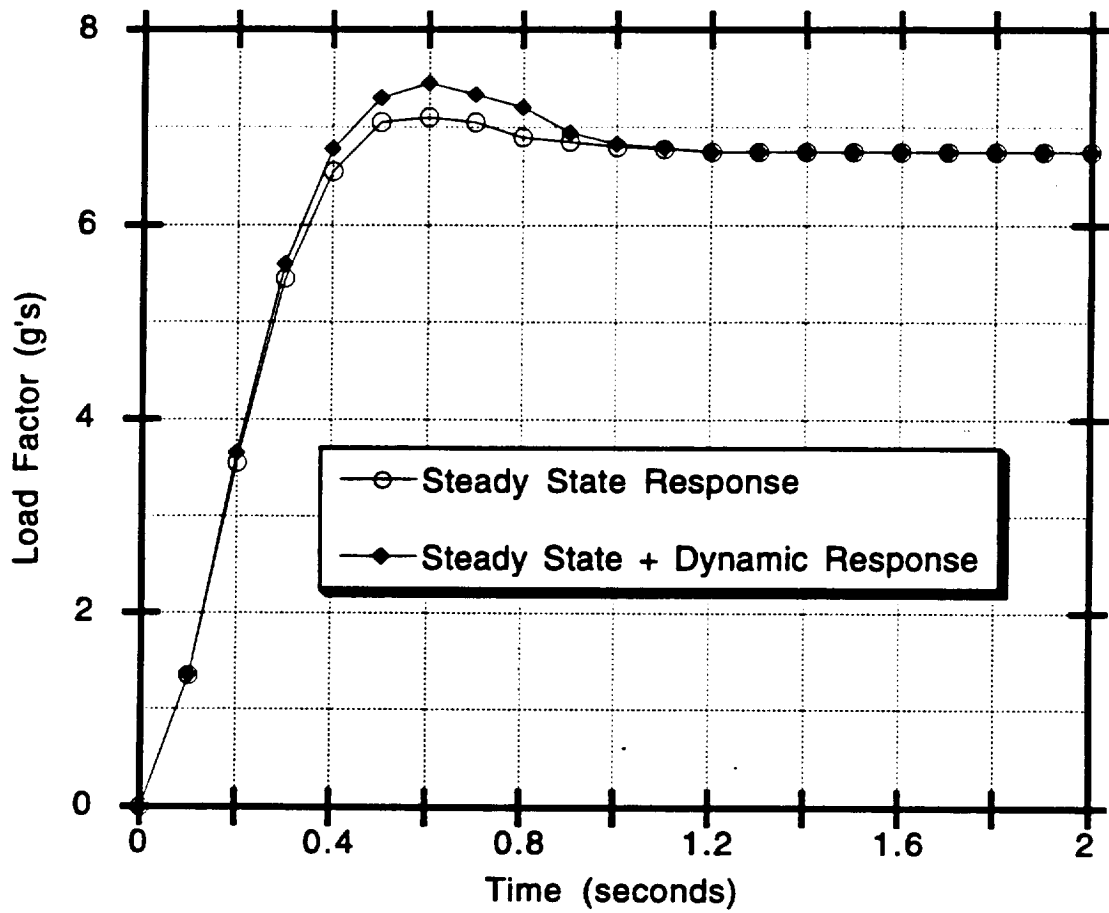
Figure 4.8

Load Factor Pitch Response With
and Without Dynamic Term

CHAPTER 5

ENGINE THRUST TRANSIENT DEVELOPMENT

The engine transient model was based on non dimensional data for a 1990 era low-bypass turbofan fighter engine. This data did not contain time responses for thrust changes from any thrust level to any thrust level, but instead, consisted of six particular throttle responses, these responses are included in Table 5.1.

Table 5.1

Throttle Response Time Histories Obtained from Contemporary Fighter Engine for Use in the Agility Module

Max afterburner -> Flight idle	Max afterburner -> Max dry
Max dry -> Flight idle	Flight idle -> Max dry
Flight idle -> Max afterburner	Max dry -> Max afterburner

Figure 5.1 illustrates the time histories of these six throttle responses. At any time step, the commanded power level may be changed by code logic. When this occurs the proper throttle response curve is enacted to provide a time history of the engine transient.

Throttle changes do not always fit one of the six throttle responses. The throttle change may start or end at a partial throttle

40

setting instead of max A/B, max dry or flight idle. In this case, the code begins its time history in the middle of the appropriate response curve. Figure 5.2 illustrates an example of this technique. The main drawback to this method is that engine response lag is not represented in a throttle change beginning at fifty percent dry power for example. Instead of an initial lag, the power increases rapidly right from the beginning of the throttle change. In reality, there would be response lag irregardless of the starting throttle level. However, information on the engine transients was limited to the six time of response curves so this method was employed.
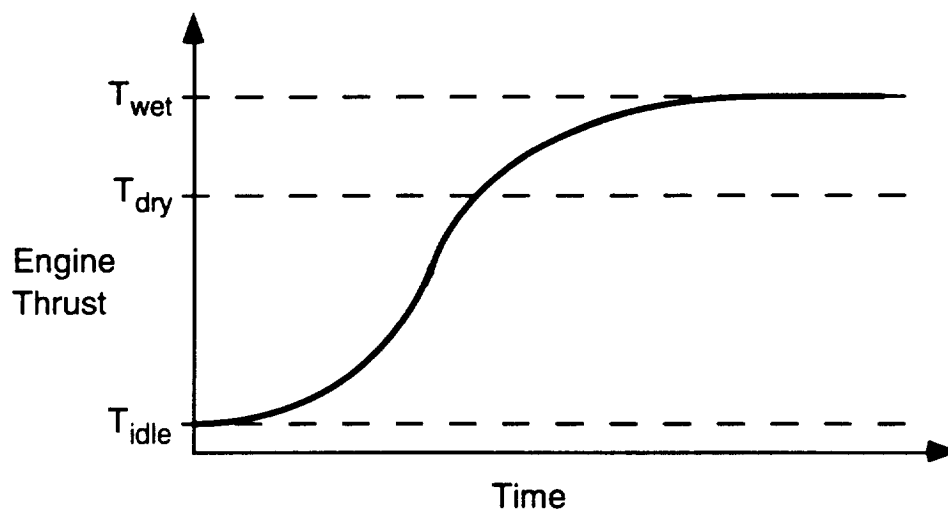
Figure 5.1a

Throttle Transient Response from
Flight Idle to Maximum Afterburner
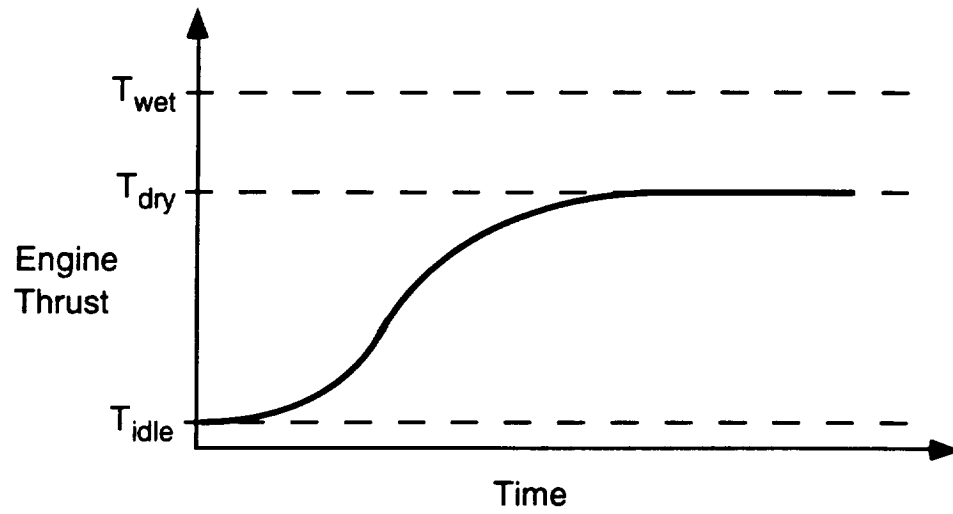
Figure 5.1b

Throttle Transient Response from
Flight Idle to Maximum Dry Thrust
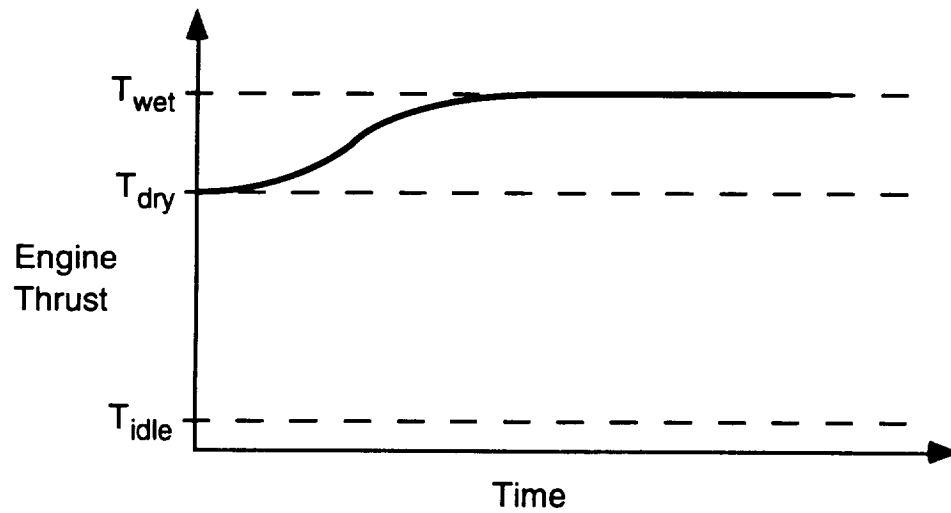
Figure 5.1c

Throttle Transient Response from
Maximum Dry Thrust to Maximum Afterburner
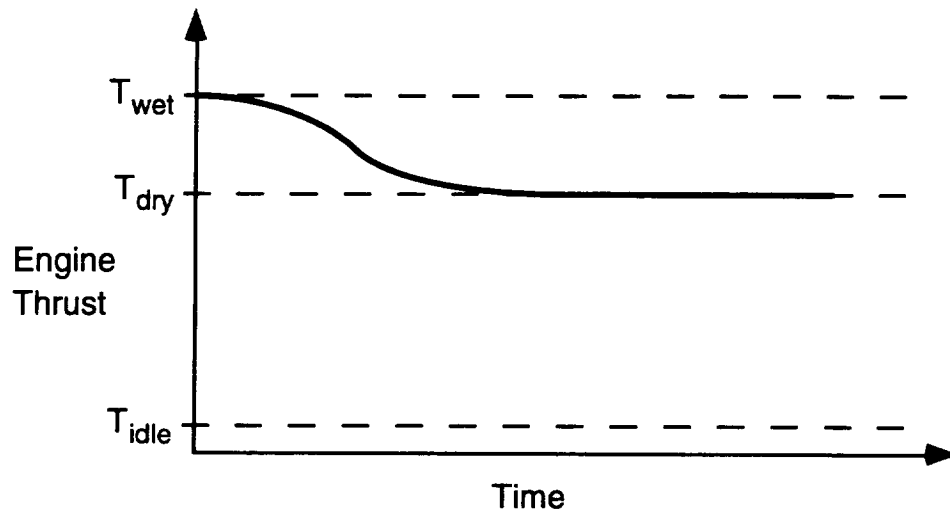
Figure 5.1d

Throttle Transient Response from
Maximum Afterburner to Maximum Dry Thrust
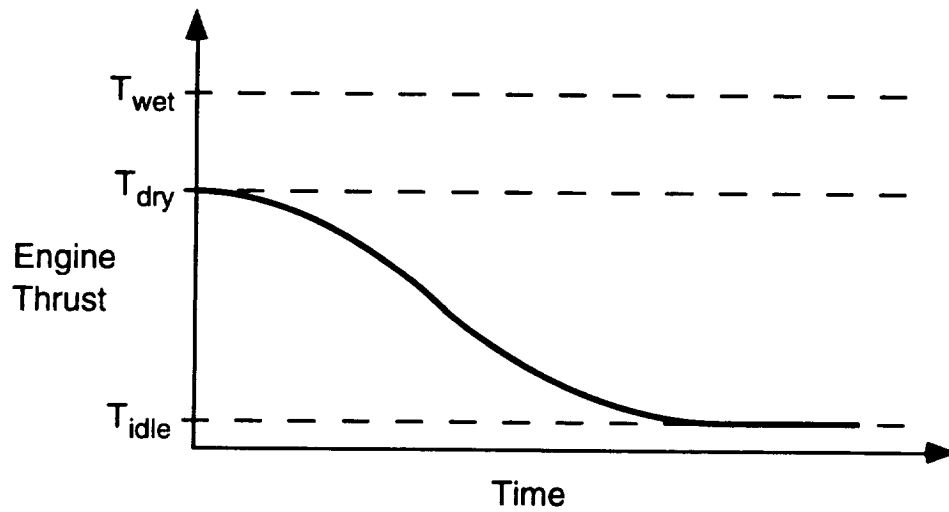
Figure 5.1e

Throttle Transient Response from
Maximum Dry Thrust to Flight Idle
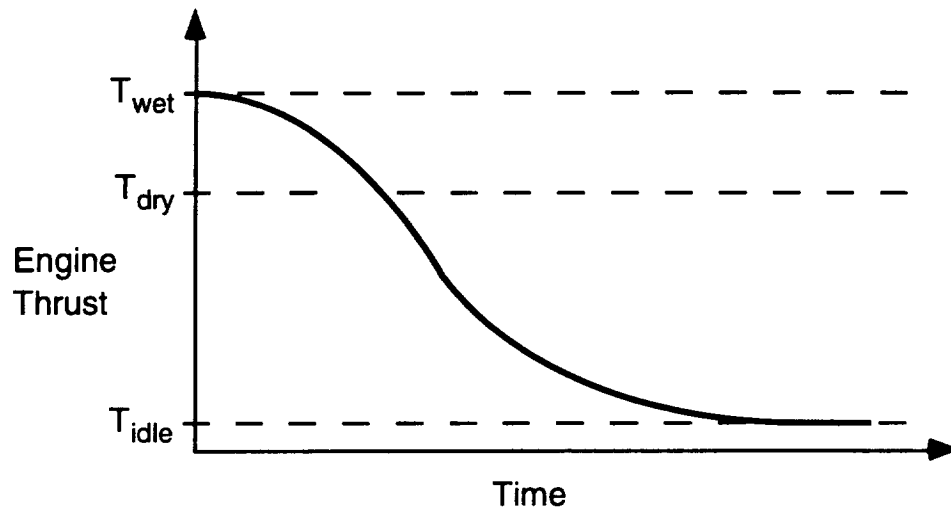
Figure 5.1f

Throttle Transient Response from
Maximum Afterburner to Flight Idle
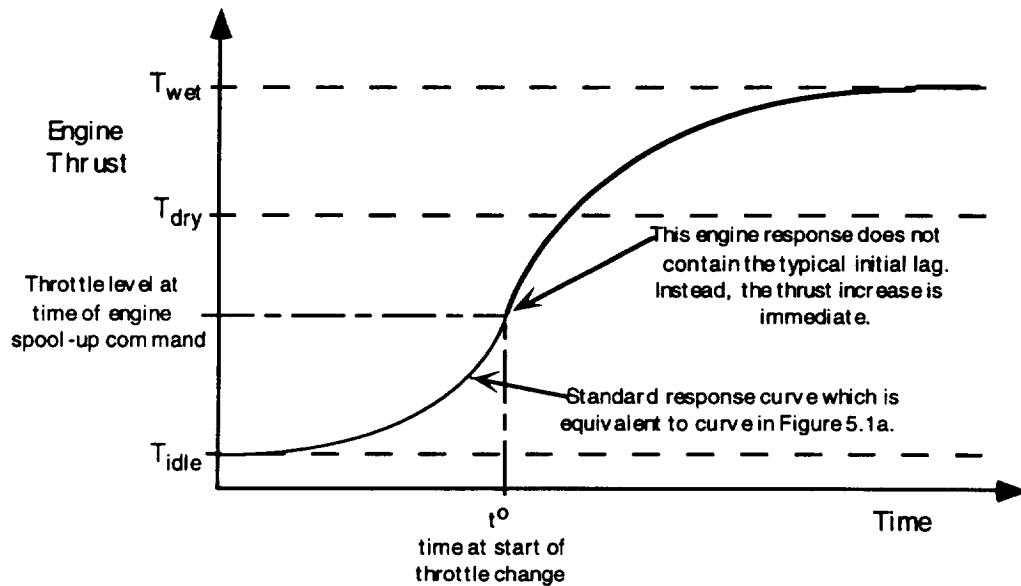
Figure 5.2

Throttle Transient Response Starting from
Partial Dry Throttle up to Maximum Afterburner

CHAPTER 6

CODE OPTIONS AND FEATURES

This chapter describes some of the operating features and simulation techniques used to conduct the aircraft through an agility maneuver. The following sections describe how the simulation package conducts agility maneuvers and how users may manipulate input parameters to customize these maneuvers.

Angle of Attack Limiting

The user has control of the maximum angle of attack allowable during metric maneuvers. This limit provides a reference for determining maximum lift coefficient. ACSYNT's aerodynamic module does not calculate a discrete stall angle of attack. Figure 6.1 illustrates a typical lift curve slope from ACSYNT. The lift slope curve does not exhibit an identifiable stall break. Instead, the slope of the curve gradually reduces to zero at extreme angle of attack. Without an obvious stall point, the definition of maximum lift coefficient is difficult to pinpoint. The inclusion of a user defined angle of attack limit provides a reference for determining maximum lift coefficient. Therefore, the angle of attack limiter is not a user option, but a necessary input.
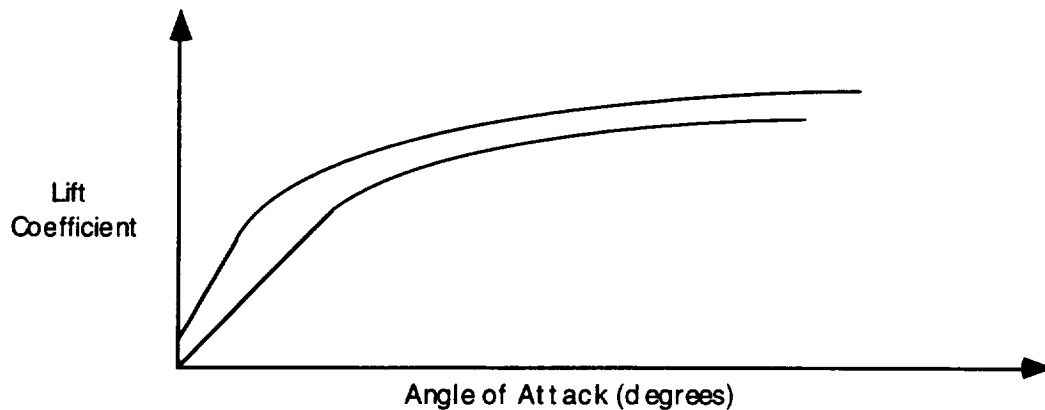
Figure 6.1

Typical Lift Curves Generated By ACSYNT

Definition of Turning Speed

The simulation package is set up to maintain a desired airspeed, determined by the code, called turning speed. This logic is incorporated to keep the maneuvering aircraft in the most favorable Mach number regime for high turn rates. There are two ways that the code specifies turning speed. Which of these methods the code uses to calculate turning speed depends on user input.

The primary definition of turning speed is similar to that of corner speed discussed in Chapter 2. The turning speed is the Mach number corresponding to the intersection of the lift-limit curve and the load-limit curve of the doghouse plot in Figure 2.1. However, the load-limit curve for turning speed does not correspond to the maximum design load factor as is the case for corner speed. Instead, the load-limit curve corresponds to the load factor specified by the user for the turn maneuver. This makes the turning

speed a variable. The turning speed for a 7g turn will be higher than that for a 4g turn. Figure 6.2 shows, for the same aircraft, various turning speeds for different turning load factors.

The second definition of turning speed is simply a Mach number input by the user. This allows complete control over what Mach number the code will try to capture. The advantage of this capability is illustrated in the following example.

Suppose a 4g turn was desired with an entry speed of Mach 0.9. From the angle of attack limit and the 4g load factor, the code calculates the turning speed to be Mach 0.35. For the Combat Cycle Time metric it would not be desirable for the code to decelerate the aircraft down to Mach 0.35 for the turn. Although the turn rate would be increasing and the turn would be completed earliest, the re-acceleration phase would be much longer. To minimize total time it would be best to turn at a higher airspeed. The lower turn rate would lengthen the turn segment, but the acceleration back to Mach 0.9 would be much shorter for an overall quicker cycle time. Thus, allowing the user to set the turning speed at Mach 0.65 or so, a better maneuver performance can be achieved.
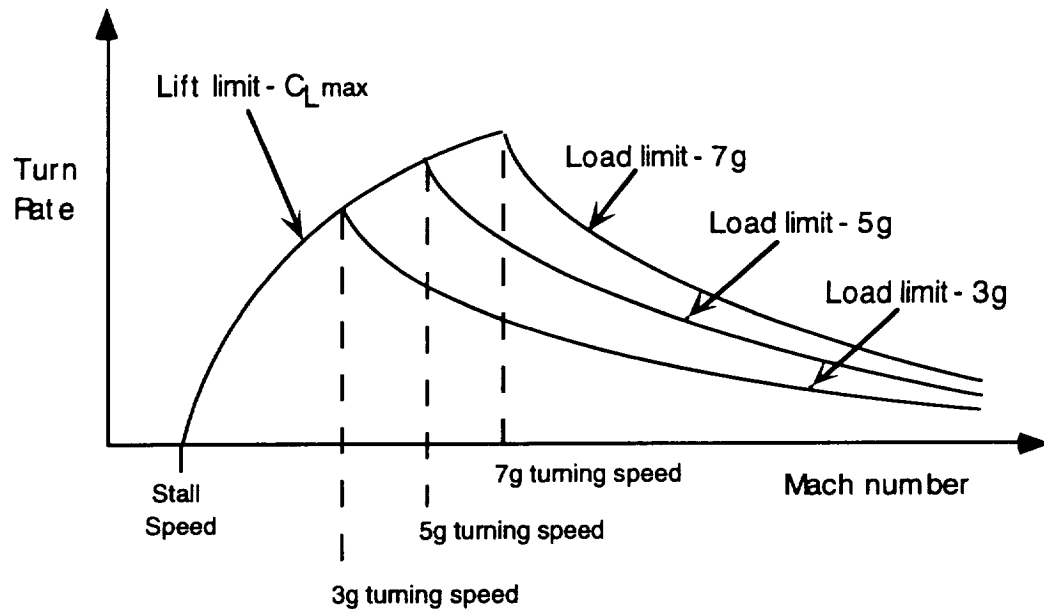
Figure 6.2

Variation of Turning Speed
With Turning Load Factor

Throttle Control and Turning Speed Capture

The simulation package maintains turning speed through throttle manipulation. In order to achieve this the user inputs throttle settings that refer to the throttle power settings discussed in Chapter 5. There are two throttle settings for each maneuver segment; one setting is for airspeeds above turning speed and the other for airspeeds below turning speed. By commanding a low power level for the above-turning-speed throttle setting, the aircraft can be controlled to decelerate back down to turning speed. Conversely, by commanding a high power level for the below-turning-speed throttle setting, the aircraft can be controlled to

accelerate back up to turning speed. Figure 6.3 illustrates how the code switches throttle commands during acceleration and deceleration through turning speed.
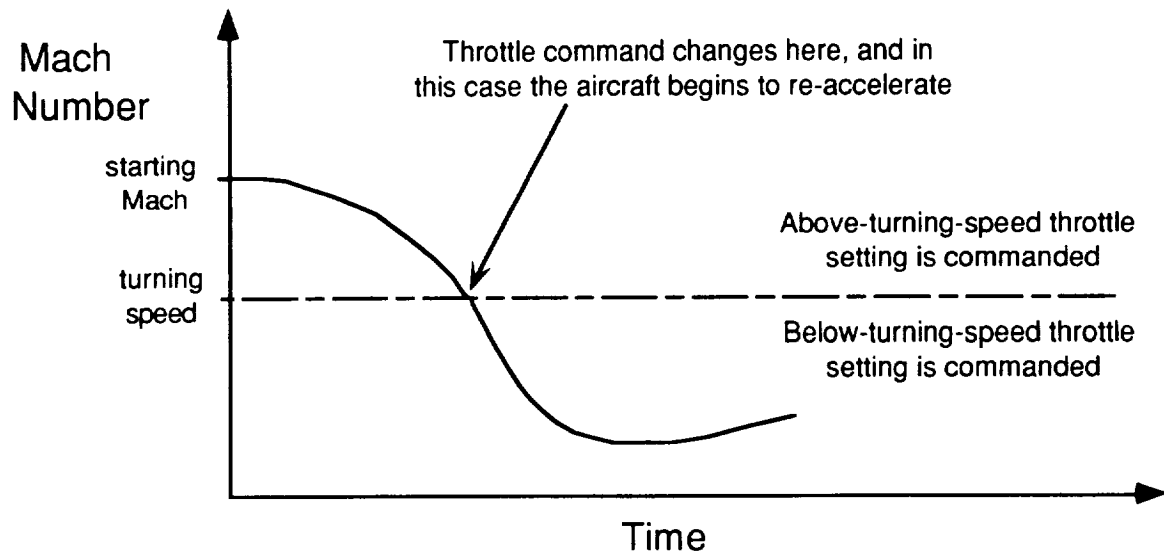
Figure 6.3

Illustration of Throttle Control Logic as
Aircraft Passes Through Turning Speed

Another input parameter can be used to alter the throttle command technique described above. This parameter is called MLEAD (Mach number LEAD). The value of MLEAD is used as a buffer zone around the turning speed. It causes the code to change throttle settings before the turning speed is actually achieved. In this way MLEAD serves as a pilot's anticipation of the approach of turning speed and his early throttle change. Figure 6.4 shows how the

parameter MLEAD affects the throttle command schedule. When the aircraft's Mach number is above turning speed+MLEAD, the above-turning-speed throttle command is selected. When the aircraft's Mach number is below turning speed-MLEAD, the below-turning-speed command is selected. In the region between these two Mach numbers (turning speed+MLEAD and turning speed-MLEAD) the throttle is changed to whatever thrust level is required to sustain the turning speed at the desired load factor. If the turn is not sustainable then the thrust is set at the maximum afterburning setting.

MLEAD>0: (**bold plot**) throttle changes at P1, and in this example, turning speed is better captured by the early throttle change

MLEAD=0: (thin plot) throttle changes at P2 (right at turning speed) which results in poor capture
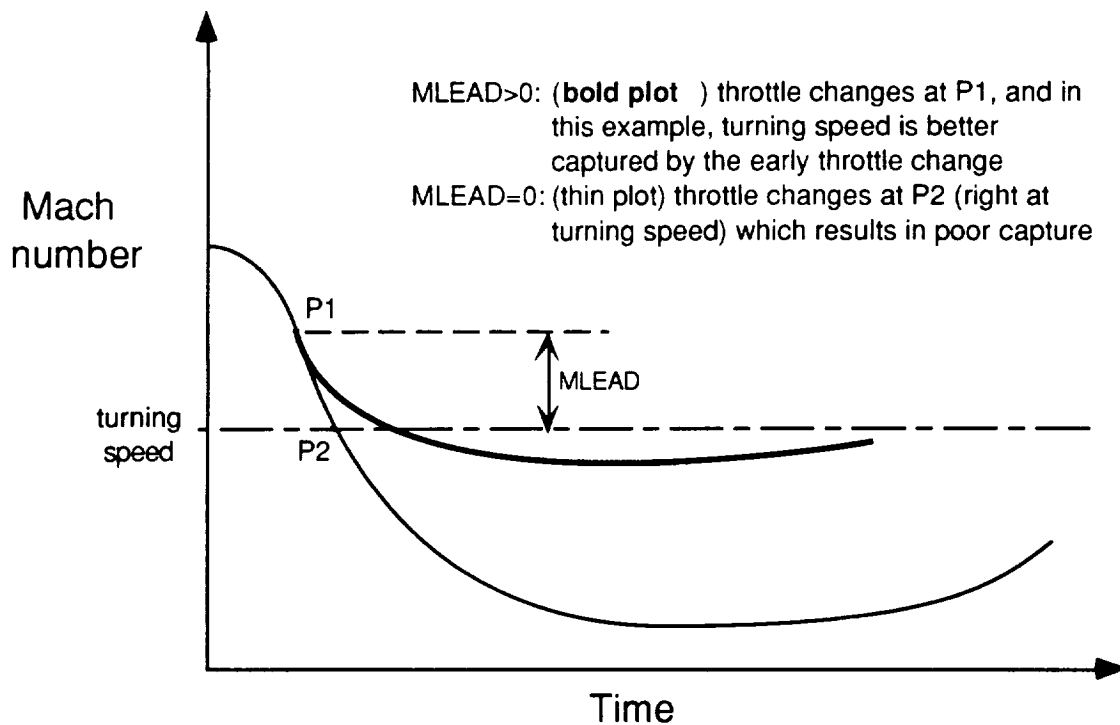
Figure 6.4

Illustration of Throttle Control Logic When
the MLEAD Parameter is Employed

Thrust Vectoring

The thrust vectoring capability of the agility module does not include pitch control thrust-vectoring. Instead it includes the ability to rotate the thrust vector out of the fuselage axis yet remain centered at the aircraft's center of gravity. This is intended to model the in-flight direct-lift capability of aircraft such as the Hawker Siddeley Harrier and McDonnell Douglas AV-8B. This capability allows the aircraft to generate some of the turning load factor through the engine. This results in higher turn rates for a

given aerodynamic load factor. However, this reduces the aircraft's ability to combat drag since the axial component of thrust is reduced.

The thrust vector angle (λ) is defined as the angle between the aircraft's fuselage axis and the thrust vector. Figure 4.3 illustrates the thrust vector angle definition. The angle can range any where from zero to one-hundred-eighty degrees. The transition rate ($\dot{\lambda}$) is another user input, and the transition is modeled linearly.

The user has control over the thrust vector angle during each maneuver segment. Each segment has two vector inputs, one setting for operation above turning speed and one for operation below turning speed. This two-setting technique for each segment allows the user to better model a pilot's control technique than a simple single setting would. Similar to the throttle control, the two-setting thrust vector control also assists in maintaining the aircraft's turning speed.

Air brake

The code user has the option of employing an airbrake during metric maneuvers. The user inputs an equivalent flat plate area for the extended airbrake and this drag is included with the aircraft's clean drag. Once the airbrake option is selected, the control and operation of the airbrake is automatic. The airbrake is automatically extended when the aircraft is flying above turning speed and, conversely, the airbrake is automatically retracted when the aircraft is below turning speed. The retraction sequence was

assumed to be instantaneous and retraction or extension occurs over one time-step.

External Stores Release and Weight/Moment of Inertia Control

At the start of an agility metric, the user specifies the desired percent fuel load. This percent includes both the internal and any external fuel the aircraft may be carrying. In addition, the user specifies the external stores and ammunition loading of the aircraft. The weight and drag of these stores is specified in the weight and aerodynamic input files of ACSYNT. The moment of inertia for the aircraft with pylons, as well as the incremental moments of inertia for fuel and stores is specified in the agility input file.

During any of the following maneuver segments the agility module has the capability of dropping stores. Each segment contains logical drop flags for four types of stores; missiles, bombs, external fuel tanks, and ammunition.

A segment's drop flags cause the store's weight and moments of inertia to be subtracted from the aircraft's. In addition, the additional drag due to these stores is also subtracted from the aircraft. The change in weight and moments of inertia as commanded by a segments drop flags is activated at the end of the maneuver segment.

When the user inputs the dimensional derivatives for the roll maneuver segment they must be referenced to a moment of inertia. For the agility module, they must be referenced to the moment of

inertia of the clean aircraft without fuel and without stores. In addition, the incremental moments of inertia due to the individual stores and fuel must be entered. With this information the code ratios the dimensional derivatives to account for the changes in weight and moments of inertia. The roll response is thus dependent on the aircraft fuel and stores loading.

CHAPTER 7

CODE VERIFICATION

Code verification consisted of two phases. The first phase was to test code logic and to ensure continuous, believable time histories of the tracked variables. This phase tested mainly the integrity of the code. The second phase was to compare the agility module's maneuver analysis with the combat analysis capability already contained in ACSYNT's trajectory module. This phase would ensure that the agility module was retrieving aerodynamic and propulsive data properly and that the physical equations used for maneuverability analysis (equations 4.4, 4.14 and 4.17) are at least consistent with an independent performance package NASA has used for years.

The combat analysis in ACSYNT's trajectory module generates the sustained and instantaneous turn rates, turn radii, specific excess power and lift and drag coefficients for a given Mach number and altitude. This information allows comparison of these parameters with the agility calculations at an isolated time step.

A third verification phase that was not performed would be to compare the agility analysis with actual flight test data for a specific fighter aircraft. The reasons this was not conducted are twofold. First, obtaining the type of information required to perform a reasonable comparison was extremely difficult. Most aircraft data consisted of the type described above: sustained and instantaneous turn rates, turn radii, specific excess power for a

given Mach number and altitude. Information on how long it took to perform an actual turn was not found. The second reason this phase was not conducted was that the agility module relies entirely on the aerodynamic and propulsion modules for information. Any discrepancy in the aerodynamic or propulsive model would manifest itself in the agility analysis.

Thus the verification was limited to the first two methods described. The following two sections detail these verification procedures.

Continuity of Tracked Variables

The first step in validating the code was to ensure that all tracked parameters were continuous over the logical operating range of the input parameters. Various maneuver segment sequences were conducted to verify that the tracked variables remained continuous through multiple turns, and various pitch and roll maneuvers.

In addition, the code features described in Chapter 6 were tested thoroughly. The angle of attack limiter, airbrake, turning speed capture and thrust-transient model all performed as designed. All glitches found were corrected and from this verification phase the integrity of the coding technique was considered satisfactory.

Agreement With ACSYNT's Combat Analysis

The second phase of verification involved coordinating the agility module maneuvers with the combat phase analysis in the trajectory module. Verification consisted of comparing the agility

module's sustained and instantaneous turn rates, radii, excess powers, angles of attack and lift and drag coefficients with those of the trajectory module. This correlation was performed over a range of Mach numbers that covered both lift limited and load limited flight regimes. Tables 7.1 through 7.3 catalog the comparison data and the descrepancies. The greatest deviation was found to be three percent. The source of this small error was attributed to roundoff error. As an example, information from the trajectory module at Mach 0.73 were compared to agility information at Mach 0.735. This was about as close of a Mach number correlation as could be performed. The agreement nevertheless was considered excellent and proof of the codes validity in determining maneuver performance at an isolated time step.

From the above discussion it may sound like ACSYNT can already do what the agility module does. However, the combat analysis in the trajectory module conducts its analysis at a frozen instant in time. The agility module performs these calculations for consecutive time steps and calculates the resulting kinematics between these time steps. In this sense it flies the aircraft through a maneuver and tracks the pertinent parameters for agility analysis.

The verification procedures indicated that the agility module performs time dependent maneuverability analysis properly. This procedure also indicates that the time-stepping simulation package is an effective method of tracking an aircraft's performance throughout a manuever.

Table 7.1

Correlation of Agility Module Parameters with Parameters

Calculated in COMBAT Phases of the Trajectory Module at Mach 0.73

Altitude:	15,000 feet		
Parameter	**COMBAT (ACSYNT)**	**Agility Module**	**Percent Difference**
Mach number	.730	.735	0.68%
Angle of attack	15.0	15.0	0%
Load factor	6.87	6.97	1.46%
Turn rate	16.24	16.4	0.99%
Lift coefficient	1.196	1.198	0.17%
Drag coefficient	.3986	.4060	1.86%
Specific excess power	-1,094	-1,119	2.29%
Turn radius	2,723	2,711	0.44%

Table 7.2

Correlation of Agility Module Parameters with Parameters
Calculated in COMBAT Phases of the Trajectory Module at Mach 0.68

Altitude:	15,000 feet		
Parameter	COMBAT (ACSYNT)	Agility Module	Percent Difference
Mach number	.680	.676	0.59%
Angle of attack	9.79	9.93	1.43%
Load factor	4.09	4.09	0.0%
Turn rate	10.18	10.40	2.16%
Lift coefficient	0.820	0.8279	0.96%
Drag coefficient	.1631	.1668	2.27%
Specific excess power	0	-7.19	N.A.
Turn radius	4,047	3,928	2.94%

Table 7.3

Correlation of Agility Module Parameters with Parameters

Calculated in COMBAT Phases of the Trajectory Module at Mach 0.53

Altitude:	15,000 feet		
Parameter	**COMBAT (ACSYNT)**	**Agility Module**	**Percent Difference**
Mach number	.530	.534	0.75%
Angle of attack	15.0	15.0	0%
Load factor	3.47	3.52	1.44%
Turn rate	10.93	11.02	0.82%
Lift coefficient	1.119	1.121	0.18%
Drag coefficient	.3458	.3540	2.37%
Specific excess power	-176	-181	2.84%
Turn radius	2,937	2,896	1.40%

CHAPTER 8

EXAMPLE STUDIES

In this chapter the influence of two parameters, thrust loading and wing loading, on the Combat Cycle Time metric are investigated. In addition, an example using the COPES optimization code in conjunction with ACSYNT to optimize the wing loading and thrust loading for minimum gross takeoff weight is presented. These studies are intended to illustrate how the agility module may be used to ascertain and optimize an aircraft configuration's agility potential. The two parameters were chosen because they are fundamental in classical energy maneuverability analysis. In these studies however, the new agility metric analysis will show that aircraft that appear to have similar energy maneuverability performance levels can have quite different levels of agility; at least as agility is defined by the Combat Cycle Time metric.

The baseline aircraft used for the studies was a fighter aircraft similar to a Northrop F-20 Tigershark. A three-view of this aircraft is shown in Figure 8.1. The weights, external dimensions and installed thrust were matched to obtain a representative fighter model. More information on this model is contained in the appendix.

The metric studied was Combat Cycle Time as defined in Chapter 2. The maneuver used for this metric was a 7g turn through 180 degrees at an altitude of 15,000 feet. The aircraft began the maneuver in straight and level flight at Mach 0.9. The values for other pertinent input parameters are also contained in the appendix.
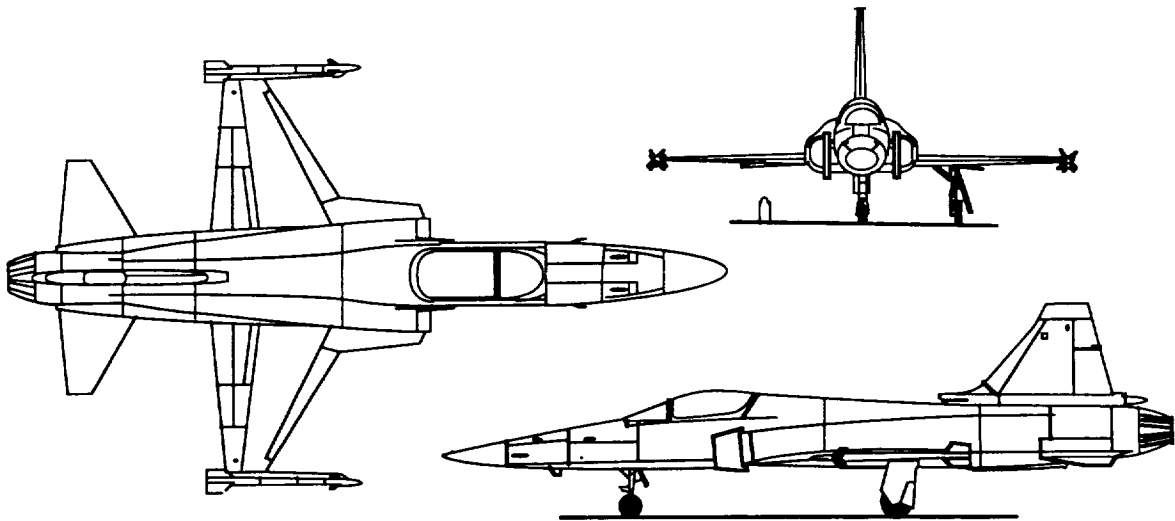
Figure 8.1

Northrop F-20 Tigershark Three View

Effect of Thrust Loading on Combat Cycle Time

This section illustrates how the ACSYNT agility module can be used to study the influence of an aircraft's thrust-to-weight ratio on the Combat Cycle Time (CCT) metric.

The Combat Cycle Time maneuver was performed using the baseline fighter configuration. For comparison, four other configurations were flown through the same maneuver. These configurations were altered only in the available level of thrust. The thrust levels were specified as a percentage of the baseline configuration's available thrust. The four percentages were 80%, 90%, 110%, and 120%. These choices were selected to bracket the baseline configuration. The full power thrust loading of the baseline

configuration was 0.94. For the 80% and 120% thrust aircraft this corresponded to thrust loadings of 0.75 and 1.13 respectively.

Although only the thrust level was changed and all other input parameters were held constant, convergence of each aircraft during ACSYNT execution resulted in slight variation in aircraft weight. This resulted in a maximum difference in wing loading of 78.3 for the 80% thrust configuration and 78.5 for the 120% configuration.

Figure 8.2 illustrates the time differences for each segment of the CCT maneuver for all five configurations. As would be expected, the highest thrust aircraft performed the maneuver in the least amount of time. The maneuver times also steadily decreased with increased available thrust. However, inspection of the separate maneuver segments reveals that the lowest thrust aircraft completed the turn segment slightly quicker than the higher thrust aircraft. Again this trend is consistent for all five aircraft; each turned slightly quicker than the next higher thrust aircraft and slightly slower than the next lowest thrust aircraft. The reason for this phenomena can be explained by looking at the time histories of Mach number and turn rate for the five aircraft.

Figure 8.3 plots the Mach number over the course of the CCT maneuver for the five configurations. The initial acceleration of each configuration is due to the engine spool-up at the start of the maneuver. Once the aircraft has completed the roll into the turn and has pitched up to the turning load factor the increased induced drag overpowers the thrust increase and the aircraft begin to decelerate.

The greatest deceleration naturally corresponds to the aircraft with the least available thrust (80%). As the available thrust increases up to 120%, the peak velocity deficit is reduced. The reduced velocity deficit coupled with the more powerful engine created significantly shorter acceleration times for the higher thrust configurations.

The turning speed for the five aircraft was Mach 0.74. Over the course of the turn only the 80% thrust configuration crossed this speed. The 90% thrust configuration barely reached turning speed just as it ended its turn. Recalling that the turning speed is where an aircraft can generate its highest turn rate, it is understandable why the lower thrust aircraft completed their turns sooner. Their higher decelerations placed them in speed regimes with higher turn rates than the greater thrust aircraft and thus were able to achieve superior turns.

The turning performance is evident in the plots of turn rate versus time in Figure 8.4. The lower thrust aircraft indeed have a higher turn rate at any given time and thus out turn the higher thrust configurations. It was observed that only the 80% thrust configuration achieved turning speed. This can be seen in the turn rate plot. The 80% thrust configuration reaches a peak turn rate around 12.5 seconds. After this the turn rate drops off as the aircraft decelerates past turning speed. At this time the aircraft is lift limited and cannot aerodynamically generate the full seven g's. This would suggest that during a continued turn through 270 or 360 degrees the lower thrust aircraft would lose its turning advantage

and fall behind the higher thrust configurations. In addition, if the starting velocity were below the turning speed, the higher thrust aircraft would be better able to accelerate to and maintain the turning speed. It is situations like this that make the development of agility criteria so difficult. The optimum configuration can be entirely dependent on the specific situation.

An additional comment on Figure 8.4 is the overshoot evident at the end of the pitch up (t=3 seconds) and pitch down (t=15 seconds) segments. These are due to the dynamic response model of the pitch maneuvers. Although a minimum damping level was specified there was still some overshoot.

Figure 8.5 illustrates the turn profile in the horizontal plane of the maneuver. These plots are what the jet contrails of the aircraft would look like to an individual watching overhead. The lower thrust configurations turn tighter and possess a positional advantage over the course of the turn segment. However, as the aircraft accelerate back to the starting velocity the lower thrust aircraft take longer and by the time the maneuver is completed they have lost their positional advantage.

Figure 8.6 shows the load factor of the five configurations over the time of the maneuver. The main interest in this figure is to note the consistency of all five configurations. Each aircraft follows almost exactly the same curve over the course of the maneuver. From this graph, which is a typical of traditional maneuverability analysis, the configurations appear to have the same level of performance. However, as previous figures and

discussion illustrate, the performance of these configurations is not identical. It is the time dependent performance of the configurations that conveys their agility potential; at least as far as defined by the Combat Cycle Time metric.

What is the overall conclusion of the impact of thrust loading on Combat Cycle Time? It depends entirely on what is considered most important. For the specific maneuver studied, the lower thrust configurations possessed a positional advantage up to the end of the turn segment. After this, the advantage was lost and the higher thrust aircraft possessed the advantage. For time considerations the higher thrust aircraft appeared to win across the board. For longer turns of 360 degrees, the lower thrust aircraft would most certainly lose. The general consensus would probably lean toward increased thrust. However, the study has alluded to the tradeoff of what type of performance is most crucial and what are its costs.
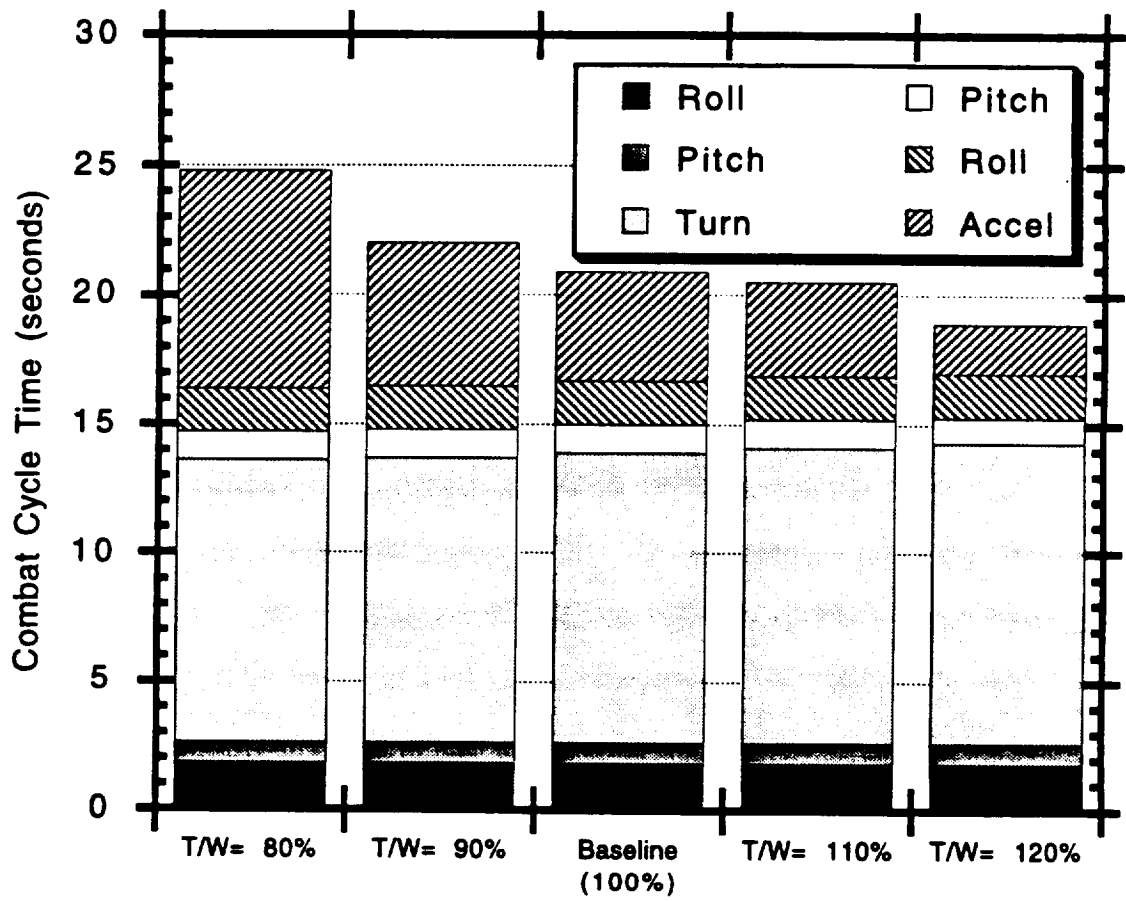
Figure 8.2

Combat Cycle Time Variation

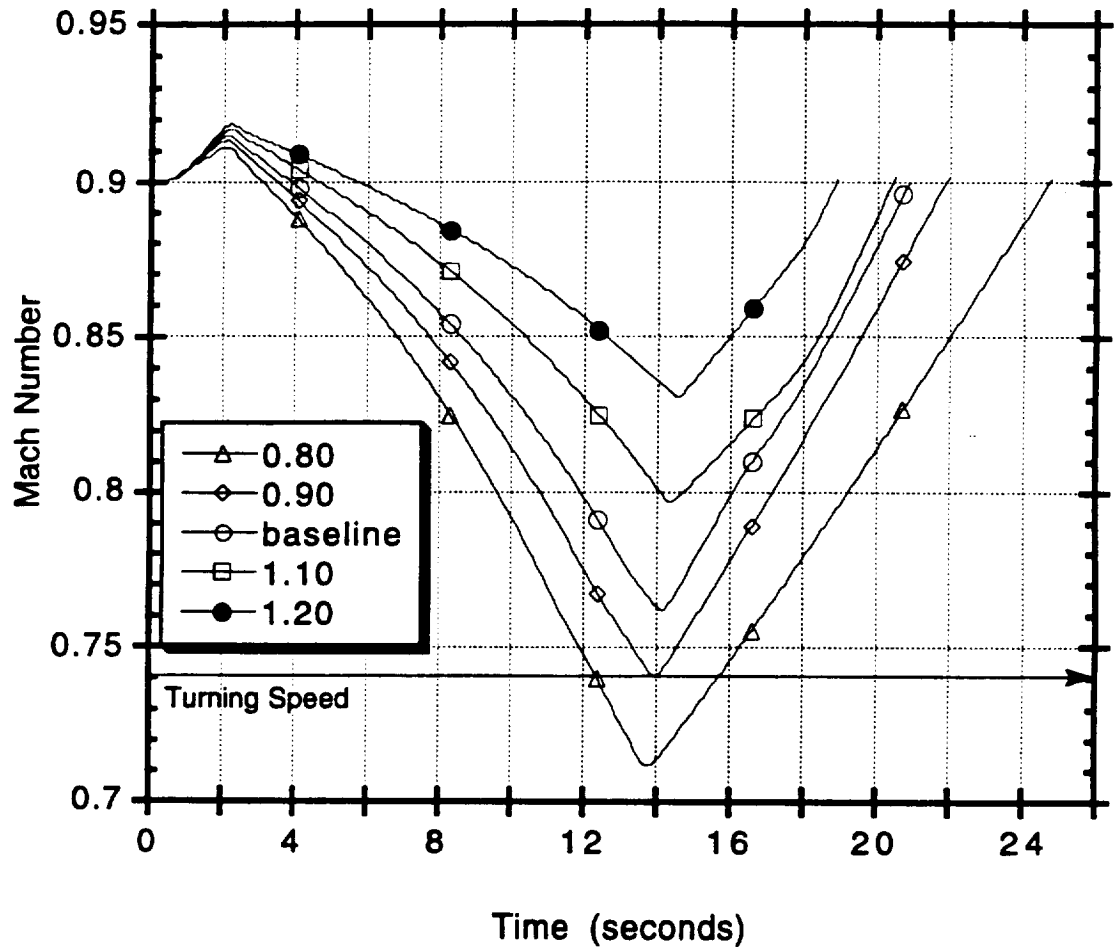for Different Thrust Loadings

Figure 8.3

Mach Number Time Histories
for Different Thrust Loadings
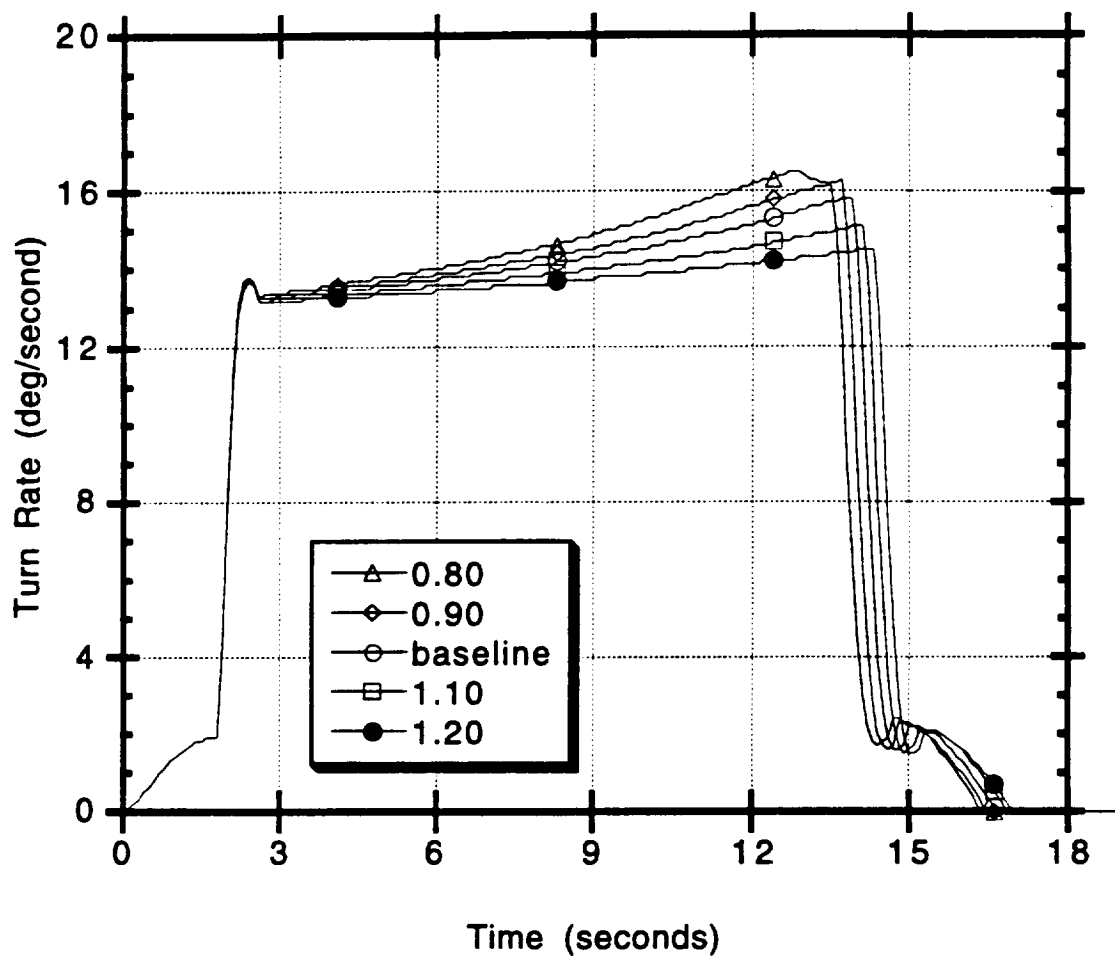
Figure 8.4

Turn Rate Time Histories

for Different Thrust Loadings
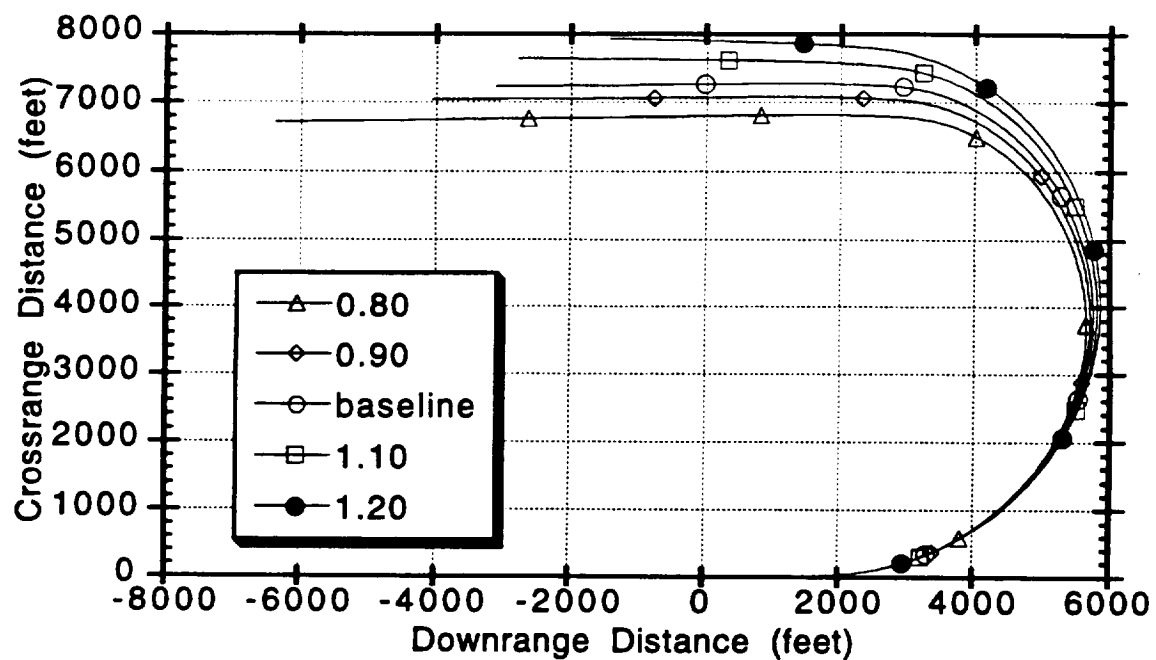
Figure 8.5

Horizontal Plane Turn Diagrams

for Different Thrust Loadings
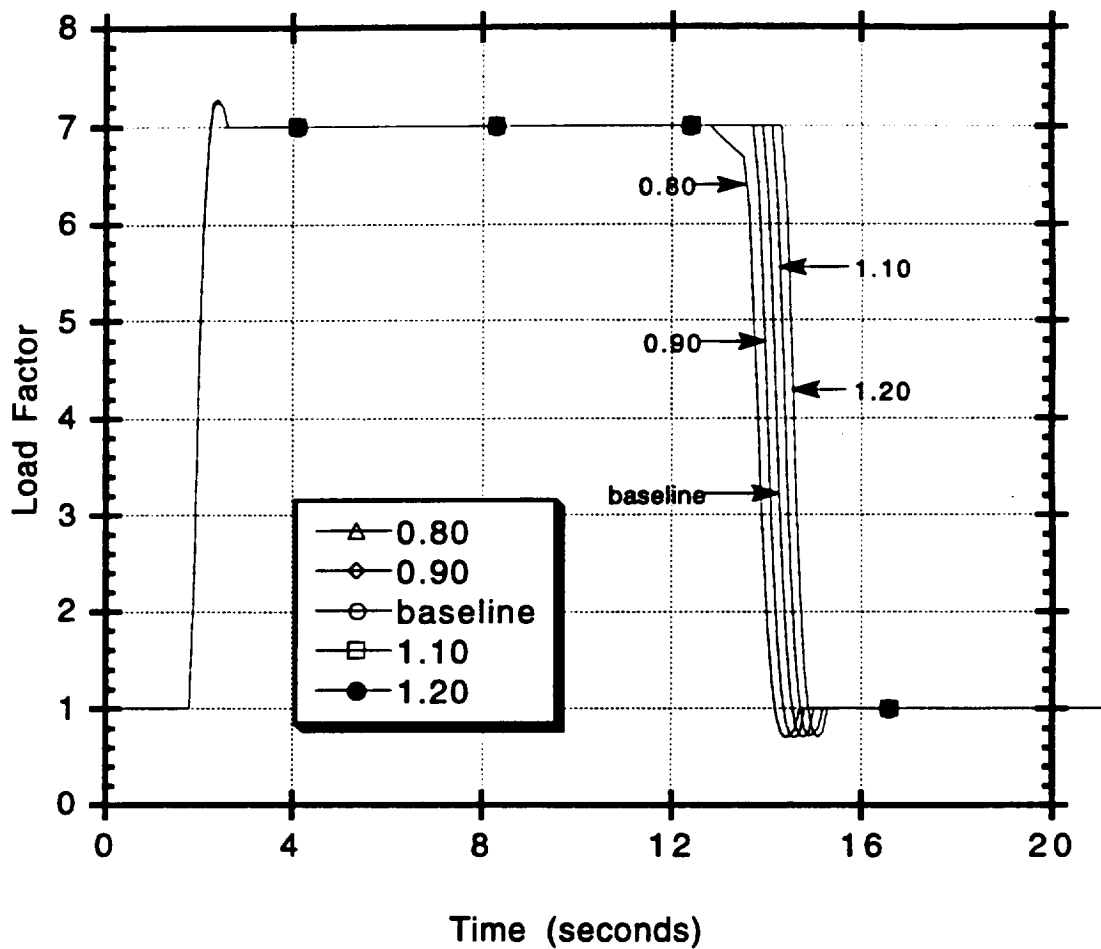
Figure 8.6

Load Factor Time Histories

for Different Thrust Loadings

Effect of Wing Loading on Combat Cycle Time

This section illustrates how the ACSYNT agility module can be used to study the influence of an aircraft's wing loading on the Combat Cycle Time metric.

Combat Cycle Time maneuvers were performed using four different wing loadings for comparison with the baseline configuration. The selected wing loadings were 65, 70, 85, and 90 pounds per square foot (psf). These choices bracketed the baseline which had a loading of 78.4 psf. The wing loading was the only change in configuration for this study. All other input parameters were held constant. However, convergence of the aircraft during ACSYNT execution resulted in some weight disparity. This resulted in a slight difference in thrust loading for the five configurations. The extremes of this disparity were a thrust loading of 0.96 for the 65 psf wing loading configuration and 1.00 for the 90 psf configuration.

Figure 8.7 illustrates the time differences for each segment of the Combat Cycle Time maneuver for all five configurations. The total time to complete the maneuver was very similar for all configurations. There was, however, a difference in the times for each maneuver segment. The higher loaded aircraft completed the turn segment slightly faster than the less loaded configurations. Conversely, the higher loaded aircraft required longer accelerations times than did the less loaded aircraft. The explanation for this is again found in the time histories of the Mach number and turn rates for the configurations.

Figure 8.8 plots the Mach number over the course of the CCT maneuver for the five configurations. As was the case in the previous study, there was an initial acceleration phase due to engine spool-up until the aircraft rolled into the turn and pitched up to the turning load factor.

In order to generate the 7 g's for the turn the higher loaded aircraft needed to produce higher lift coefficients. This in turn increased their induced drag. The result was the greater the wing loading the greater the deceleration and the resultant velocity deficit. This explains the longer acceleration phases of the higher loaded configurations.

The greater deceleration also allowed the higher loaded configurations to approach their turning speeds. Similar to the previous study, the quicker approach to turning speed provided higher turn rates. This explains why the higher loaded aircraft completed the turn in a shorter amount of time.

In the case of different wing loadings the approach to turning speed is more pronounced. Since the wing loadings were different, the turning speed for each configuration was different. The horizontal lines in Figure 8.8 designate the turning speed for the various wing loadings. As the wing loading decreased the turning speed decreased as well. This along with the reduced deceleration of the less loaded aircraft kept these aircraft far from their optimal turning speeds. Figure 8.8 illustrates that the lower the wing loading the greater the difference between the turning speed and the minimum speed obtained during the entire maneuver. Only the 90 and

80 psf aircraft ever reach turning speed while the 65 psf aircraft never came within Mach 0.12 (17%) of its turning speed.

The differences in turn rate are illustrated in Figure 8.9. Here it can be seen that as the turn progressed a higher loaded aircraft produced a turn advantage over a less loaded aircraft. However, as soon as the turning speed was passed the now lift limited aircraft lost its turn rate advantage. For extended turns the higher loaded aircraft would eventually lose the turn advantage but in this case it still completed the turn first.

Figure 8.10 plots the turn profile in the horizontal plane of the maneuver. This graph shows the higher loaded aircraft had tighter turn radii. Not only did the higher loaded aircraft have a turn advantage in terms of time but they also held a spatial turn advantage. By the time the entire maneuver was completed and the aircraft had re-accelerated to the starting velocity all five configurations flew roughly abreast one another. Yet the higher the wing loading the tighter the ending position.

Figure 8.11 shows the load factor time history of the five aircraft. As in the thrust loading study all five configurations had very similar time histories. The only difference is the time of pitch-down for the five cases and the upper right-hand corner of the 90 psf aircraft. Since this configuration achieved its turning speed and became lift limited, the load factor dropped off toward the end of the turn. This again illustrates the importance of time dependent performance analysis as the load factor plot shows little discrimination between the five aircraft.

The overall conclusion for this particular maneuver is that higher wing loading improves turn performance with little detrimental impact on Combat Cycle Time (remember total maneuver times were very similar). However, it was illustrated that the results of this study were highly dependent on the particular type of maneuver. Had the turn been extended to 270 or 360 degrees the higher loaded aircraft would have lost its turning advantage and created an excessive velocity deficit that would lengthen the acceleration phase. This again reinforces the difficulty in developing robust agility criteria that provide the best overall performance for a variety of situations and tasks.
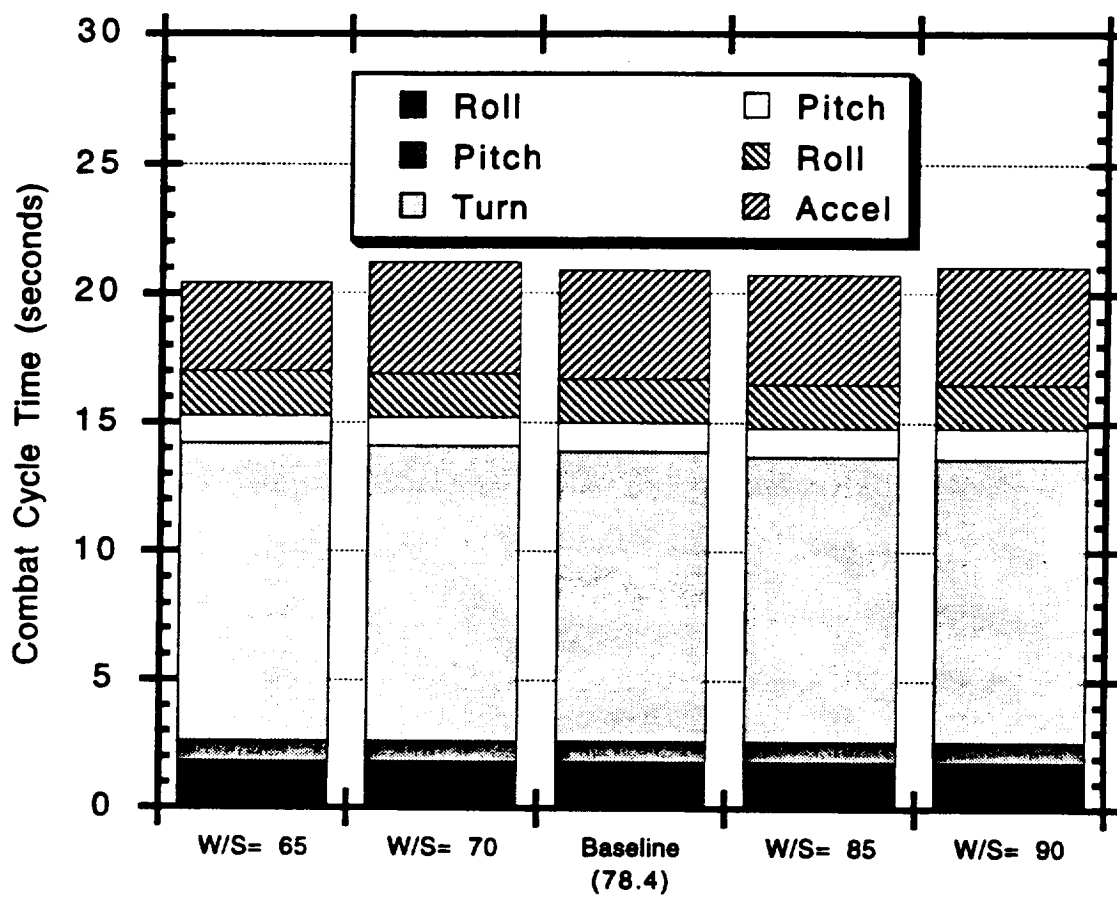
Figure 8.7

Combat Cycle Time Variation
for Different Wing Loadings
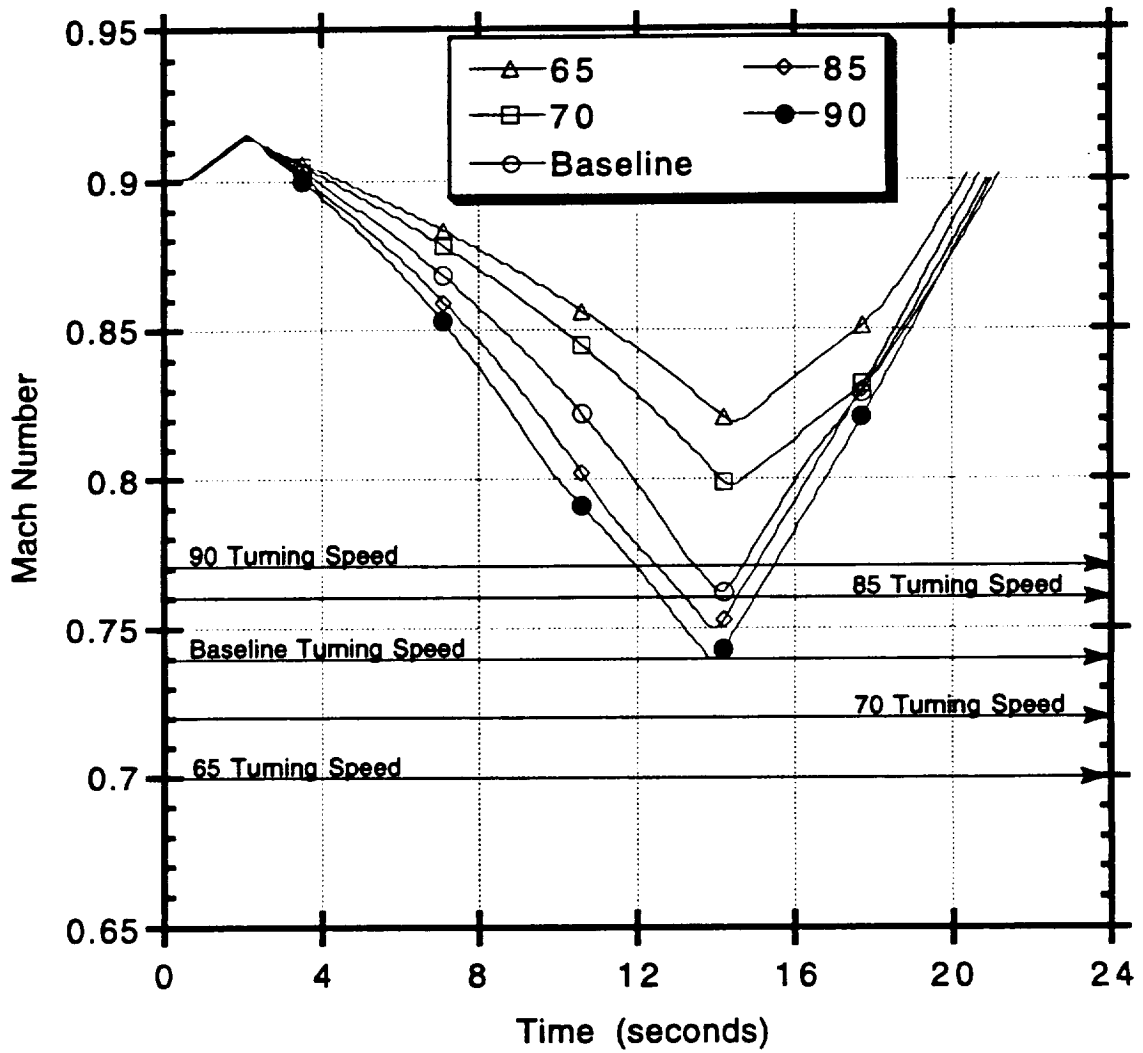
Figure 8.8

Mach Number Time Histories

for Different Wing Loadings
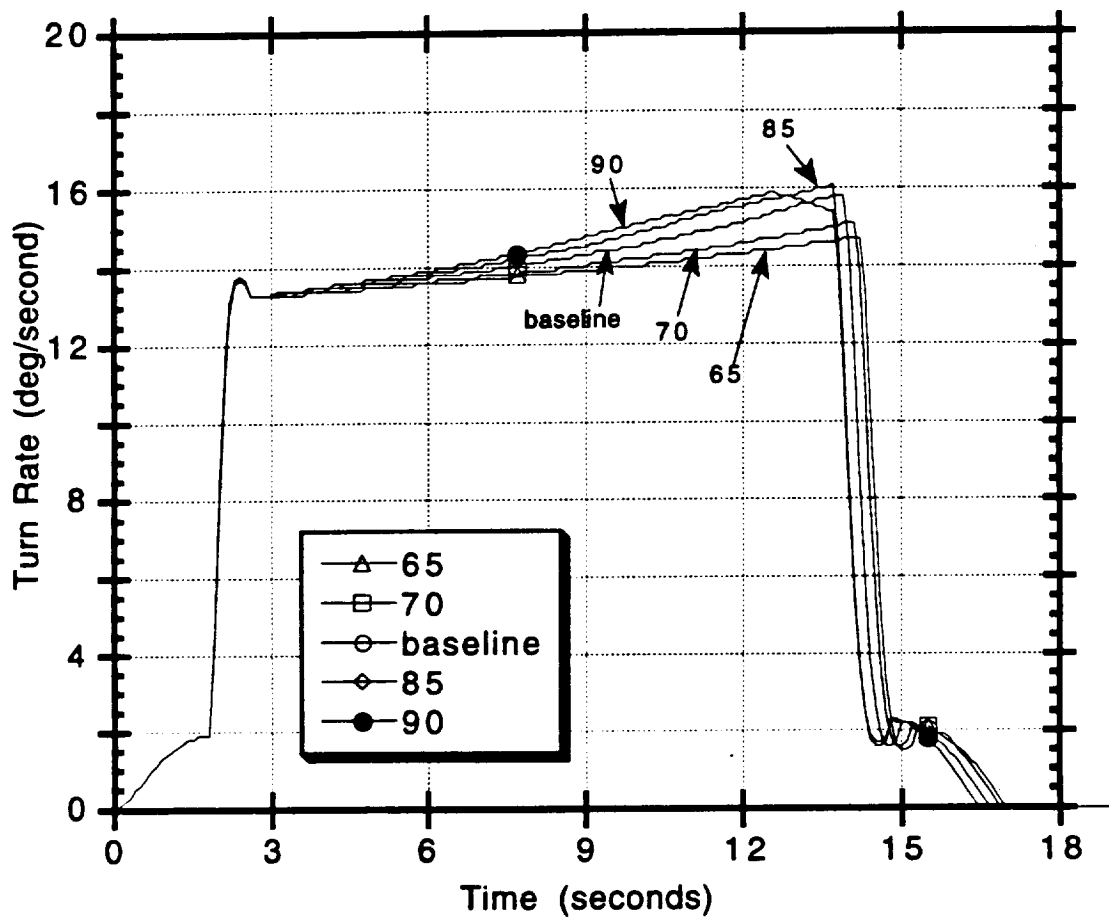
Figure 8.9

Turn Rate Time Histories
for Different Wing Loadings
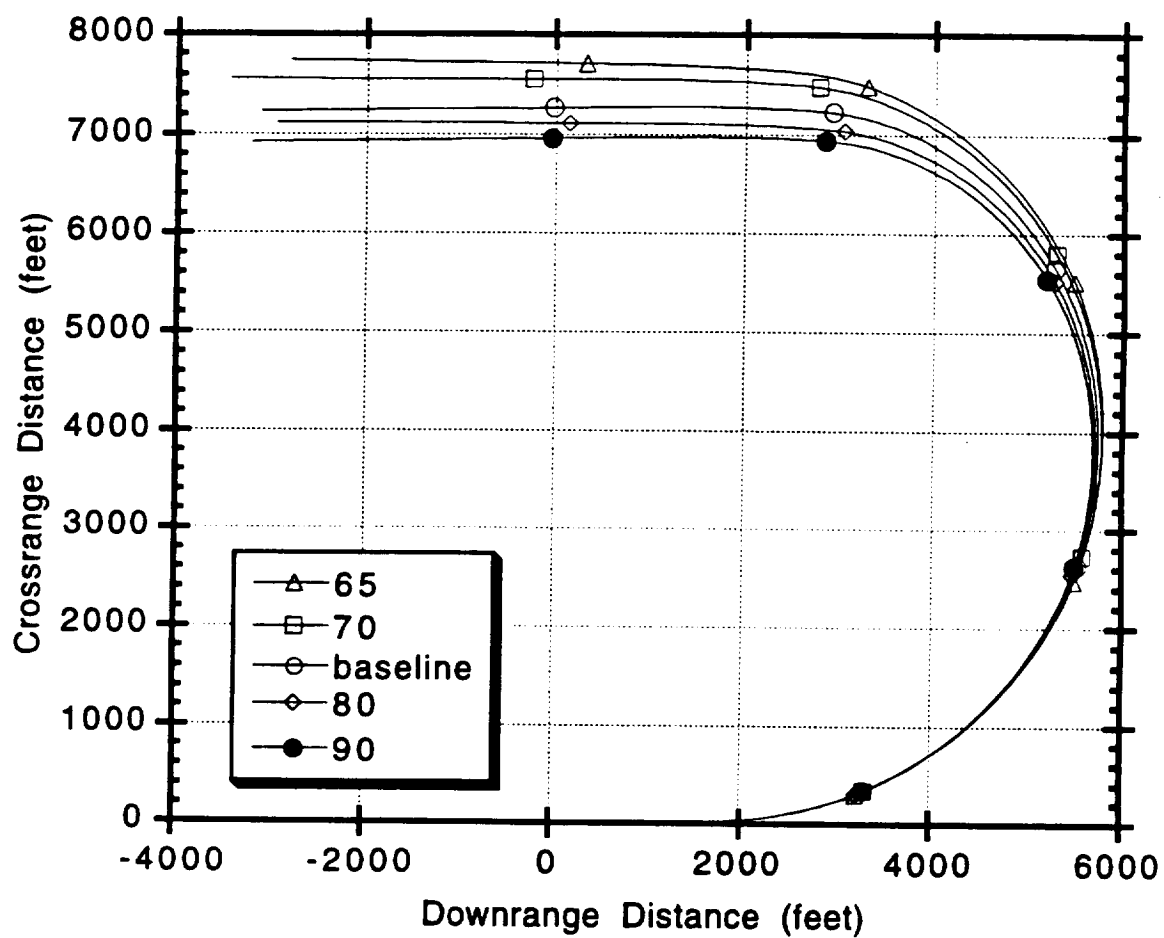
Figure 8.10

Horizontal Plane Turn Diagrams
for Different Wing Loadings
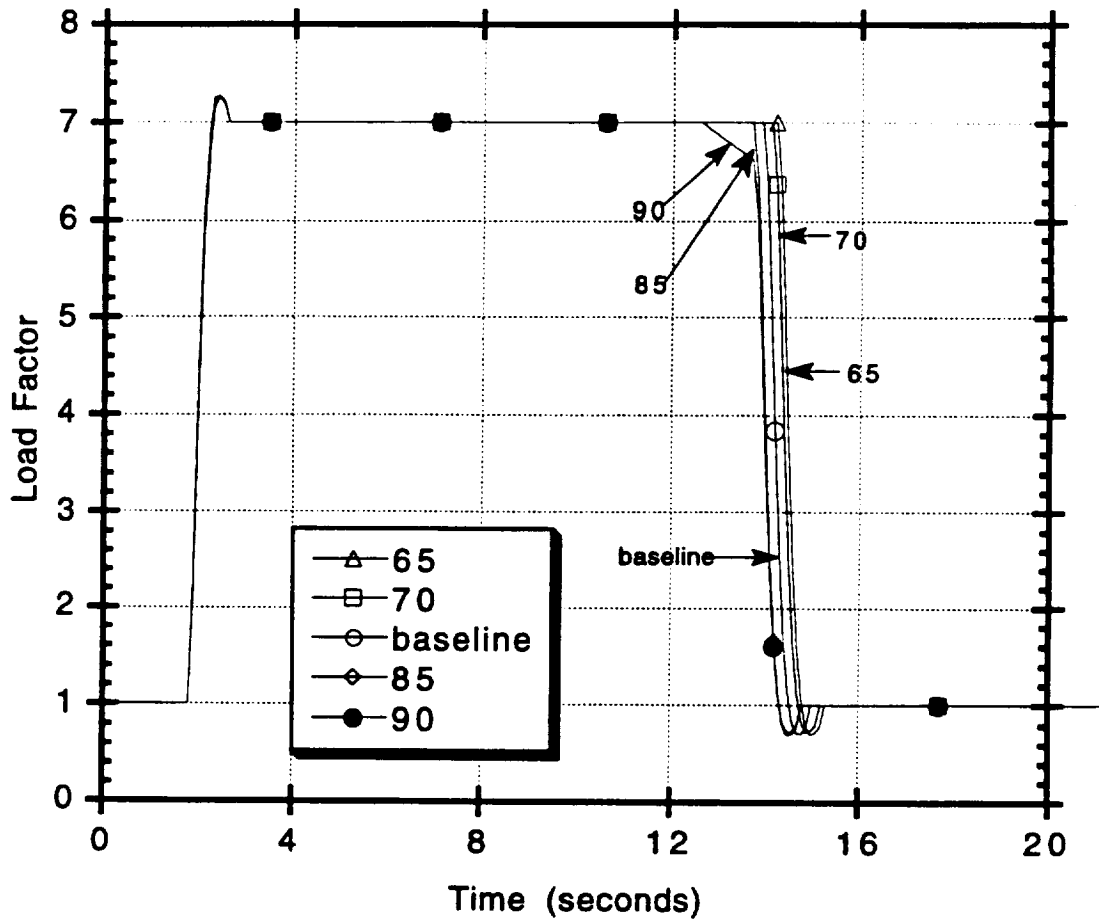
Figure 8.11

Load Factor Time Histories

for Different Wing Loadings

Use of Combat Cycle Time as a Constraint In Aircraft Optimization

This section illustrates how the agility module can be used in configuration optimization. This capability is the real power of ACSYNT and it is these types of optimization studies that will be used to determine the impact of agility technologies and constraints on the overall aircraft configuration. The overall optimization technique will first be discussed and then the particular example will be presented to illustrate the optimization opportunities of the agility module.

The basic optimization method used by COPES in conjunction with ACSYNT consists of an objective variable, design variables and constraint variables. The objective variable is the parameter that is being optimized and can be either maximized or minimized. Design variables are the parameters whose values are varied to provide a design space. These design variables are given upper and lower bounds. The constraint variables are parameters that further limit the design space. In the case of ACSYNT typical constraints are mission range or a sustained turn requirement at altitude. Only the design variable space that satisfies all constraints can provide possible solutions. The optimizer evaluates aircraft configurations over this design space and attempts to find the design point that produces the desired extrema of the objective variable.

In this example the objective variable was gross takeoff weight. Naturally the objective was to minimize the takeoff weight. The constraint for this optimization was to complete the same Combat Cycle Time maneuver used previously within 20.00 seconds.

The design variables were the wing area and engine size. Table 8.1 lists the design variables bounds, the constraint variable value, and the pertinent parameters of the starting configuration and the optimized configuration. This information is also illustrated in Figure 8.12.

The tradeoff in this case is wing loading versus thrust loading. A decrease in wing loading allows a decrease in thrust loading and vice versa. However, a larger wing adds weight to the vehicle. Conversely a larger engine also adds weight. These two trends are the source of the tradeoff. Some combination of wing and engine size will satisfy the agility constraint and provide the overall lowest takeoff weight. From Table 8.1 and Figure 8.12 it can be seen that the trends drive the wing to as small a value as possible. This resulted in only a moderate increase in engine size. Evidently the agility criterion is much more sensitive to engine size than wing loading.

The lower boundary on wing loading was reduced to see where the wing size would stabilize. As it turns out, the wing continued to shrink all the way down to 90 square feet. However, this portion of the design space is really irrelevant. The only constraint applied was the Combat Cycle Time maneuver. Any functional aircraft configuration would have many more constraints such as takeoff and landing performance. These constraints would require a much more reasonable wing size. This example does show, however, the capability of ACSYNT to use agility constraints in configuration optimization.

One note on the engine size variable: the engine deck used had an engine much larger than needed for the baseline aircraft. ACSYNT provides a parameter called engine scale factor (ESF) that 'rubberizes' the engine. This parameter proportions the engine thrust, airflow, fuel flow and dimensions. The engine scale factor required to match the engine deck with the thrust level of the baseline aircraft was 0.438 (43.8%).

Table 8.1

Design Space Boundaries and Final Results
for Combat Cycle Time Optimization

Design and Constraint Variable Boundaries

Design variable	Lower bound	Upper bound
Wing area (ft^2)	150.0	250.0
Engine scale factor	0.200	1.00

Constraint variable	Lower bound	Upper bound
Combat Cycle Time (sec.)	5.00	20.0

Optimization Results

Configuration:	Original	Optimized
Combat Cycle Time (sec.)	21.40	20.00
Wing area	200.0	150.0
Engine scale factor	0.420	0.438
Takeoff weight	19,234	18,904
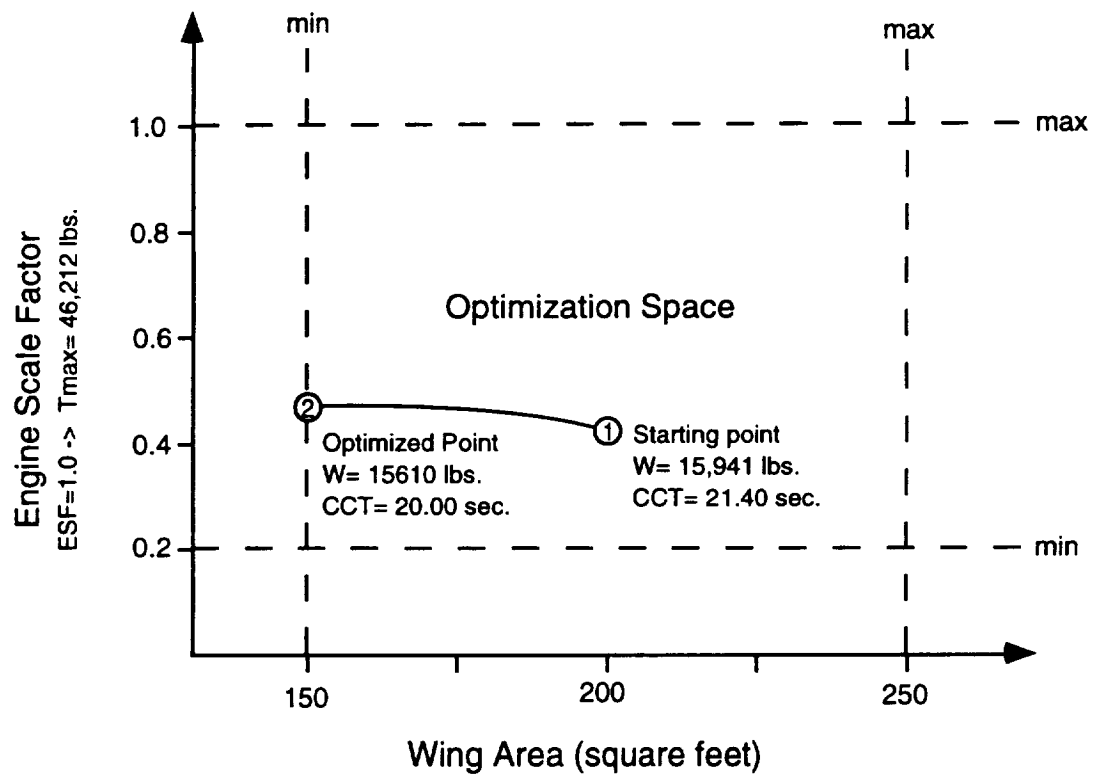
Figure 8.12

Optimization Path for Minimization
of Aircraft Takeoff Weight

CHAPTER 9

CONCLUSIONS AND RECOMMENDATIONS

This project involved designing the overall architecture of the module and developing the quasi-simulation subroutines. While this is the core of the agility module it is not the entire package. This chapter will summarize the present state and capabilities of the module and suggest future work efforts.

The present agility module is in working order and should be an effective tool in analyzing an aircraft configuration's agility potential. The example studies of the effect of thrust loading and wing loading illustrate how the module can be used to perform trade studies on parameters important to agility metrics.

The module is also capable of providing constraints for ACSYNT's optimization capability. Once agility criteria have been developed the module can be used to optimize an aircraft configuration for agility requirements as well as contemporary mission requirements.

The present module is best suited for functional type metrics. It is particularly suited to metrics such as combat cycle time, pointing margin, and dynamic speed turn. Although the transient metrics may be analyzed and the architecture is well suited for transient maneuvers, the analytical models are not as robust as for the functional type segments. However, once ACSYNT is capable of generating stability derivatives and the flight control module is

incorporated, the transient maneuver analysis capabilities may be improved.

One major concern in the code development was computer run time. A time stepping simulation with numerous tracked variables could produce a lengthy run time, especially for functional long-term maneuvers. However, certain measures were taken to reduce computer time. As stated in Chapter 4, the analytical models of the transient pitch and roll maneuver segments were simplified as much as possible. When the added complexity of multi-step control response and dynamic load factors provided little difference in time response, these elements were dropped from the model. The amount of time ACSYNT spent in the agility module was found to be about 30% greater than most of ACSYNT's other modules. While this is definitely added length, time was reduced as much as possible without hindering analytical performance.

The agility module's architecture has an important characteristic for future improvements. Since industry has not yet settled on a single definition of agility, an accepted group of metrics, nor quantifiable requirements, the adaptable architecture will allow future metrics and requirements to be incorporated with the least amount of rework. The simulation's time-stepping technique of analysis and the menu list of maneuver segments should allow the necessary adaptability.

Future work efforts should involve development of subroutines dedicated to performing specific agility metrics. Presently, combat cycle time is the only dedicated subroutine. References 6,7,9 and

13-17 discuss many of the agility metrics developed by industry. Most of these are appropriate for inclusion in the agility module.

Another task for future work is to continue the verification of the routine. A comparison between actual flight test data and the agility module would better prove the integrity of the code. The requirement for this comparison is flight test data for a particular aircraft performing a maneuver close to a metric maneuver. Complete time histories for relevant parameters such as Mach number, turn rate and spatial position would be needed.

ACSYNT does not have the capability to analyze maneuver flaps that change their deflection over the course of a maneuver. Thus the correlation of flight test data with the agility module should be done with caution since most contemporary aircraft employ variable geometry during maneuvers. For the first comparison, an older aircraft without variable geometry would be best.

REFERENCES

1. Gilbert, William P., et al. "Control Research in the NASA High-Alpha Technology Program." AGARD Conference Proceedings AGARD-CP-465. Symposium of the Fluid Dynamics Panel. Madrid, Spain. October 2-5, 1989.

2. Wanstall, B., and J.R. Wilson. "Air Combat Beyond The Stall." Interavia Aerospace Review, Vol. 45, May 1990, 405-407.

3. Herbst, Wolfgang B. (MBB). "X-31A." SAE Paper 871346. SAE Aerospace Vehicle Conference. Washington, DC. June 8-10, 1987.

4. Dorn, M. "Aircraft Agility: The Science and the Opportunities." AIAA Paper AIAA-89-2015. AIAA/AHS/ASEE Aircraft Design, Systems and Operations Conference. Seattle, Washington.
    July 31 - August 2, 1989.

5. McAtee, Thomas. "Agility in Demand." Aerospace America, May 1988, 36-38.

6.   Tamrat, B.F.   "Fighter Aircraft Agility Assessment Concepts and Their Implication on Future Agile Fighter Aircraft."   AIAA Paper AIAA-88-4400.   AIAA/AHS/ASEE Aircraft Design, Systems and Operations Meeting.   Atlanta, Georgia.   September 7-9 1988.

7.   Skow, A.M.   "Agility As a Contribution to Design Balance."   AIAA Paper AIAA-90-1305.   AIAA/SFTE/DGLR/SETP Fifth Biannual Flight Test Conference.   Ontario, California.   May 1990.

8.   Butts, Stuart, and Alan Lawless.   "Flight Testing for Aircraft Agility."   AIAA Paper AIAA-90-1308.   AIAA/SFTE/DGLR/SETP Fifth Biannual Flight Test Conference.   Ontario, California.   May 1990.

9.   Liefer, Randall K., et al. "Assessment of Proposed Fighter Agility Metrics."   AIAA Paper AIAA-90-2807.   AIAA Atmospheric Flight Mechanics Conference.   Portland, Oregon.   August 20-22, 1990.

10.   Roskam, Jan.   Airplane Flight Dynamics and Automatic Flight Controls Part 1.   Lawrence, Kansas: Roskam Aviation and Engineering Corporation, 1982.

11. Roskam, Jan. _Airplane Design Part VI: Preliminary Calculation of Aerodynamic, Thrust and Power Characteristics._ Lawrence, Kansas: Roskam Aviation and Engineering Corporation, 1987.

12. McRuer, Duane, and Irving Ashkenas. _Aircraft Dynamic and Automatic Control._ Princeton, University Press, 1973.

13. Bitten, R. "Qualitative and Quantitative Comparison of Government and Industry Agility Metrics." AIAA Paper AIAA 89-3389. AIAA Atmospheric Flight Mechanics Conference. Boston, Massachusetts. August 14-16, 1989.

14. Skow, A.M., et al. "Advanced Fighter Agility Metrics." AIAA Paper AIAA 85-1779. AIAA Atmospheric Flight Mechanics Conference. Snowmass, Colorado. August 18-21, 1985.

15. Yajnik, Kirit S. "Energy-Turn-Rate Characteristics and Turn Performance of an Aircraft." _Journal of Aircraft_, Vol. 14, May 1977, 428-433.

16. Riley, D., and M. Drajeske. "Status of Agility Research at McDonnell Aircraft Company and Major Findings and Conclusions to Date." ICAS Paper ICAS-90-5.9.4. ICAS, Congress, 17th. Stockholm, Sweden. September 9-14, 1990.

17. Riley, D., and M. Drajeske. "An Experimental Investigation of Torsional Agility in Air-to-Air Combat." AIAA Paper AIAA 89-3388. AIAA Atmospheric Flight Mechanics Conference. Boston, Massachusetts. August 14-16, 1989.

APPENDIX A

DESCRIPTION OF BASELINE AIRCRAFT FOR VERIFICATION AND EXAMPLE STUDIES

This section describes the theoretical model of the Northrop F-20 Tigershark fighter aircraft used during verification of the agility module and during the example studies of Chapter 8.

The overall weight, engine thrust and external dimensions of the Tigershark were matched as best as possible for the available information. The aerodynamics and component weight breakup were completely generated internally by ACSYNT. In addition, the engine performance was obtained from an engine deck obtained from NASA-Ames and not necessarily the General Electric F-404 used on the Tigershark. This data should thus not be considered real data from the Tigershark. This aircraft was simply used as a typical modern aircraft in the fighter class.

The general configuration data for the Tigershark model is:

```
**** AGILITY TEST MODEL (F-20 WITH 2 AIM-9L'S) DEC92'-JAN93'****

DISTANCES IN FEET     WEIGHTS IN LBS.   FORCES IN LBS.    PRESSURES IN LBS/FT**2


     GENERAL              FUSELAGE                        WING   HTAIL   VTAIL

WGROSS 18201.   LENGTH          46.5   AREA              200.0   61.8    39.6
W/S       91.0  DIAMETER         3.9   WETTED AREA       292.3   70.9    77.6
T/W       0.62  VOLUME         426.0   SPAN               26.7   15.3     6.4
N(Z) ULT 13.5   WETTED AREA    463.8   L.E. SWEEP         32.7   32.2    36.3
CREW       1.   FINENESS RATIO  11.9   C/4 SWEEP          25.0   25.0    25.0
PASENGERS  0.                          ASPECT RATIO       3.56   3.79    1.04
                                       TAPER RATIO        0.23   0.24    0.28
     ENGINE               WEIGHTS      T/C ROOT           0.05   0.04    0.04
                                       T/C TIP            0.05   0.04    0.04
NUMBER     1.                 W    %WG ROOT CHORD         12.2    6.5     9.6
LENGTH     9.5  STRUCT.    5279. 29.0  TIP CHORD           2.8    1.5     2.7
DIAM.      2.2  PROPUL.    2323. 12.8  M.A. CHORD          8.5    4.6     6.8
WEIGHT  1023.1  FIX. EQ.   4110. 22.6  LOC. OF L.E.       21.9   36.6    33.3
TSLS    11234.  FUEL       5126. 28.2
SFCSLS    0.75  PAYLOAD    1162.  6.4
```

The maneuver specifications for the Combat Cycle Time metric of Chapter 8 were:

```
          NSEG=7,            JMAX=500,          DT=0.1,
     IYY=14000.0, 300.0, 0.0, 0.0, 0.0, 0.0, 0.0,
     IXX=10500.0, 500.0, 0.0, 0.0, 0.0, 0.0, 0.0,
     ETADE=1.0,        LP=-7.0,          LDA=75.0,
     AMAX=15.0,        FBRAKE=5.0,       LAMDOT=45.0,
     MLEAD=0.05,       KARB=0,           IPRINT=1,
     SEND
MANEUV. MACH   ALT.   LOAD HEAD   BANK  AILN  WCOMBP    A M B T  THR    THRVECT
SEGMENT                FACT CHANGE ANGLE DEFL                      - +   -    +
------- ----- ------- ---- ------- ----- ---- --------- - - - -  - -  ---- ----
* METRIC 0.90 15000                                0.60 0 0 0 0  1 2   0.   0.
  ROLL   0.00          1.0     0.0  81.8  5.0            0 0 0 0
  PITCH  0.00          7.0     0.0   0.0  0.0            0 0 0 0
  TURN   0.00          7.0   166.5   0.0  0.0            0 0 0 0
  PITCH  0.00          1.0     0.0   0.0  0.0            0 0 0 0
  ROLL   0.00          1.0     0.0   0.0 -5.0            0 0 0 0
  ACCEL  0.90          1.0     0.0   0.0  0.0            0 0 0 0
```

The user's manual included in this appendix provides explanation of the above parameters.

95

AGILITY MODULE USER'S MANUAL
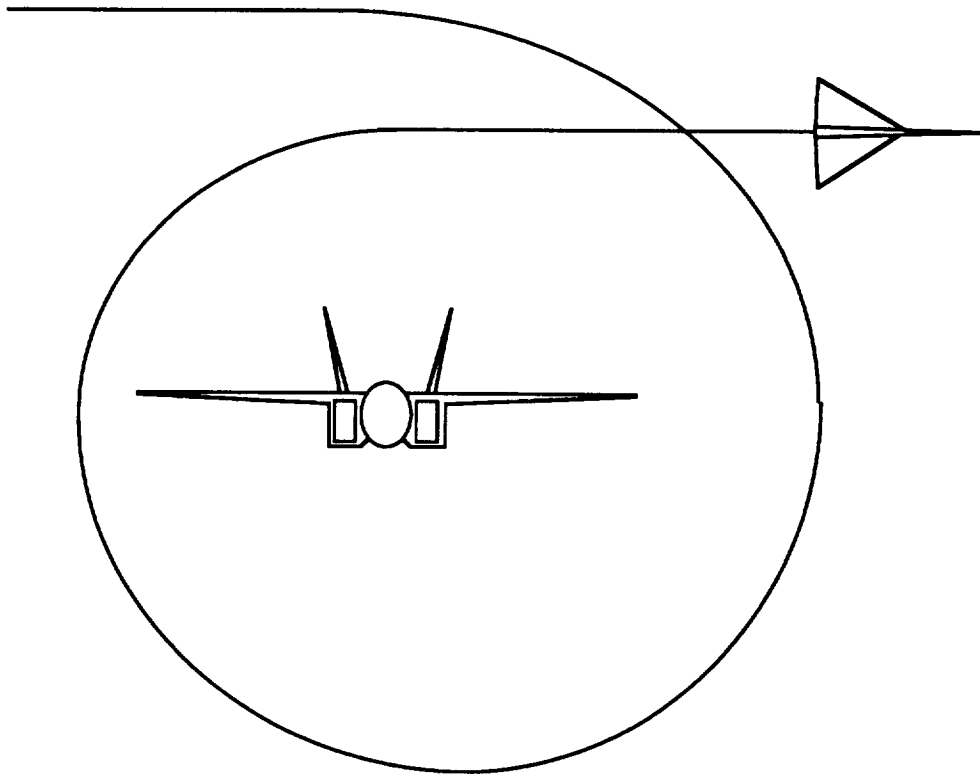
A. Introduction

Much of present fighter research has focused on improving aircraft agility. The problem is that agility is a poorly defined concept. There have been many new ideas to improve an aircraft's combat effectiveness and many of these ideas have developed into a unit of merit or metric. Most agility metrics can be separated into two categories; transient and functional. The transient metrics deal with an aircraft's ability to perform quick actions such as rolls, pitches and nose pointing maneuvers. Functional metrics deal with longer time scale maneuvers such as transitions from one spatial location and orientation to another location and orientation, or transition from one energy level to another. Typically, functional metrics have transient type maneuvers within them. For both transient and functional metrics, time is almost always the driving criterion; the more agile aircraft performs the metric in the least amount of time.

The architecture of this agility module does not cater to one specific agility metric but is designed so that a number of metrics may be analized. This routine can analyze functional metrics and track the position and energy level of an aircraft through a variety of trajectories. Functional metrics typically consist of some transient segments (rolls and pitches) so they have been includeded in the module. However, these models are rudimentary and while satisfactory for functional metric analysis, they are not as appropriate for discrete transient metrics. Yet, the pieces are there and as ACSYNT's stability derivative and control system analysis improves, the transient segment analysis can be improved.

The agility module can only analyze those metrics that lie in an horizontal plane. The altitude is specified by the user and this altitude is maintained; there is no diving or climbing.

98

The architecture of the agility module consists of a series of subroutines that 'fly' an aircraft through a level maneuver. The basic output of the module is the time to complete the maneuver. It is assumed that maneuvers consist of discrete actions like rolling to a bank angle, pitching to a load factor, turning to a heading angle or accelerating to a Mach number. These actions are refered to as maneuver segments. It is the combined sequence of these segments that represent the aircraft's maneuver flightpath and performance. There is a subroutine that performs each of the segment categories (ROLL, PITCH, TURN, ACCEL). The controlling subroutine (AGILCON) calls these maneuver segment subroutines in the user specified order.

The maneuver segment subroutines perform their operations in time steps. Each of the segment subroutines track the following sixteen state variables through the duration of the segment:

Mach number	Gross thrust (pounds)	Net thrust (pounds)
Axial acceleration (g's)	Angle of attack (degrees)	Load factor (g's)
Turn rate (deg/sec)	Heading angle (degrees)	Roll rate (deg/sec)
Bank angle (degrees)	X position (feet)	Y position (feet)
Thrust vector angle (degrees)		Lift coefficient
Drag coefficient		
Turn radius (feet)		

The coordinate system of the maneuver arena

The geometry of the maneuver arena is illustrated in figure B.1 The X and Y variables represent the horizontal plane at the given metric altitude. The aircraft starts at the origin with its nose pointing in the positive X direction. The heading angle is referenced to the positive X direction so the aircraft begins with a zero heading angle.

Running agility metrics

There are two methods to run agility metrics. The first is to pick a standard metric like "Combat Cycle Time". This metric

99

automatically calls the maneuver segment routines in the required order to perform the combat cycle time metric.

The second method is to build up a user-defined metric out of the individual maneuver segments (ROLL, PITCH, TURN, ACCEL), in any order.

Up to 50 maneuver segments can be implemented in the agility module. There are no restrictions on the type of these segments. However, a new metric must begin with a METRIC segment (see description of maneuver segment options).

The doghouse plot and corner speed

The general character of the agility module is to operate on the upper boundary of what is frequently refered to as the doghouse plot. This is a graph of turn rate versus speed or Mach number (see figure B.2). The upper boundary of this graph indicates the maximum turn rate for a given Mach number.

As shown in figure B.2, there is a peak in the upper boundary. This peak represents the highest turn rate for any Mach number. The Mach number corresponding to the peak is usually called corner speed.

The aircraft's turn rate is limited by different constraints depending on which side of corner speed it is flying. Above corner speed, the aircraft can aerodynamically generate a higher load factor than the aircraft's structure can withstand. The aircraft is said to be load limited with the max turn rate determined by the max designed load factor. Below corner speed, the aircraft is operating at its maximum lift coefficient and cannot aerodynamically generate the design load factor. In this region the aircraft is said to be lift limited.

From the above discussion, the definition of corner speed can be inferred; the Mach number that produces the max design load factor at maximum lift coefficient is the corner speed.

Turning speed (MTURN)

The general logic of the code centers around a certain Mach number called "turning speed" (MTURN). This speed is used as a

dividing line between two sets of user input; a throttle and thrust vector command for above MTURN and a throttle and thrust vector command for below MTURN.

MTURN is specified one of three ways. The first method designates MTURN as the corner speed calculated for the particular metric altitude, load factor and max angle of attack. The other two methods, which will be addressed later, are incorporated to give the user more control over MTURN for metrics that do not involve turns.

The user may use another variable to adjust the throttle and thrust vector command schedule. If the variable MLEAD (Mach LEAD) is used, the throttle schedule described above is altered. This command strategy attempts to better capture MTURN by anticipating the approach of turning speed (by a factor of MLEAD) and starting the throttle change earlier (see figure B.3).

Figure B.4 shows the three regions of throttle command created by the parameters MTURN and MLEAD. The above-corner-speed command is used only if the Mach number is above MTURN+MLEAD. Conversely, the below-corner-speed command is used only if the Mach number is below MTURN-MLEAD. If the Mach number lies in the region between MTURN+MLEAD and MTURN-MLEAD, the throttle command is the thrust required to sustain the turning load factor at MTURN.

Roll methodology

Aircraft roll maneuvers use a minimum-time control strategy. The roll begins with a step input aileron deflection. As roll rate increases and the roll progresses, there is a point in time where a reversal step input of the aileron would decelerate the roll rate to zero just as the desired bank angle was captured. This time is calculated and the time history of the roll then generated. A single degree of freedom decaying exponential function is used as a time response model.

Pitch methodology

The pitch routine uses a short period approximation transfer function for the time response. The control input is a step from the

101

starting trimmed control deflection to that required to trim at the ending angle of attack.

The internally calculated damping derivatives are adjusted so that the damping ratio is at least 0.70. Also, the pitching moment slope is constrained to be -0.1 or less. Therefore, negatively stable aircraft (positive slope) are constrained to a positively stable response. These damping ratio and pitch slope constraints are incorporated to approximate the effects of a flight control system.

Turn methodology

The turn segment flies the aircraft through a level turn. The specified load factor is maintained as long as the aircraft is not lift limited. If it is lift limited, the maximum angle of attack is maintained and the load factor drops off as the aircraft decelerates.

At each time step, the bank angle is calculated to maintain a level turn. Therefore, as load factor drops off the bank angle will decrease.

Throttle methodology

The throttle subroutine generates time responses from any starting thrust level to any ending thrust level. The thrust transient models used are from a modern ('90) fighter class turbofan engine. The type of transients modelled are idle to dry, idle to wet, wet to idle, wet to dry, and dry to idle. Throttle changes starting or ending between idle and dry or between dry and wet do not have their own time responses but are interpolated from the five responses stated above.

Thrust vectoring

The thrust vector is referenced to the aircraft body axis and can be directed to any angle between the centerline (zero) and the opposite direction of the centerline (180). Vectoring in the normal direction would be an angle of 90 degrees. There is a user defined rate at which the vector angle changes.

The logic is set so that the normal component of thrust and the lift force add up to the desired load factor. Therefore, for

equivalent load factors, a vectored thrust turn would be conducted at a lower angle of attack than a corresponding non-vectored thrust turn.
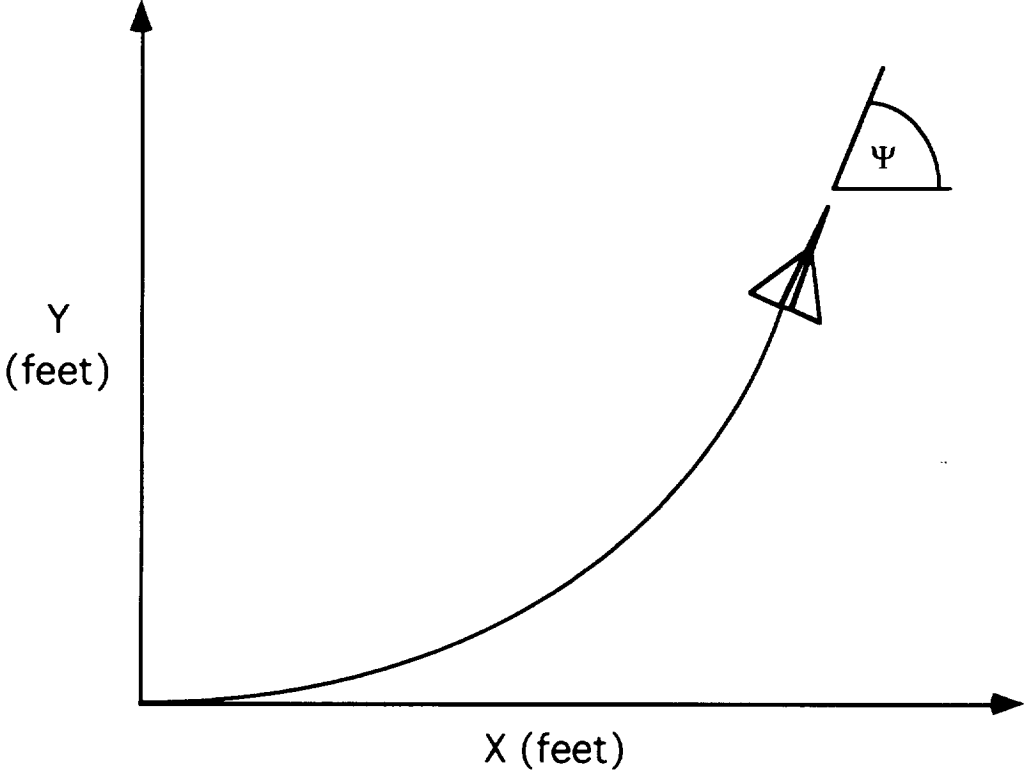

Figure B.1. Coordinate System Of
The Maneuver Arena
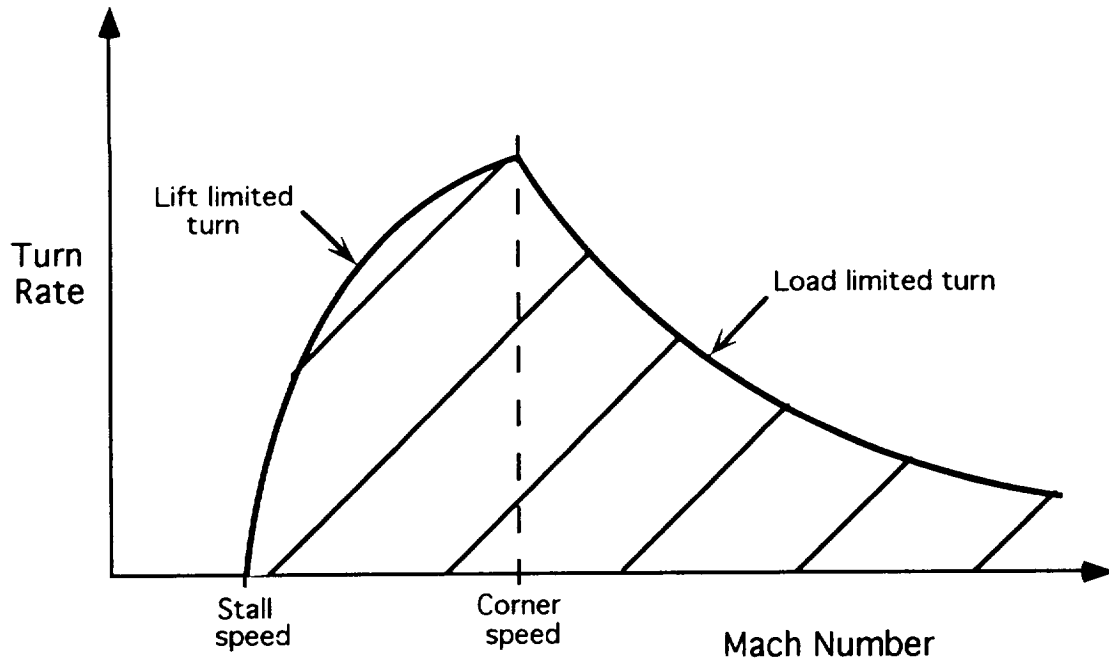
Figure B.2. The Doghouse Plot

MLEAD>0: (**bold plot**) throttle changes at P1, in this example, MTURN is better captured by the early throttle change

MLEAD=0: (thin plot) throttle changes at P2 (MTURN) results in poor capture
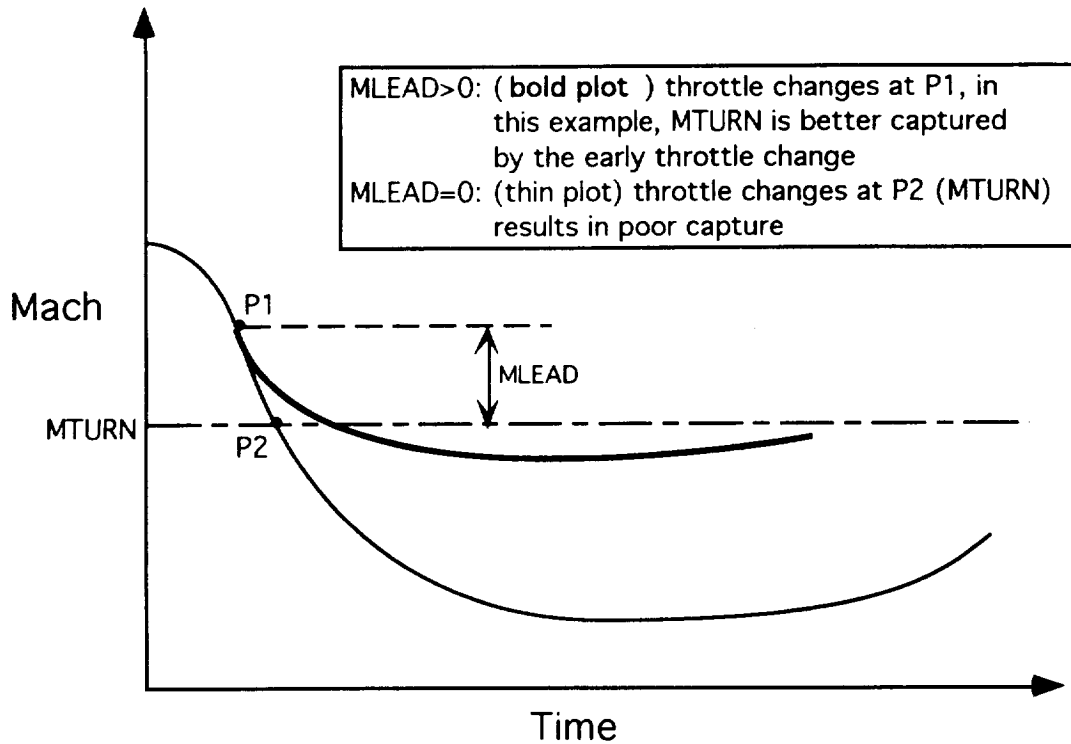
Figure B.3. Effect Of MLEAD During Deceleration To Capture Turning Speed

Thrust equal to drag at turning speed and load factor is commanded

Throttle command for below turning speed is commanded

Throttle command for above turning speed is commanded

MLEAD   MLEAD

MTURN

Mach Number

Figure B.4. Throttle Command As A Function OF Mach Number

1. Combat Cycle Time

The standard combat cycle time metric takes an aircraft through a level turn of a specified heading change. The idea is to turn at high 'g', capture the new heading angle and then accelerate back to the starting Mach number. The figure of merit for this metric is the time to complete the entire maneuver. Figure C.1 illustrates the combat cycle time circuit.
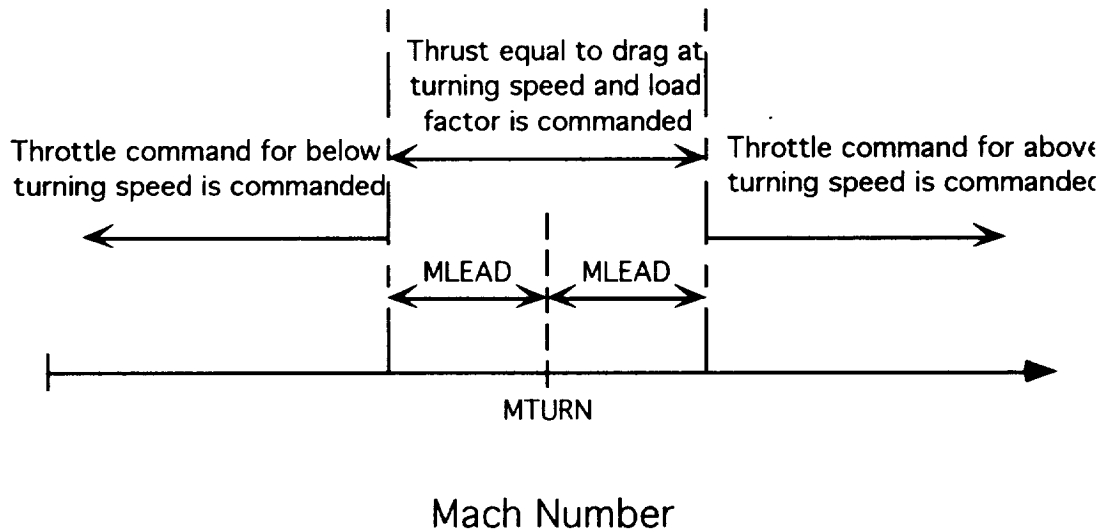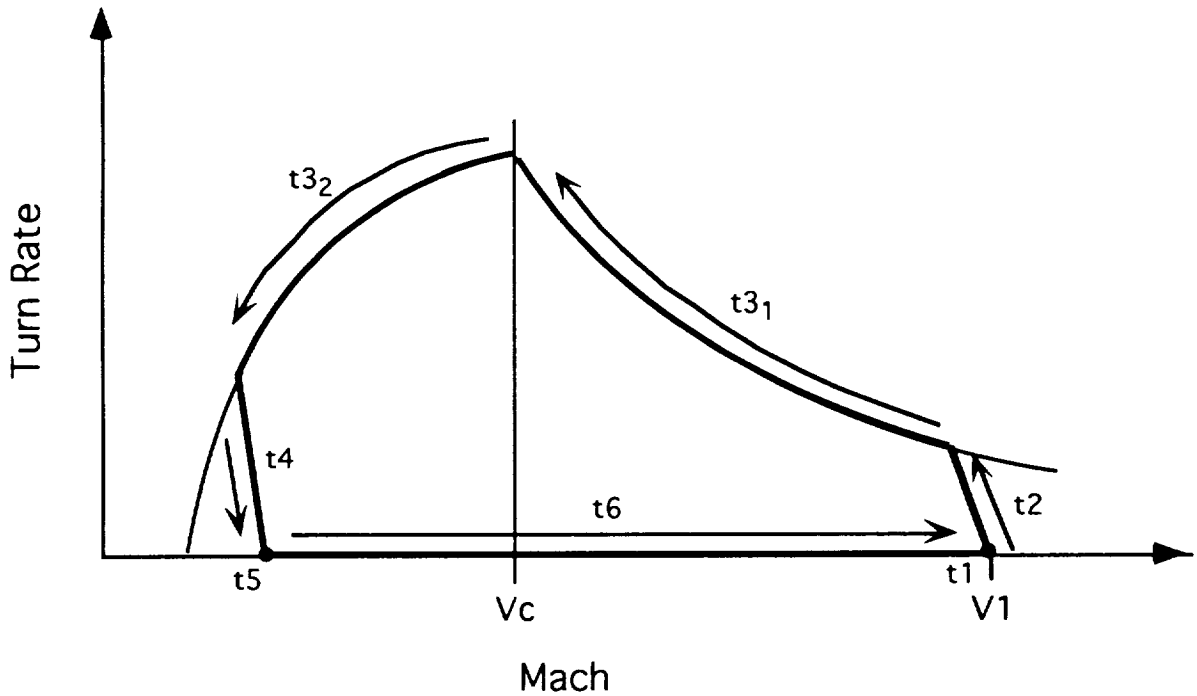

Legend:

V1 - starting and ending speed
t1 - time to bank into turn
t2 - pitch up to load factor
t31 - accelerate back to starting Mach level turn
t32 - time spent in lift limited level turn

Vc - corner speed
t4 - pitch down to unity load factor
t5 - roll to wings level
time spent in load limited t6 - time to number

106

Figure C.1. Combat Cycle Time Maneuver Circuit

```
┌─────────────────────────────┐
│ D.  Input  File  Architecture │
└─────────────────────────────┘
```

The agility module must be entered in the ACSYNT control block. The minimum entries are the read and execute rows. The execute entry should be -12. The negative sign causes agility to be executed after weight convergence. If agility output is desired in the main ACSYNT output file, an entry must be placed in the output row of the module call matrix. If this entry is not made, output will only be written in agility's output file.

An input block must also be included in the input file; figure D.1 illustrates a sample input block.

1. Agility Namelist ($AGILIN)

	-------------------- Real format --------------------	
Name	**Default**	**Description/units**
DT	0.1	Time step increment (seconds)
IYY*7	20000.0	Pitch axis moment of inertia array. There are seven elements which correspond to: IYY(1)= clean aircraft, zero fuel IYY(2)= added IYY due to internal fuel IYY(3)= " external fuel IYY(4)= " ammunition IYY(5)= " missiles IYY(6)= " bombs

IYY(7)=   "
                external tanks
If WCOMBP (in agility formatted
      input) is >1.0 (ie. it is the
      actual weight of the
      aircraft) then only the first
      elements are used.
Non-dropable stores, pylons, etc,
should be included in IYY(1).
(slug*ft^2)

IXX*7	8000.0	Lateral axis moment of inertia array. The description of IYY applies here also. (slug*ft^2)
ETADE	2.5	Efficiency of the pitch control surface. ETADE is 1.0 for an all moving tail. For an elevator it is less than one. See appendix for calculation method.
LP	-7.0	Roll damping dimensional derivative (1/sec)
LDA	75.0	Aileron effectiveness dimensional derivative (1/sec)
AMAX	15.0	Angle of attack limit (degrees)
FBRAKE	3.0	Airbrake equivalent flat plate area (ft^2)
MLEAD	0.04	Mach number lead. If accelerating through corner speed, the above-corner power setting will be engaged at MLEAD below corner speed. If decelerating through corner speed, the below-corner-speed power setting will be

engaged at MLEAD above corner speed. If the Mach number is between MTURN+MLEAD and MTURN-MLEAD the throttle command will be thrust equal to the drag at the turning condition (MTURN and the turning load factor).

• This variable can have pronounced effects on the capture of turning speed and the entire metric in general.

---------------------- Integer format --------------------------

Name	Default	Description
KARB	0	Airbrake toggle variable: 0= Do not use airbrake 1= Use airbrake Note: if the airbrake is used, then an internal variable controls when it is and when it is not used. This variable deploys the airbrake while above turning speed and retracts it below turning speed.
NSEG	1	Number of maneuver segments in formatted input block (50 maximum)
IPRINT	0	Output print controller: 0= Print summary output only 1= Print standard output 2= Print detailed output (see section E)
JMAX	500	Maximum number of time steps allowed per metric. If the time step (DT) is 0.1, the default value (500) would allow for fifty

seconds of maneuver time. The maximum number is 750. If more are required the variable arrays must be increased in the /TRACK/ and /POWER/ common blocks as well as the dimension of TIME() in the AGILE subroutine.

2. Formatted Input

The formatted input block is where the maneuver sequence is specified. A series of segments such as ROLL, PITCH and TURN are implemented to build the desired metric. In addition, there are certain segment types that perform an entire standard agility metric. In either case the beginning of a new metric is designated by the input of a "METRIC" segment.

The maneuver segment options are:

METRIC: This segment tells the code to start a new metric. Inputs are the starting flight conditions.

ROLL: Here the aircraft is rolled to a specified bank angle. The load factor entered under this row is the starting load factor. The ROLL subroutine maintains this load factor for the duration of the roll. For convenience, table D.II lists the proper level turn bank angles for common load factors.

PITCH: The pitch segment rotates the aircraft to a desired load factor. The starting bank angle is maintained for the duration of the pitch.
WARNING: for aircraft that are statically unstable, the pitch routine fudges the pitching moment slope to be slightly negative to prevent the response equation from blowing up.

TURN: This segment turns the aircraft to a specified heading angle. The heading angle input in this column is not the

110

number of degrees to turn through but the actual desired heading angle. The aircraft is always assumed to start a metric with a zero heading angle. The subroutine tries to maintain the specified load factor but if the aircraft decelerates to the lift limited region the maximum angle of attack will be held and the load factor will thus decay.

ACCEL: The accel segment accelerates or decelerates the aircraft to a specified Mach number. This segment begins with and maintains a wings level 1g horizontal flight path.

CCT: This segment 'flies' the aircraft through an entire combat cycle time metric (see figure C.1).

The formatted input is organized into sixteen columns, these are:

MANEUV. SEGMENT   This list contains the type of maneuver segments (see segment description)

MACH   Mach number, represents:
                    starting Mach in METRIC segments
                    turning Mach in TURN or CCT segments
                    ending Mach in ACCEL segments

ALT.   Metric altitude in feet, used only in METRIC segment

LOAD FACT   Load factor, used by all but METRIC and ACCEL segments

HEAD ANGLE   Ending heading angle, used by TURN and CCT segments

BANK ANGLE   Ending bank angle in degrees, used only by ROLL segments

AILN DEFL   Aileron deflection in degrees, used by ROLL and CCT segments

WCOMBP	Specifies aircraft weight, used only by METRIC segments
	<1.0 - fuel fraction (total usable fuel)
	>1.0 - actual aircraft weight in pounds

A,M,B,T   Drop flags for ammunition, missiles, bombs, and external fuel tanks respectively. Used by every segment but only if WCOMBP in the METRIC segment is less than 1.0. The drop flags recompute weight, moment of inertias and drag at the *end* of each segment.

0 - include store weight and drag
1 - subtract store weight and drag for
    the remainder of the metric

THR   '+': Throttle command for operation above
      turning speed
'-': Throttle command for operation below
      turning speed
Throttle commands are:
    1: maximum power (full A/B)
    2: maximum dry power
    3: maintain starting trimmed flight
       power
    4: thrust = drag (@turning speed and
       load factor)
    5: flight idle
Throttle commands may be entered under any or all segments but they are required under the METRIC segments. If they are only entered in the METRIC segments then these throttle commands are used for the entire metric.

THRVECT   '+': Thrust vector angle command for
      operation above turning speed
'-': Thrust vector angle command for
      operation below turning speed
      Zero degrees refers to thrust along
      axial direction while ninety degrees
      refers to thrust normal to body axis.

Notes: The turning speed (**MTURN**) is calculated one of three ways:

1: If there are no TURN or CCT segments in the input file then MTURN is designated as the starting Mach number.
2: If there are TURN or CCT segments, then MTURN is the corner speed for the given metric altitude, turning load factor and maximum angle of attack.
3: However, if the Mach entry under the TURN or CCT segment is nonzero, the corner speed designation (2) is overwritten with this Mach entry.
If there are or more TURN segments within one metric, the turning speed will be set by the information in the last TURN segment.

It is up to the user to ensure that the tracked variables are continuous from one segment to the next.
Some examples are-
The load factor for a roll should be equivalent to the ending load factor of the previous segment.
If a turn is desired following a roll, a pitch segment is required to transition from the rolling load factor to the desired turning load factor.
The starting Mach number of an acceleration segment should be the ending Mach number of the previous segment.

Table D.I summarizes the required inputs for different segment types.

Table D.I Required Inputs For Maneuver Segments

MANEUV. SEGMENT	MACH	ALT.	LOAD FACT	HEAD CHANGE	BANK ANGLE	AILN DEFL	WCOMBP	A	M	B	T	THR -	THR +	THRVECT -	THRVECT +
* METRIC	X	X					X	X	X	X	X	X	X	X	X
ROLL			X		X	X		X	X	X	X				
PITCH			X					X	X	X	X				
TURN	X		X	X				X	X	X	X				
ACCEL	X							X	X	X	X				
CCT	X		X	X		X		X	X	X	X	X	X	X	X

113

```
*** AGILITY ***
              NSEG=7,                JMAX=500,           DT=0.1,
          IYY=14000.0, 300.0, 0.0, 0.0, 0.0, 0.0, 0.0,
          IXX=10500.0, 500.0, 0.0, 0.0, 0.0, 0.0, 0.0,
          ETADE=1.0,        LP=-7.0,           LDA=75.0,
          AMAX=15.0,        FBRAKE=5.0,        LAMDOT=45.0,
          MLEAD=0.05,       KARB=0,            IPRINT=1,
          SEND
MANEUV. MACH  ALT.  LOAD  HEAD  BANK  AILN  WCOMBP     A M B T  THR    THRVECT
SEGMENT             FACT CHANGE ANGLE DEFL                       - +    -    +
------- ----- ----- ---- ------ ----- ---- ----------- - - - -  - -   ---- ----
* METRIC 0.90 15000                              0.60  1 0 1 1  1 2   0.   0.
  ROLL   0.00        1.0   0.0  83.6  5.0             0 0 0 0
  PITCH  0.00        9.0   0.0   0.0  0.0             0 0 0 0
  TURN   0.00        9.0 169.3   0.0  0.0             0 0 0 0
  PITCH  0.00        1.0   0.0   0.0  0.0             0 0 0 0
  ROLL   0.00        1.0   0.0   0.0 -5.0             0 0 0 0
  ACCEL  0.90        1.0   0.0   0.0  0.0             0 0 0 0
```

Figure D.1. Sample Input File

Notes on figure D.1:

As in other ACSYNT namelists, $AGILIN is indented one space.

After the namelist, three lines are read before the formatted input is read. These three lines are for the format column header. Any fewer or any more lines will mess up the input.

The formatted input statement is:

FORMAT(2X,A6,F6.2,F8.0,F5.1,F7.1,F6.1,F5.1,
       F10.2,I2,I2,I2,I2,1X,I2,I2,IX,F5.0,F5.0)

Table D.II Bank Angles Required To Coordinate Level Turns

Load Factor	Bank Angle		Load Factor	Bank Angle
1.0	00.0		5.5	79.5
1.5	48.2		6.0	80.4
2.0	60.0		6.5	81.2
2.5	66.4		7.0	81.8
3.0	70.5		7.5	82.3
3.5	73.4		8.0	82.8
4.0	75.5		8.5	83.2
4.5	77.2		9.0	83.6
5.0	78.5		9.5	84.0

Equation: bank angle= $\cos^{-1}(1/load\ factor)$

Example: Suppose a 4.5 g turn was desired. According to the above table, a roll to a bank angle of 77.2 degrees should be performed first. After the roll a pitch to 4.5 g's would then hold the aircraft in a level turn.

E   Output File Architecture

The agility module has three levels of output, these are:

Summary-   only the total time to complete each metric

Standard-   summary output plus the time per segment breakdown and some other key parameters (see output example below)

Detailed-   standard output plus complete time track of state variables.

The output is contained in three files, these are:

fort.30-   contains the summary and standard output and
            the entire time tracks of the following:
            Mach number   Net thrust
            Axial acceleration   angle of attack
            Load factor   Turn rate
            Roll rate   Bank angle
            X position   Y position
            Segment type indicator

fort.31-   contains the entire time tracks of the following:
            Gross thrust   Percent core thrust
            Percent A/B thrust   Lift coefficient
            Drag coefficient   Turn radius

ACSYNT- The user can choose any of the three output
         levels for the ACSYNT output file. The selected
         output level holds for all metrics. This is done by
         specifying the output control variable IPRINT in the
         namelist.

                    IPRINT=
                         0: Summary

                         1: Standard

                         3: Detailed

| F.   COPES Interface |

COPES has access to 25 variables in the agility module. The
first five elements in this array are reserved for the total times
required to complete the first five metrics. Elements 6 through 25
are open to the user. However, use of these elements requires
modification of the code. The user must alter the subroutines to
extract the desired parameter and then assign it an element location
in the COPES array.

Construction of the pitch control surface effectiveness (ETADE)

The method used to calculate the pitch control surface effectiveness is straight out of Jan Roskam's Aiplane Design Series Part 6. The equation below corresponds to equation 10.94 on page 437 of Roskam's text. In this equation, the parameter $\alpha_{\delta e}$ is equivalent to ETADE used below. The attached figures were copied from this text and are included here for convenience.

$$\text{ETADE} = K_b * [c_{l\delta}/(c_{l\delta})_{theory}](c_{l\delta})_{theory} * (k'/c_{l\alpha h})[(\alpha_\delta)_{CL}/(\alpha_\delta)_{cl}]$$

where:

Kb is the elevator span factor obtained from Figures 8.51 and 8.52. Note: in Figure 8.52, the abscissa η should be considered as the $\Delta\eta$ of Figure 8.51.

$[c_{l\delta}/(c_{l\delta})_{theory}]$ is found from Figure 8.15.

$(c_{l\delta})_{theory}$ is found from Figure 8.14.

k' is found from Figure 8.13.

$[(\alpha_\delta)_{CL}/(\alpha_\delta)_{cl}]$ is found from Figure 8.53.
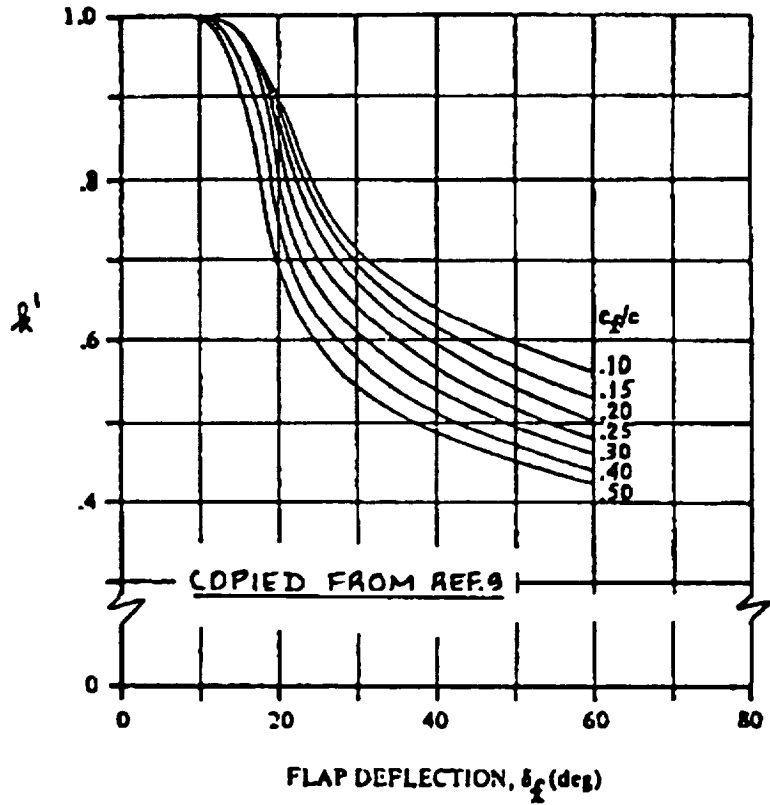
Figure 8.13 Correction Factor for Nonlinear Lift Behavior of Plain Flaps
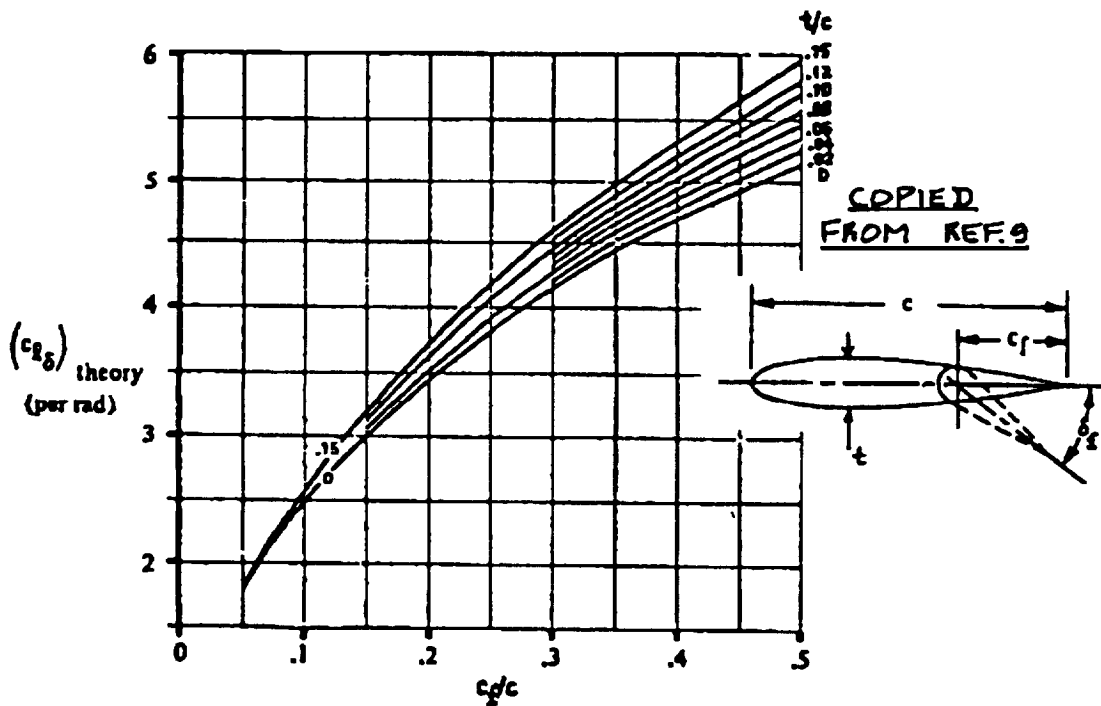
Figure 8.14 Lift Effectiveness of a Plain Flap
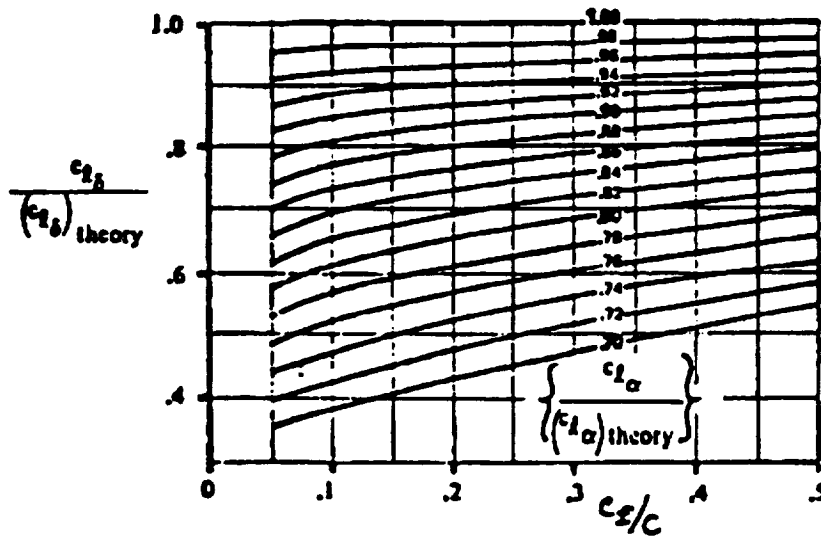
118

Figure 8.15 Correction Factor for Plain Flap Lift
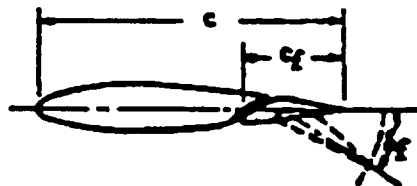
Figure 8.16 Single Slotted Flap Geometry

FLAP DEFLECTION, δ_f (deg)
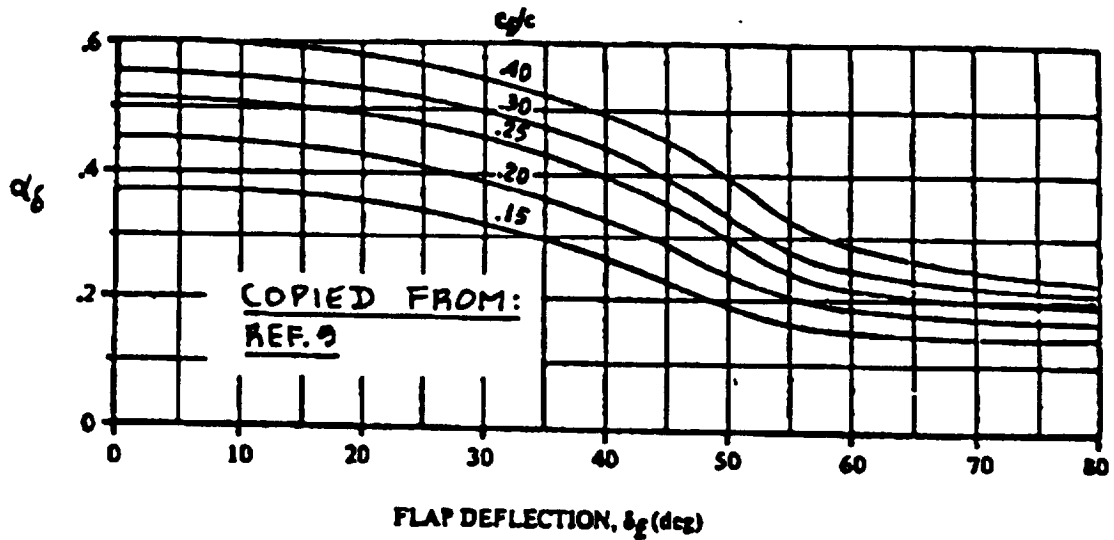
Figure 8.17 Lift Effectiveness of a Single Slotted Flap
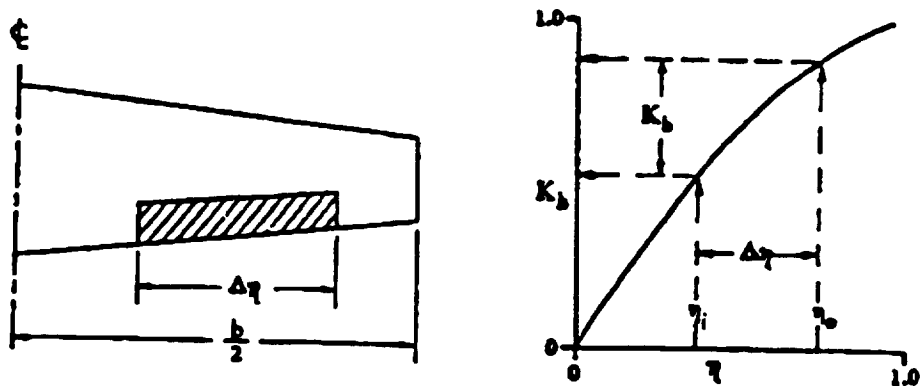
Figure 8.51 Procedure for Estimating K_b
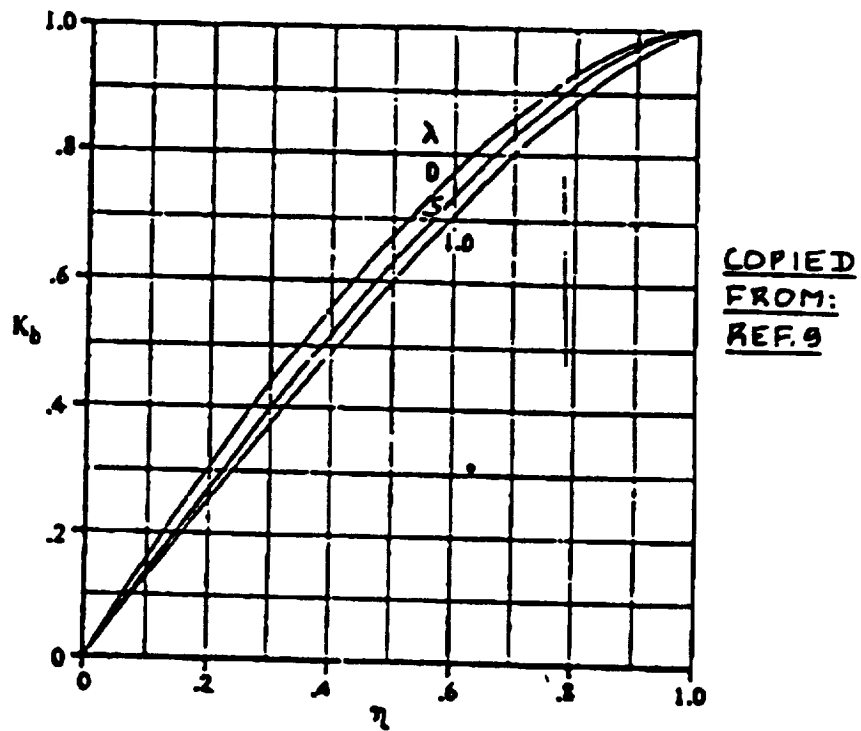
COPIED
FROM:
REF.9

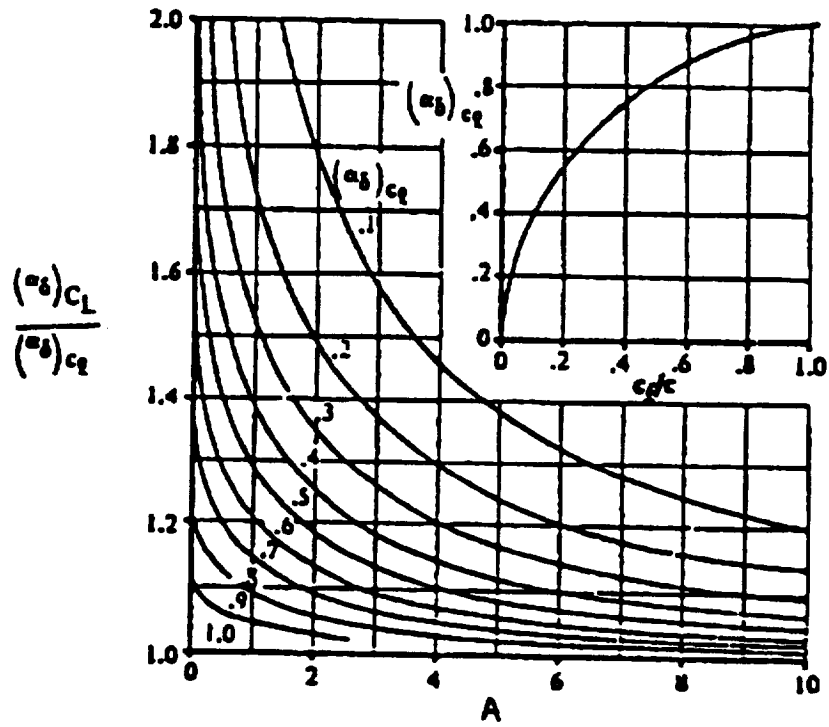Figure 8.52 Effect of Taper Ratio and Flap Span on K_b

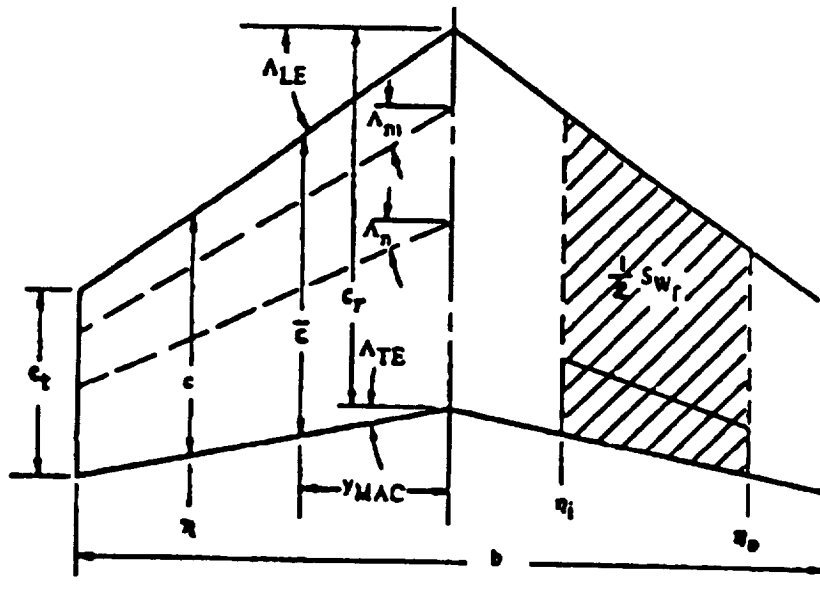**Figure 8.53 Effect of Aspect Ratio and Flap-Chord Ratio on the Three-Dimensional Flap Effectiviness**

Figure 8.54 Definition of 'Flapped' Wing Area